

UNIVERSITY OF BIRMINGHAM

**GEOHERMAL SYSTEMS IN THE CHALK OF THE SOUTH EAST OF ENGLAND:
METHODS OF PREDICTING THERMAL TRANSPORT IN A FRACTURED
AQUIFER**

BY

RYAN LAW

BA (Hons). Earth Sciences, Oxford University

MSc. Hydrogeology. University of Birmingham

Supervisors

Dr R. Mackay

Dr J H Tellam

Hydrogeology research group

School of Earth Sciences

August 2009

UNIVERSITY OF
BIRMINGHAM

University of Birmingham Research Archive

e-theses repository

This unpublished thesis/dissertation is copyright of the author and/or third parties. The intellectual property rights of the author or third parties in respect of this work are as defined by The Copyright Designs and Patents Act 1988 or as modified by any successor legislation.

Any use made of information contained in this thesis/dissertation must be in accordance with that legislation and must be properly acknowledged. Further distribution or reproduction in any format is prohibited without the permission of the copyright holder.

ACKNOWLEDGEMENTS

I am grateful to my supervisor Professor Rae Mackay for his support, intellectual input and for allowing me such a long leash to develop the project.

I would like to thank Arup Geotechnics for their support of this work which went far beyond the financial. In particular I would like to thank Duncan Nicholson, without whose foresight and energy, this project would never have started. In addition, his input into the project, particularly during the early stages was extremely valuable. Also, Karen Mayo from Arup Geotechnics for her assistance with the fieldwork on this project.

I would also like to thank Mick Riley from the University of Birmingham for his assistance with some mathematical aspects of the work.

Also, thank you to my wife Sue, for inadvertently starting me off on the long geothermal road.

ABSTRACT

There has recently been a steady increase in the number of licenses granted for the abstraction of water from the Chalk aquifer beneath London to supply 'open loop' geothermal systems (Environment Agency, 2007). However, there has been little research conducted on how the water re-injected by these systems, which often differs in temperature by as much as 10°C, will interact with the fractured Chalk aquifer in both the short and long term.

An analytical solution developed by Bodvarsson (1989) was used to show that, for most configurations of a geothermal system, thermal transport would be governed by fractures. It was then proved that the United States Geological Survey SUTRA code could be used to construct a more detailed model of the aquifer. A thermal test was devised to collect hydrogeological and thermal data. This test, along with conventional site investigation techniques, was used at a site in central London. A detailed numerical model of the geothermal system and the aquifer was then constructed in SUTRA. The results showed that the fracture zones found during testing would affect the system performance. Building on these results a procedure was developed for designers, to ensure such systems function in an appropriate way.

Contents

1	AIMS AND OBJECTIVES.....	1
2	BASIC PRINCIPLES	4
2.1	Energy transport in the ground	4
2.1.1	Conduction	4
2.1.2	Convection	6
2.1.3	Dispersion	7
2.1.4	Diffusion	8
2.2	Energy storage.....	9
2.2.1	Groundwater flow and temperature	10
2.3	Ground properties	11
3	GEOHERMAL SYSTEMS	15
3.1	System configurations	18
3.2	The United Kingdom.....	22
3.3	Basic hydrogeology and geothermal systems	25
3.3.1	Background hydraulic gradient in the Chalk.....	27
3.3.2	Fracture basics	27
3.3.3	Evidence of thermal breakthrough.....	29
3.4	Existing research.....	31
4	THE GEOLOGY OF LONDON.....	33
4.1	Research history.....	33
4.2	Geological History	34
4.3	Quaternary	35
4.4	Palaeogene-Eocene.....	37
4.5	Palaeogene-Paleocene	38
5	THE CHALK.....	3
5.1	Chalk matrix.....	6
5.2	Discontinuities and fracturing.....	6
5.3	Permeability and transmissivity	8

5.4	Fracture geometry	13
	Summary	14
6	FRACTURE FLOW AND MODELS	15
6.1	Treatment of single fractures	15
6.2	Scaled conceptual models	18
6.2.1	Discrete Models	20
6.2.2	Continuum models	21
6.3	Scale of interest	23
	Open loop geothermal model.....	24
6.3.1	Fracture geometry	25
6.3.2	Porosity and permeability	25
6.3.3	Scale of interest and the conceptual model	27
6.3.4	Summary	29
7	THERMAL TRANSPORT IN FRACTURES	30
7.1	Background	30
7.2	Conceptual model (thermal breakthrough)	31
7.3	Numerical models	45
7.3.1	Representation of thermal transport in SUTRA	46
7.4	Summary	50
8	SUTRA TEST	52
8.1.1	Analytical solution	55
8.1.2	Analytical solution parameters	56
8.1.3	Analytical Solution Results	58
8.2	Numerical modelling	59
8.2.1	Geometry	59
8.2.2	Boundary conditions	60
8.2.3	Grid	62
8.2.4	Fluid injection	65
8.2.5	Model Operation	68

8.2.6	Model Results	68
8.3	Summary	69
9	SITE INVESTIGATION TECHNIQUES.....	70
9.1	Suite of tests.....	71
	CCTV survey.....	71
9.2	Flow logging	72
9.3	Pumping tests	72
9.4	Tracer test	73
9.5	Thermal test	74
9.6	Application to a proposed site	75
9.7	The site	75
9.8	Borehole specification	77
9.9	Initial Development and Geophysical Logging	79
9.10	Geophysical surveys	79
9.11	CCTV Survey	83
9.12	Flow logs.....	86
9.13	Pumping tests.....	87
9.13.1	Correction of groundwater level data	87
9.13.2	Step drawdown tests	87
9.13.3	Constant rate tests.....	87
9.13.4	Combined abstraction and recharge trial	88
9.13.5	Tracer test.....	88
9.13.6	Thermal test.....	90
9.14	Summary	94
10	SITE INVESTIGATION INTERPRETATION	96
10.1	Flow logging and CCTV	96
10.2	Pumping tests.....	96
10.3	Tracer test.....	100
10.4	Thermal test.....	104

10.5	Summary	110
11	APPLICATION OF A NUMERICAL MODEL TO A PROPOSED SITE.....	111
11.1	Parameters	111
11.1.1	Building heating and cooling demands.....	111
11.1.2	Representation of hydrogeology.....	117
11.1.3	Model construction	120
11.1.4	Boundary conditions	123
11.1.5	Grid	124
	Fluid injection	126
11.2	Model results	128
11.2.1	Peak heat rejection rates	129
11.2.2	52 week rejection and abstraction cycle	130
11.2.3	Yearly heat rejection cycle	131
11.3	Conclusions	132
11.4	Summary	132
12	CONCLUSIONS AND FURTHER WORK.....	134
12.1	Literature review of geology	135
12.2	Literature review of fluid flow in fractured material	135
12.3	Conceptual model development for Chalk	136
12.4	Site Investigation techniques	137
12.5	Construction of a numerical model	138
12.6	Summary	138
12.7	Recommendations for further work.....	141
	APPENDICES	154
	PUBLISHED PAPERS	154

Figures

Figure 3-1 Energy sources and temperature profile with depth (UK).....	16
Figure 3-2 The expansion and compression cycle of a heat pump (after Strathclyde University)	17
Figure 3-3 Closed geothermal system (no direct contact between the ground and the fluid transporting the heat).....	20
Figure 3-4 Open geothermal system (direct usage of fluid from the ground)	21
Figure 3-5 Number of heat pumps sold in Europe – after Sanner, 2009	22
Figure 3-6 Hydrogeology and open geothermal systems	26
Figure 3-7 Comparing fluid velocities for a homogenous and fractured medium.....	28
Figure 3-8 Temperature data from an operational geothermal system, London.....	30
Figure 4-1 Chronology of principal Quaternary deposits and oxygen isotope stages (Sumbler, 1996) after Ellison, 2004.	36
Figure 4-2 Palaeogene lithostratigraphy and chronology (after Knox, 1996).....	39
Figure 4-3 Schematic diagram showing the relationship between the informal lithological units in the Lambeth Group in central London (after Ellison, 2004).....	40
Figure 5-1 Sketch map of the extent of Chalk in England after Bell et al (1999)	4
Figure 5-2 Typical stratigraphy of the Chalk after Mortimore 1983,1986.....	5
Figure 5-3 Conceptual model of fracture systems in the Chalk (after Bloomfield, 1996).....	13
Figure 6-1 Fracture models	19
Figure 7-1 Different representations of thermal transport.....	33
Figure 7-2 Reduced geometry for the analytical model	35
Figure 7-3 Type curve for $\theta \leq 0.01$ (After Bodvarsson, 1982). The zone of interest for a geothermal system with typical flow rates and borehole spacings is highlighted	41
Figure 7-4 Representation of Figure 7-3 showing the thermal front for two different conditions.....	42
Figure 8-1 Fracture model (1D).....	53
Figure 8-2 Matrix model geometry.....	54
Figure 8-3 Results from the analytical solution.....	58
Figure 8-4 Representation of the geometry used in the numerical model	60
Figure 8-5 Boundary conditions for numerical model	61

Figure 8-6 Representation of grid used in the numerical model	65
Figure 8-7 Block representation of a fracture plane and injection nodes	67
Figure 8-8 Numerical modelling (NM) results using SUTRA 3D and analytical results (AM)	68
Figure 9-1 Borehole configuration	78
Figure 9-2 Geophysical survey – borehole 1	80
Figure 9-3 Geophysical survey – borehole 2	82
Figure 9-4 CCTV survey, potential fracture at 86mbgl – borehole 2	84
Figure 9-5 CCTV survey, potential fracture at 84mbgl – borehole 1	84
Figure 9-6 CCTV survey, potential fracture at 80 mbgl – borehole 1	85
Figure 9-7 Close up of results from the flow logging (_s_unpumped conditions; _p_pumped conditions; _r_recharge)	86
Figure 9-8 Tracer test response (courtesy of the BGS)	89
Figure 9-9 Plastic insulated containers for heated water storage	91
Figure 9-10 Schematic section of thermal test equipment	91
Figure 9-11 Equipment being lowered into the borehole	92
Figure 9-12 Results of the thermal test	94
Figure 10-1 Eden Hazel Analysis for Borehole 1 and Borehole 2	97
Figure 10-2 Jacob’s straight line interpretation for Borehole 1 and Borehole 2 respectively	99
Figure 10-3 Calibrated versus observed breakthrough tracer concentrations at the outlet of the doublet discharge borehole	103
Figure 10-4 Results of the thermal test	104
Figure 10-5 Basic elements of the thermal test	106
Figure 10-6 Modelled versus observed response for the thermal test	108
Figure 10-7 Modelled results for a single fracture and two fractures	109
Figure 11-1 Heat rejection to the ground and absorption from the ground for the proposed system ..	115
Figure 11-2 Type curve developed by Bodvarsson for $\theta \leq 0.01$	119
Figure 11-3 Representation of the numerical model	122
Figure 11-4 Boundary conditions for numerical model	124
Figure 11-5 Block representation of a fracture plane and injection nodes	127

Figure 11-6 Calculated temperature in the abstraction borehole. Peak cooling.	129
Figure 11-7 Calculated temperature in the abstraction borehole. 52 weeks.....	130
Figure 11-8 Calculated temperature in the abstraction borehole. 50 years.	131
Figure 12-1 Flow chart representing the recommended procedure to be undertaken in the design of an open loop geothermal system in the Chalk.	140

Tables

Table 2-1 Thermal properties of rock and other materials (Bose, J.E, Parker, J.D, and McQuiston, F.C 1985, De Vries & Afgan 1975, Walton 1984).....	14
Table 4-1 Geological units of relevance to geothermal systems (open or closed) in London (Arup, 2006).....	2
Table 5-1 Transmissivity in the Chalk aquifer after McDonald, 2001.....	11
Table 7-1 Parameters used for the Chalk.....	40
Table 8-1 Parameters used in the analytical solution.....	58
Table 8-2 Example injection and abstraction rates.....	67
Table 9-1 Summary of ground conditions at the site.....	76
Table 10-1 Summary of calculated transmissivity.....	99
Table 10-2 Material properties used to model the thermal injection test.....	107
Table 11-1 Estimation of ground temperature changes.....	114
Table 11-2 Model injection and abstraction rates.....	127
Table 11-3 Parameters for the three models.....	128

1 AIMS AND OBJECTIVES

This PhD aims to understand and predict the interaction between an ‘open loop’ geothermal system and the Chalk aquifer beneath central London. Such systems abstract water from the aquifer at ambient temperatures (approximately 13°C in London) before re-injecting to the aquifer at a different temperature. Large scale, modern developments in London, often have much larger cooling demands than heating demands and the aquifer represents a good ‘cold’ resource. It is normally the case that the water re-injected by these systems is much warmer (between 5 and 10°C) than the ambient temperature of the aquifer.

The installation of open loop geothermal systems in London has seen an unprecedented rise since 2004. As the number of installations grow, so does the potential impact upon the aquifer. To date, not enough research has been completed on the interaction between a geothermal system and a fractured aquifer such as the Chalk. This PhD aims to address two main issues:

1. How will the geothermal system alter the ambient temperature of the aquifer over both the short and long term
2. Will the geothermal system be prone to short circuiting and subsequent system shut down due to rapid, fracture driven, thermal transport between the injection and abstraction borehole

The first concern is one of environmental sustainability and must be properly addressed to ensure that the Environment Agency can manage the resource appropriately. The second is related to the performance of the system. Rapid thermal breakthrough will cause a feedback loop to develop between injection and abstraction boreholes. This can cause a number of problems. For systems that are used for cooling, the re-injection temperature is likely to rise

quickly in response to a rise in the abstraction temperature. As the maximum temperature of re-injection is limited by the licence granted by the Environment Agency, the system will become in danger of breaching this licence and thus becoming inoperable. Conversely, for systems that are used for heating purposes, the temperature of re-injection will drop and start to approach freezing, again causing the system to become inoperable.

To adequately understand the type of thermal transport that may occur between an injection and abstraction borehole an accurate picture of the hydrogeological and thermal characteristics of the Chalk aquifer beneath a site must be developed. In addition, a sufficiently robust method of predicting the effects of the geothermal system must be developed. The former should be achievable with a thoughtful site investigation and testing programme. To assist with developing this programme, a push-pull thermal test has been designed for this PhD. The latter should be achievable with the development of appropriate analytical and numerical models. The complexity of the models needs to match the accuracy and reliability of the field data as well as both the project budget and schedule. Two modelling approaches are therefore proposed:

1. An analytical model to enable an initial assessment of the likely type of thermal transport (fracture or homogenous) for a geothermal system. This model should be easy to construct, without the need for either an expensive site investigation or a time consuming numerical modelling exercise and would be for use at an early stage in the design process.
2. A detailed, transient 3-dimensional model based on the specific geological parameters that will accurately predict the interactions between the geothermal system and the aquifer. This model will require the collection of sufficient and accurate data.

The final objective of the PhD is to develop an appropriate procedure for designers of open loop systems to follow to ensure that a geothermal system will operate appropriately over its lifetime.

It is proposed that the following steps are undertaken to achieve the objectives of this PhD:

1. A literature of review of the principles of thermal transport
2. A literature review of the geology of central London and the Chalk structure
3. A review of existing research and data on open loop geothermal systems in the Chalk aquifer
4. A literature review of modelling fluid flow in fractured material
5. The development of analytical and numerical models that best represent the thermal transport displayed by the Chalk for typical geothermal flow rates and conditions
6. A review of site investigation techniques and the development of a push pull thermal test
7. Application of the site investigation techniques to a proposed site to collect sufficient data for the construction of a detailed numerical model. Use of the model to predict the behaviour of a proposed geothermal system
8. Development of a standard set of procedures to be followed during the design stages of an open loop geothermal system to ensure efficient operation and environmental sustainability

2 BASIC PRINCIPLES

Before discussing geothermal systems in more detail, this chapter covers the basic physical principles upon which all systems are based. There are two strands to consider:

- Energy transport
- Energy storage

2.1 Energy transport in the ground

The movement of energy, in particular heat, in the ground can occur in the following ways:

1. *Conduction* within a solid due to a temperature gradient between two points.
2. *Convection* due to the movement of groundwater
3. *Dispersion* due to movement of groundwater coupled with the irregularities in the rock structure
4. Molecular *diffusion*

2.1.1 Conduction

Conduction is the transfer of energy through a material. The most often used example is that of a rod of steel that has one end within a fire. Heat travels along the rod due to conduction. *Thermal conductivity* is the physical property of a material that characterizes the rate at which heat travels through it. The value of thermal conductivity determines the heat flow, i.e. the thermal energy passing per unit time per unit area for a temperature change of 1-degree Kelvin per unit length. *Thermal conductivity* is a measure of the ease with which heat can be

propagated through a material and is analogous to permeability in the flow of groundwater.

The heat flow equation is:

$$Q = \lambda A dT / dx$$

Eq 2-1

where:

Q Heat flow (W/m²)

A Cross sectional area of the material (m²)

dT / dx Temperature / thickness gradient (°C/m)

λ Thermal conductivity (W/m°C)

The thermal conductivity of a material varies as a function of pressure and temperature. The thermal properties of the ground are dependent upon the rock minerals, the pore fluid, the microstructure of the ground (Guéguen & Palcianskas, 1994), and the partial saturation of the ground (Ahrens, 1995). Because the ground is made up of rock, pore spaces, water and air a bulk thermal conductivity can be applied, assuming local thermal equilibrium, that takes these additional parameters into account. (Eq 2-2 – Walton, 1984, for a fully saturated case)

$$\lambda_A = \phi \lambda_F + (1 - \phi) \lambda_S$$

Eq 2-2

where:

λ_A Thermal conductivity of the aquifer material (W/m°C)

λ_F Thermal conductivity of the fluid (W/m°C)

ϕ	Porosity
λ_s	Thermal conductivity of the solid (W/m°C)

2.1.2 Convection

Convection is the transfer of energy by the movement of the medium itself. An example of convection would be the transport of heat from a hairdryer where heat is transferred by the movement of air. There are two forms of convection:

- Free convection, also known as natural convection, results from buoyancy effects due to temperature difference within a medium (for the geothermal systems being considered in this thesis buoyancy effects will be minimal)
- Forced convection, is precipitated by some form of gradient (Isaacs, 1996) leading to the movement of an energy carrying medium such as pressure gradients driving the movement of air or water. Convective flux is dependent upon the density of the medium carrying the heat, its specific heat capacity, its temperature and the velocity at which the medium is moving.

$$f_{convection} = \rho C T v_x$$

Eq 2-3

where:

$f_{convection}$	Convective heat flux (W/m ²)
ρ	Density (kg/m ³)
C	Specific heat capacity (J/kg°C)
T	Temperature (°C)

v_x Velocity tensor (m/s)

2.1.3 Dispersion

Thermal dispersion is analogous to solute dispersion. It is caused by the movement of groundwater through the irregular structure of the rock matrix. A full discussion of dispersion is not warranted here but readers are referred to Sauty et al, 1978 for further information. Although thermal dispersion is relatively small compared to convection or conduction it cannot be ignored, particularly if the rock structure is relatively complex. The thermal dispersion coefficient (D_L) contains a component for pure diffusion (D_e) and a component for dispersion due to advection ($\alpha_L v$). This analogy permits the same numerical scheme for both mass and heat transport (Eq 2-4) (Sauty *et al.* 1978, 1982)

$$D_L = D_e + \alpha_L v$$

Eq 2-4

where:

α_L Longitudinal thermal dispersivity (m²/s)

v Average linear groundwater velocity (m/s)

Willemsen and Groeneveld (1989) have questioned this analogy, and Hufschmiedt (1985) presents data in which the dispersivity for heat transport is smaller than that for solute transport by a factor of three, presumably because of greater mixing of the heat locally. However, it is customary for the analogy of Sauty *et al.* (1982), to be used, as no proven

alternative has yet been established. Therefore, the relationship between longitudinal thermal dispersivity (α_L) and the apparent length scale (L_s) is that of Eq 2-5 (Xu and Eckstein 1995)

$$\alpha_L = 0.83(\text{Log}L_s)^{2.414}$$

Eq 2-5

The transverse dispersivity is generally assumed to be one tenth of the longitudinal value (Gelhar, 1993).

2.1.4 Diffusion

Thermal diffusivity is a measure of the rate of heat propagation spatially in a transient heat transfer process due to conduction. The higher the thermal diffusivity of a material, the higher the rate of temperature propagation.

$$\alpha = \frac{\lambda}{\rho C_p}$$

Eq 2-6

Where:

α Thermal Diffusivity (m^2/s)

λ Thermal Conductivity ($\text{W}/\text{m}^\circ\text{C}$)

C_p Specific Heat ($\text{J}/\text{kg}^\circ\text{C}$)

ρ Density (kg/m^3)

According to this relation, thermal diffusivity will affect any conductive transient heat transfer process within the sample medium. Thermal diffusion is a relatively slow process when

compared to advection. However, over the lifetime of a geothermal system (25 to 50 years) the affects cannot be ignored.

2.2 Energy storage

The ground is a very effective energy store. The quantity of energy that can be stored by a given volume of ground is large compared to the rate at which the energy can be added or removed. The energy storage capacity of the ground is determined by the heat capacity of the materials that make up the ground. Each material has a specific heat capacity, by definition, this is the quantity of energy required to raise the temperature of a unit of mass of a substance by a unit change in temperature (Eq 2-7).

$$C = \frac{E}{m\Delta T}$$

or

$$E = mC\Delta T$$

Eq 2-7

where:

E Change in heat in Joules

m Mass in kg

C Specific heat capacity in J/(kg°C)

ΔT Change in temperature in °C

Specific heat capacity is pressure and temperature dependent. The standard units for C , the specific heat capacity, are J/(kg°C). The amount of thermal energy that can be stored is dependent upon the thermal capacity of the ground material and the water or air contained

within its void space. The volume of air and or water is important as the specific heat capacity of pure water (4,182 J/(kg°C)) is much greater than the specific heat capacity of air (1,000 J/(kg°C)) and most types of rock ~ (900 J/kg°C). Therefore, the more porous and saturated the ground is, the greater the proportion of water per unit volume and therefore the greater the heat storage capacity.

A bulk specific heat capacity that represents both the ground and the water can be determined in a similar manner to bulk thermal conductivity (**Eq 2-8**).

$$c_v = \phi c_w \rho_w + (1 - \phi) c_s \rho_s$$

Eq 2-8

where:

- c_v Volumetric thermal capacity (J/kg°C)
- $c_w ; c_s$ Specific heat capacity of water and solid respectively (J/kg°C)
- $\rho_w ; \rho_s$ Density of water and solid respectively (kg/m³)

2.2.1 Groundwater flow and temperature

In aquifers where there is groundwater flow one dimensional specific discharge can be defined by Darcy's Law (Eq 2-9) in terms of density and viscosity (Fetter, 2001)

$$q_x = -\left(k \frac{\rho g}{\eta}\right) \frac{dh}{dx}$$

Eq 2-9

where:

η Dynamic viscosity (kg/ms)

g Gravitational acceleration (m/s²)

k Permeability (m²)

$\frac{dh}{dx}$ Hydraulic gradient

As dynamic viscosity is dependent upon temperature, the hydraulic conductivity is also temperature dependent to an extent, illustrating the coupled processes that exist between heat and hydraulic flows in an aquifer: water flow is controlled by the hydraulic gradient and additional flow is induced by thermal gradients. The thermally-induced flow of water will cause a shift in the temperature isotherms and alter the thermal gradient, hence changing water flow (Freeze and Cherry, 1979).

2.3 Ground properties

The thermal properties the density and the porosity of the ground material, provide important controls on the total amount of heat stored/ abstracted and the ease with which it migrates through the ground / is lost to the surrounding environment.

The thermal storage capacities and conductivities of different ground types display a range of values (Table 2-1), depending upon the mineral composition. Variation in mineralogy will affect the thermal properties of a lithology; for example, sandstone with a high quartz content

will have a higher thermal conductivity than sandstone with a low quartz content. As such, thermal properties may change, even throughout one formation, according to depositional environment and locality. In addition, the saturation and porosity of the lithology will strongly affect the thermal conductivity of the material. The thermal conductivity of water ($0.6 \text{ W/m}^\circ\text{C}$) is at least 4 times less than most rock types (ca. $2.4 \text{ W/m}^\circ\text{C}$). The thermal conductivity of air ($0.02 \text{ W/m}^\circ\text{C}$) is two orders of magnitude less, which shows that composition of the pore contents in the rocks will strongly affect the thermal conductivity.

As there will be variations in thermal and hydrogeological properties in all ground types, the ability to accurately represent a lithology on a small scale is limited. However, on a larger scale, a lithology should become more homogenous and thus more easily represented in a mathematical manner.

Igneous Rocks	Thermal Conductivity (W/m°C)	Specific Heat (KJ/(Kg°C))
Amphibolite	2.60 – 3.81	0.85
Andesite	1.56 – 2.42	0.50
Basalt	2.08 – 2.42	0.71 – 0.88
Diorite	2.08 – 2.94	0.92
Gabbro	1.56 – 3.64	0.75
Granite (10% Quartz)	2.25 – 3.29	0.88
Granite (25% Quartz)	2.60 – 3.64	0.89
Granodiorite	2.08 – 3.46	0.88
Metamorphic Rocks		
Gneiss	1.73 – 5.71	0.38
Marble	2.08 – 5.54	0.38
Quartzite	5.19 – 6.92	0.35
Schist	2.08 – 4.50	0.39
Slate	1.56 – 2.60	0.38

Sedimentary Rocks	Thermal Conductivity (W/m°C)	Specific Heat (KJ/(Kg°C))
Chalk	2.10 – 2.70	0.89
Claystone	1.90 – 2.94	0.90
Dolomite	2.77 – 6.23	0.88
Limestone	2.42 – 3.81	0.92
Sandstone	2.08 – 3.46	1.00
Shale (wet/ no quartz)	1.04 – 1.56	0.88
Shale (dry/ no quartz)	0.87 – 1.38	0.88
Siltstone	1.38 – 2.42	0.90
Other materials		
Air	0.025	0.994
Clay	2.90	0.937
Concrete (dense)	1.73	0.84
Organic matter	0.25	0.80
Quartz	8.80	0.79
Water	0.57	4.18

Table 2-1 Thermal properties of rock and other materials (Bose, J.E, Parker, J.D, and McQuiston, F.C 1985, De Vries & Afgan 1975, Walton 1984)

3 GEOTHERMAL SYSTEMS

Geothermal systems, or at least those with which this PhD is concerned, use the thermal mass of the ground as a heat source or sink. Geothermal energy being defined by the European Parliament, Energy Committee (2008) as '*the energy stored in the form of heat beneath the surface of the solid earth*'.

The temperature of the ground at depths of between 5 and 100m is approximately stable throughout the year (Figure 3-1). In the United Kingdom, the ground temperature over this depth range is approximately 12°C, although this is variable depending upon the location of the site (Met Office, 2007). The processes by which this temperature is maintained are complex. Figure 3-1 shows the main energy inputs and outputs that control the temperature of the ground over a one year period. The principal energy gain to the ground is solar (an average of 157 W/m² over the year for the UK – (Met Office, 2007)). The principal losses from the ground are those associated with changing the phase of water (evaporation) 85 W/m², radiation 51 W/m² and conduction / convection 21 W/m². The energy gain from the dissipation of heat from the heated core of the Earth at these shallow depths is several orders of magnitude smaller, approximately 20-100 mW/m² depending upon the location of the site. The effects of deep geothermal energy fluxes only start to become apparent at greater depths than this PhD is concerned with. The majority of the energy used by shallow geothermal systems (<200m) therefore ultimately comes from the sun: thus such systems, despite the term geothermal, are in reality buried solar collectors.

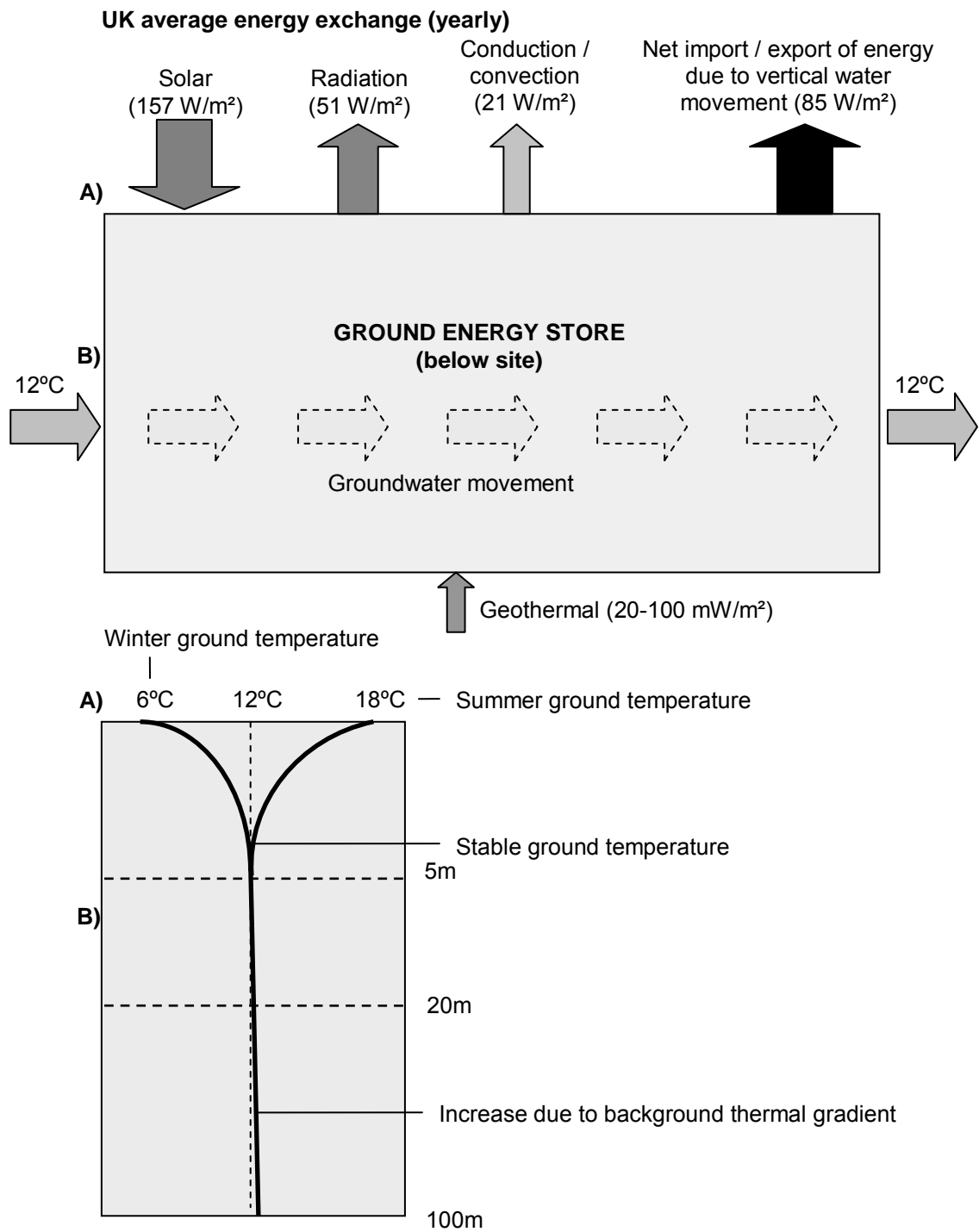


Figure 3-1 Energy sources and temperature profile with depth (UK)

Geothermal systems (in heating mode) withdraw energy from a large volume of ground and transfer it to a smaller volume (a building). In cooling mode, energy is taken from a small volume (a building) and transferred to a larger volume, the ground.

In general, the temperature of the ground at shallow depths (<200m) in the winter is lower than that desired to heat a building. A geothermal system often uses a Ground Source Heat Pump (GSHP) to increase this temperature to that required for space heating. GSHPs operate in the same way as refrigerator units, using electricity to circulate a fluid (often ammonia based), through a compression and expansion cycle (Figure 3-2). In heating mode, during the expansion cycle (when the liquid becomes a gas) heat is abstracted from the ground loop side of the heat pump. During the compression cycle this heat is then released from the circulation fluid and transferred to the building side of the heat pump. This method of transferring energy from one source to another is efficient, particularly when compared to conventional methods of heating such as a gas or oil boiler.

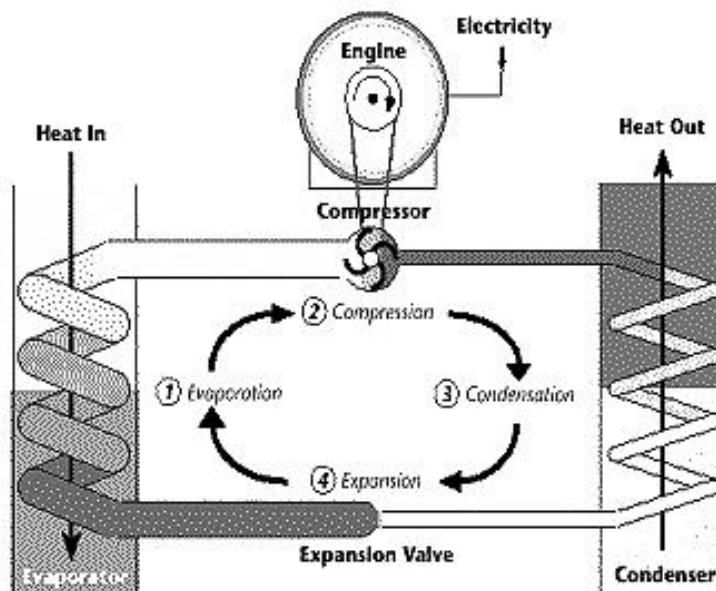


Figure 3-2 The expansion and compression cycle of a heat pump (after Strathclyde University)

The ratio of the units of electricity used by the heat pump (the base energy) to the units of heat supplied to the building is termed the Co-efficient of Performance (COP). GSHPs can function with COPs as high as 5 for heating, depending on the input and output temperatures (Natural Resources, Canada, 2002). For comparison, a modern gas boiler will function with an efficiency of approximately 0.9 (Natural Resources, Canada, 2002). Heating a building with a GSHP is therefore more efficient in base energy units. When comparing such systems the efficiency of the electricity generation should also be taken into account (conversions of energy to electricity are typically 0.4). With this in mind, the renewable resource of a system using a GSHP is ‘*the additional energy supplied by the ground over and above that used by the system*’ as defined by the European Parliament, Energy Committee (2008)

For cooling purposes, the equivalent COP of the GSHP is termed the Energy Efficiency Ratio (EER). This is calculated by dividing the energy removed from the building (in Btu/hr) by the energy input into the system (in Watts). This is also referred to as the COP_c and can be as high as 20 (Natural Resources, Canada, 2002) due to the ground temperature being much closer to that required by the building for cooling than for heating. With an EER of 20 the renewable portion of this system is significant and GSHP cooling is regarded as the most energy efficient method of cooling a building.

3.1 System configurations

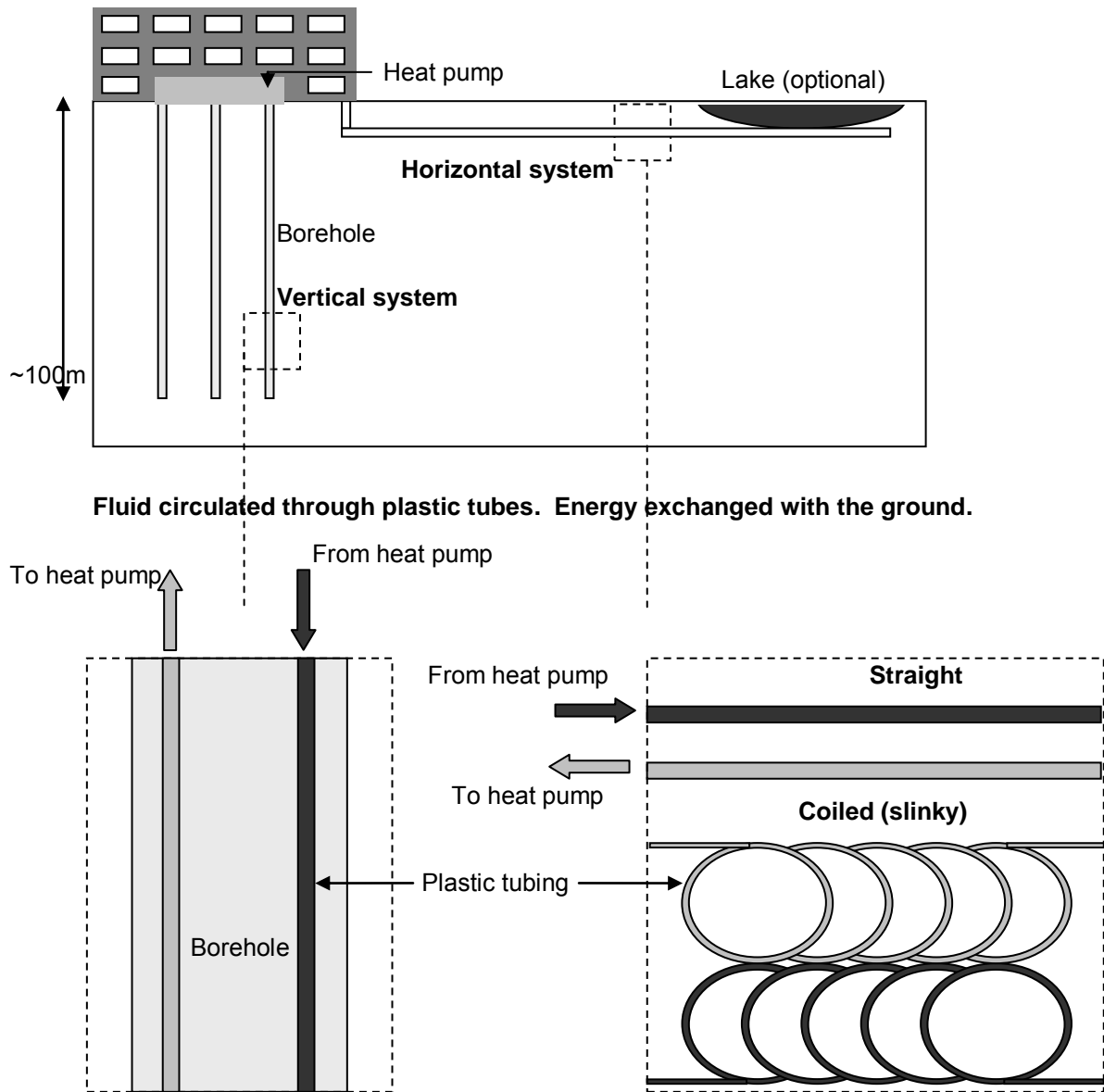
There are two main types of geothermal systems used to heat and cool buildings.

- Closed (Figure 3-3) - *conduction*. In closed systems there is no direct contact between the fluid circulating in the geothermal pipework and the ground. Fluid is circulated through a closed circuit of plastic tubing. The energy from the ground is transferred to

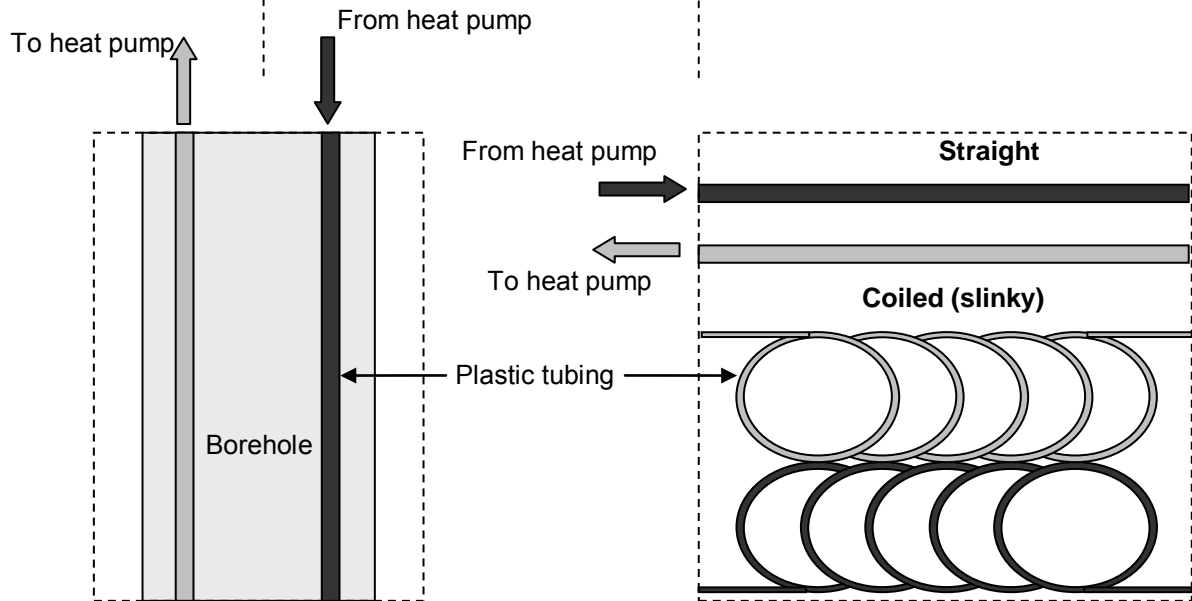
the fluid in the circuit through the process of conduction due to the temperature gradient between the fluid in the circuit and the surrounding ground. Closed systems can be vertical or horizontal and can also be placed within the foundations of a building. Typical energy yields for a closed system are approximately 40 – 60 watts per metre of borehole length for a vertical system and 35 watts per square metre of trench area for a horizontal system (Brandl, 2006)

- Open (Figure 3-4) - *convection*. In open systems, water is extracted directly from the ground. The extracted water is normally passed through a heat exchanger / GSHP and energy transferred to the building. The used groundwater is then either discharged to a surface water source or re-injected into the aquifer. As energy is transferred through the processes of both convection and conduction a greater energy yield can be achieved per borehole for an open system than a closed system.

As an example, a vertical, open borehole in the Chalk aquifer of London will typically yield between 210 and 420 kW of energy, depending upon the borehole flow rates and the operational efficiency of the heat exchanger. A vertical closed borehole of a similar length will only yield 12 kW in favourable ground conditions (approximately 30 times less). In an urban setting such as London, where space is at a premium it is clearly preferable to install open systems.

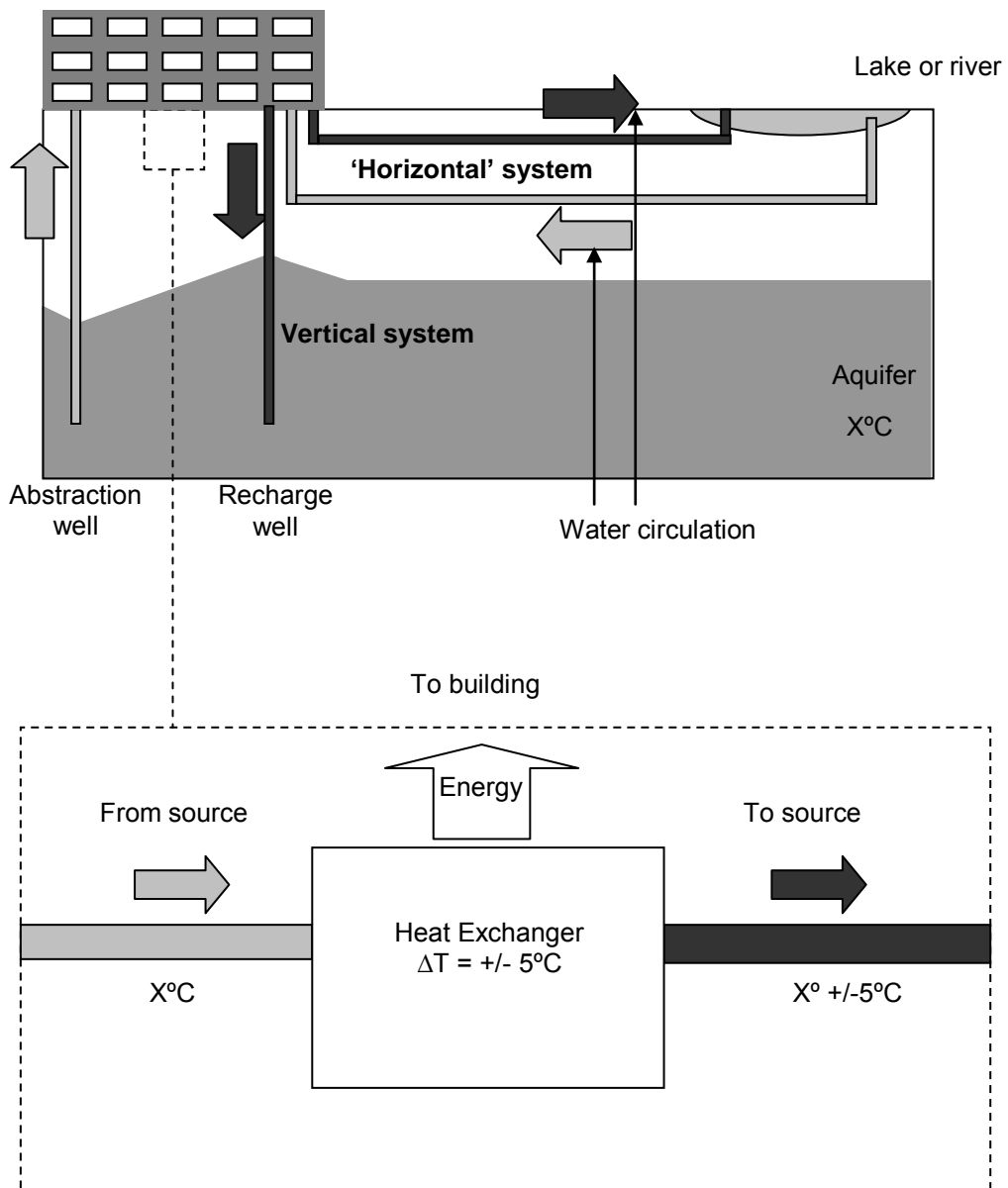


Fluid circulated through plastic tubes. Energy exchanged with the ground.



Typical energy:	
Vertical	45-60 W/m
Horizontal	35 W/m²
Surface area for 100 kW	
Vertical	450 m²
Horizontal	2860 m²

Figure 3-3 Closed geothermal system (no direct contact between the ground and the fluid transporting the heat)



Typical energy:
Flow of 10 l/s per borehole* 210 kW

Surface area for 100 kW
Vertical <10 m²

*Based on a ΔT of 5°C for the heat exchanger.

Figure 3-4 Open geothermal system (direct usage of fluid from the ground)

3.2 The United Kingdom

Other European countries are more advanced than the United Kingdom in their deployment of geothermal systems (Figure 3-5). This is despite the fact that the United Kingdom has good potential for such systems.

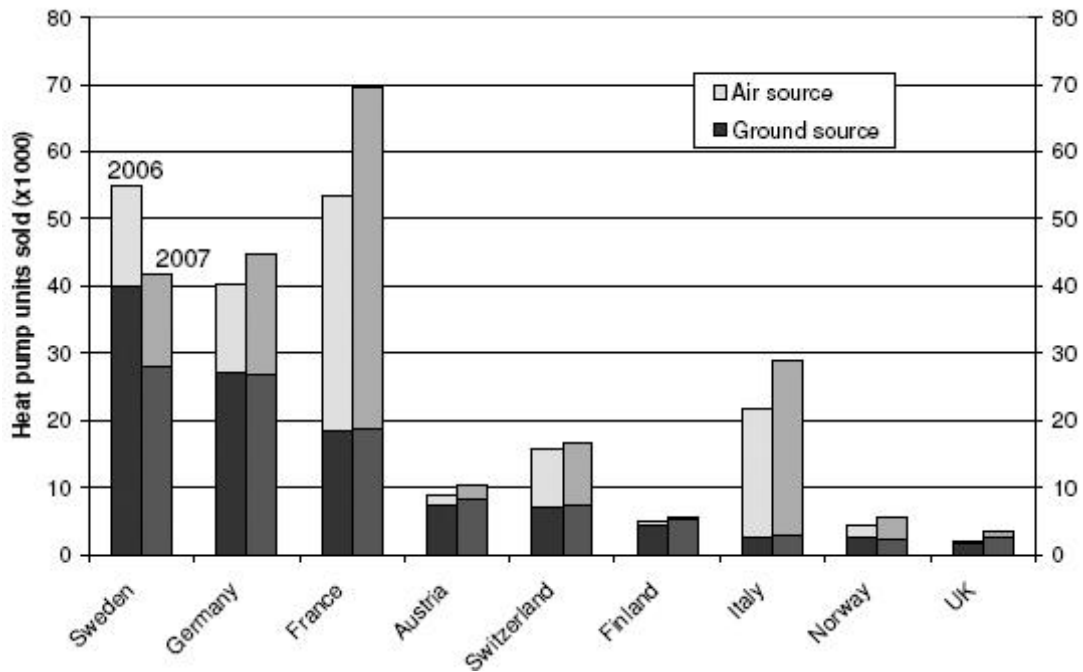


Figure 3-5 Number of heat pumps sold in Europe – after Sanner, 2009

Recent changes in the United Kingdom planning regulations have resulted in a growing interest in geothermal systems. Planning in the United Kingdom has to date been governed by the Part L regulations (conservation of fuel and power, UK government). In addition, there may be specific local requirements that will need to be taken into account depending on the siting of the project. Amendments to the Part L regulations, particularly with respect to the conservation of fuel and power came into effect on 6th of April 2006. These new regulations have placed a greater emphasis on carbon dioxide emissions. Any developer must now show that the annual carbon dioxide emission rate of the completed building, as

calculated using an approved calculation tool, do not exceed the target set by reference to a notional building with the characteristics that match those of the proposed building.

Local planning stipulations may go over and above those stipulated in Part L. For example, the London Plan (2004) states that ‘The Mayor will and boroughs should require major developments to show how the development would generate a proportion of the site’s electricity or heat needs from renewables, wherever feasible’ (Policy4A.9). The Mayor’s Energy Strategy expects 10% of a new development’s energy demand to come from renewable energy generated on site. At this stage this caveat only applies to planning applications which must be referred to the Mayor according to Parts I - IV of the Town and Country Planning (Mayor of London) Order 2000. Examples of major developments to be referred to the Mayor’s office include >500 person dwellings, >30,000 sq m commercial space in the city and >20,000 sq m and >15,000 sq m commercial space in and outside Central London respectively. Each borough is able to define what it considers to be a major development. This policy may or may not be adopted by other parts of the country in the future.

Of note is that the strategy relates to all energy uses of the building and what goes on within it. This includes energy use for heating, hot water, cooling, ventilation, lighting, cooking appliances, computers, lifts, processes, floodlighting, etc., depending on the building type. This is a step further than the Part L requirements.

As the total energy demands of significant new developments in central London are often greater than 5 MW (Arup, 2006) it has proved difficult to find suitable methods of meeting

the 10% reduction target. In central London, where wind turbines are impractical and space is limited for photovoltaic cells there are few possibilities available to developers to meet these targets. As the majority of new buildings proposed for central London have predominant demands for cooling (Arup, 2006), one of the most practical solutions has been to make use of the Chalk aquifer beneath central London as a source of cool water. As discussed previously, a high COP_c can be achieved when using a geothermal system. Indeed, a number of projects have already been constructed in London where the aquifer has been used to cool the building, e.g. Portcullis House and the Greater London Authority (GLA) building with the used water being discharged to the river.

Recent environmental policy (Environment Agency, 2005) regarding the Chalk aquifer stipulates that to maintain groundwater levels, abstraction licenses will only be granted if a significant proportion of the abstracted water is re-injected into the aquifer. This is a recent stipulation and did not apply to Portcullis House or the GLA building mentioned above. The re-injection of water at a different temperature to that at which it is abstracted poses many problems for an open system. The principal concern is the nature of the thermal transport between the abstraction borehole and the injection borehole. Of particular interest is the thermal breakthrough time between the injection and abstraction boreholes at a proposed site and whether the thermal transport is rapid enough to cause short-circuiting between the abstraction and injection boreholes. In addition, the pattern of thermal transport in the aquifer may also cause abstraction boreholes in the vicinity of the proposed system to be affected. If this is the case, how can potential systems best be designed to avoid these issues? There have been a number of cases reported in the literature (Packsoy, 2003, Allen, 1996) where a lack of knowledge about the hydrogeology caused such thermal interference problems to occur. An

understanding of the nature of the thermal transport beneath a site will therefore be important for both the designers of open geothermal systems and the Environment Agency to allow it to legislate and effectively control any adverse affects of such systems.

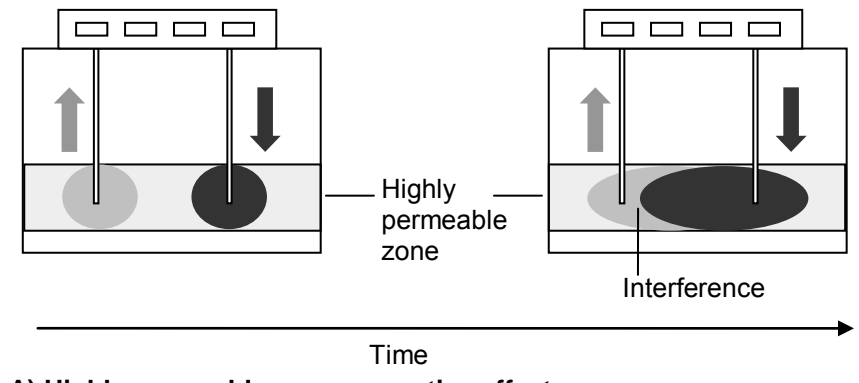
3.3 Basic hydrogeology and geothermal systems

The hydrogeology beneath a site will alter the performance of a geothermal system in a number of ways (Figure 3-6). In general, the hydrogeology affects open systems to a greater extent than closed systems. The majority of potential problems are associated with regions of anomalous flow – that is when the flow within the aquifer does not behave in a uniform manner. This is usually due to fractures or highly permeable zones (Allen, 1996).

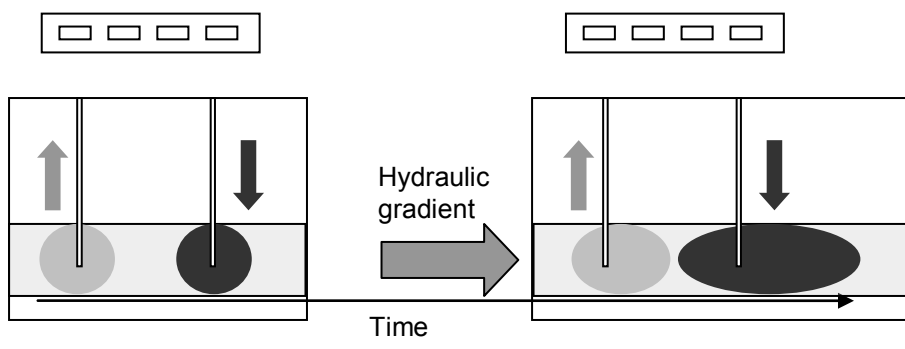
Figure 3-6A highlights the effect of a highly permeable zone upon the performance of an open system. The zone causes two primary problems; the first is that flow between the two boreholes is channelled into a smaller surface area than expected and thus travels at a faster velocity between the abstraction and injection boreholes than would be otherwise expected. The second compounding effect is that the volume of rock exposed to the moving water is reduced by the permeable zone, resulting in a lower thermal storage capacity than an equivalent homogenous medium. The potential for rapid thermal transport between the injection and abstraction borehole is therefore increased.

A highly permeable zone may not necessarily always have a completely negative effect. For the case where the background hydraulic gradient is sufficiently high to overcome the effects of the gradient between the abstraction and injection boreholes (3.3.1) there will be little thermal interference between the two (Figure 3-6 B). In practice however, this rarely occurs.

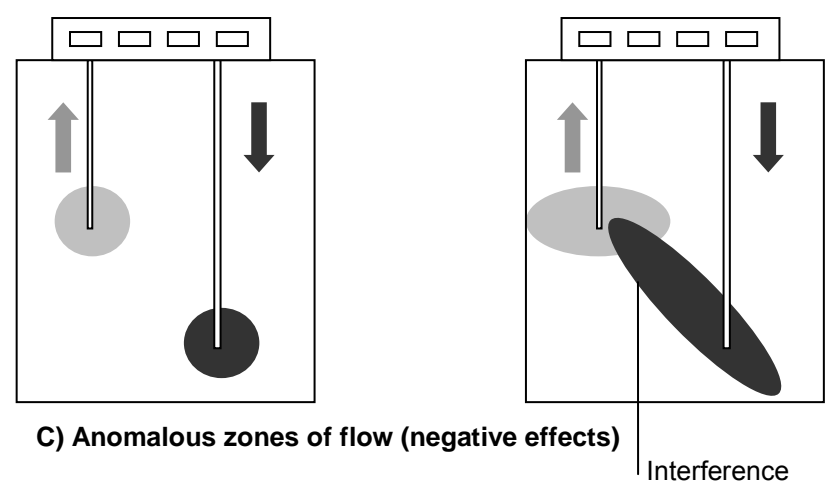
Figure 3-6C shows how the effects of unexpected flow regimes can cause connections between the abstraction and injection boreholes. This sort of connectivity is unlikely in a fractured sedimentary aquifer such as the Chalk but can occur in igneous rocks.



A) Highly permeable zone – negative effects



B) Highly permeable zone – positive effects of a background hydraulic gradient



C) Anomalous zones of flow (negative effects)

Figure 3-6 Hydrogeology and open geothermal systems

For closed systems, hydrogeology is less important. Indeed, closed systems can be situated in almost any geological unit. Abnormalities in the flow regime generally enhance the performance of the system by removing or adding energy to the system at a faster rate than would normally be expected.

3.3.1 Background hydraulic gradient in the Chalk

The typical background hydraulic gradient for the Chalk in central London is in the region of 0.001m/m (Environment Agency, 2005). A medium to large scale new development is likely to occupy a site with a footprint of approximately 100m in length. Therefore, abstraction and injection boreholes will be separated by a maximum of approximately 100m. Within the Chalk, typical drawdowns for a borehole abstraction rate of 15 l/s range from 3 to 5 m (McDonald, 2001). These are matched by equivalent injection heads. The hydraulic head difference expressed as a linear gradient between the injection and abstraction boreholes will therefore lie between 0.06 and 0.1. Thus the flow regime will be dominated by that generated by the injection and abstraction boreholes.

3.3.2 Fracture basics

For an open system, fractures can channel the total flow into an appreciably smaller volume than the total available volume of material between an abstraction and injection borehole. The velocity of the water within these fractures will therefore be greater, quite possibly orders of magnitude greater, (Figure 3-7) than if the water was channeled through the total available volume.

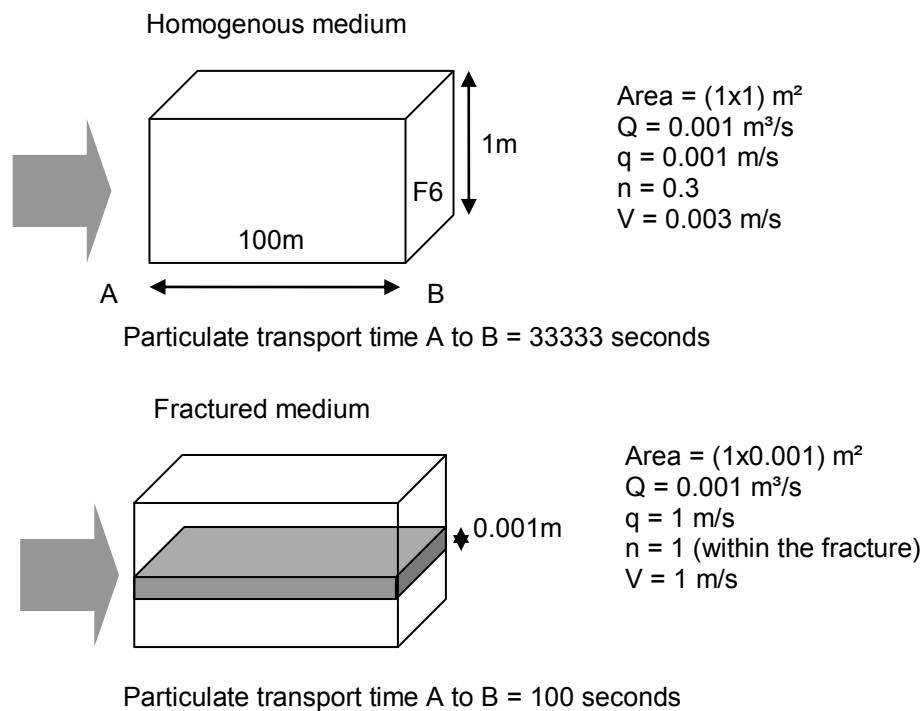


Figure 3-7 Comparing fluid velocities for a homogenous and fractured medium

The difference in calculated transport time does not necessarily represent the thermal transport time, which will be dependent not only upon the velocity of the fluid but also upon the rate at which the material surrounding the fracture can exchange energy with the fluid in the fracture. If the fluid has a low enough velocity and the material surrounding the fracture has a high enough thermal conductivity, it is possible that heat could be removed from the fluid in the fracture at a rate that is at least equal to the rate at which it can be transmitted by convection in the fracture. Therefore, even though the rate of fluid transport through the fracture is more rapid than for a homogenous medium, the movement of the thermal front may be rather similar in the two cases. The thermal transport rate is therefore not only dependent on the velocity of the water but also the thermal conductivity and the thermal storage capacity of the surrounding material. The velocity of the water is in turn dependent upon the nature and size of the fracturing in the material.

3.3.3 Evidence of thermal breakthrough

When this PhD was started there were no data available to corroborate the theory that thermal breakthrough was a potential problem for open geothermal systems in the Chalk aquifer. This was primarily due to very few abstraction and injection systems having been installed, in addition to the lack of any published data on such systems.

During the course of this PhD many open geothermal systems have been installed in the Chalk beneath central London. The majority of the systems were installed without considering how the structure of the Chalk would alter the performance of the system. It was largely thought that the volumes of rock and water involved would be sufficient to dissipate energy away from the site.

Data were obtained from an operational system in 2008 that shows the occurrence of thermal breakthrough. The data presented below (Figure 3-8) are from an abstraction and injection borehole at an operational site in central London. The data points are for July and show the temperature of injection and abstraction. The peaks in abstraction temperature directly correlate to peaks in injection temperature (within 12 to 48 hours). This breakthrough time can only be caused by fracture flow as the velocity of the water (calculated from the system flow rates) would be too slow to reach the abstraction borehole in a homogenous medium. Over the summer period of approximately 3 months, the average temperature in the abstraction borehole increased by 1°C.

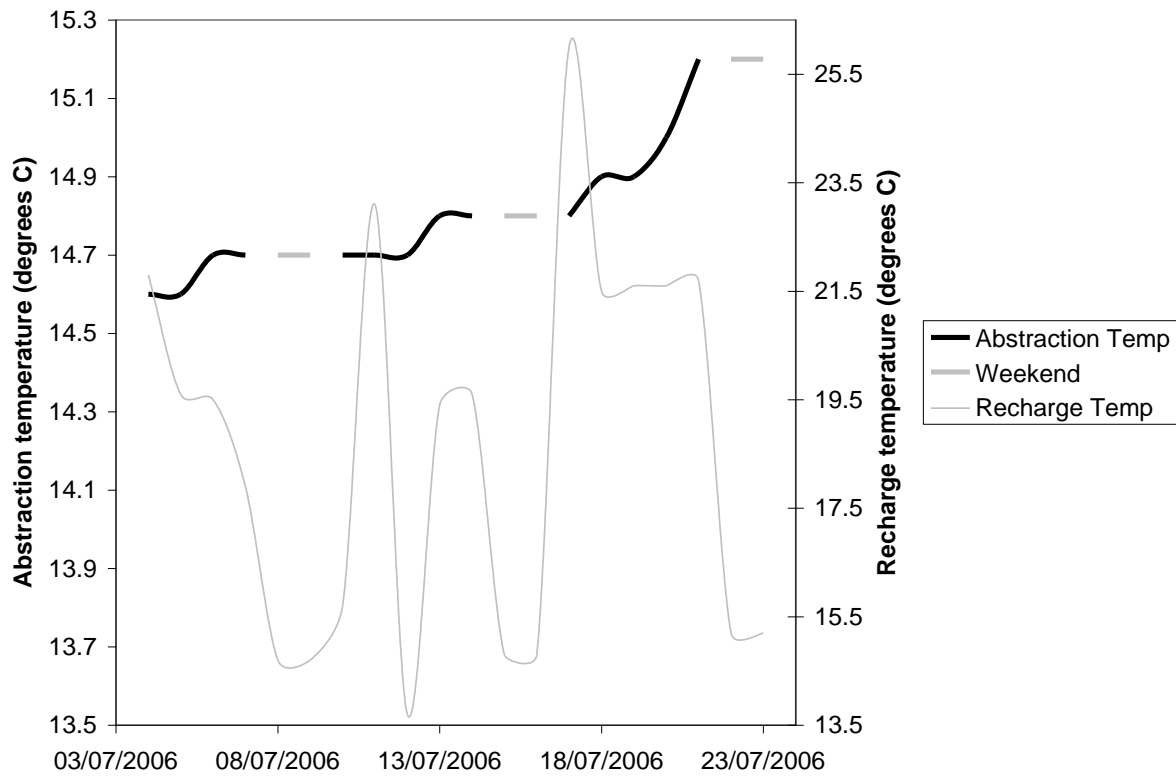


Figure 3-8 Temperature data from an operational geothermal system, London

Clearly there is no imminent danger of this system shutting down due to failure; an abstraction temperature at the end of the summer of 15°C is still a relatively cool source compared to a conventional air source chiller. However, it can be seen that this system is operating with a delta T (difference between abstraction and injection temperature) of approximately 10°C. The current recommended temperature limit for a discharge licence from the Environment Agency is 24°C. With an end of summer temperature (for the first year of operation) of 15°C the system is already unable to operate at its maximum capacity without breaking the discharge license consent.

3.4 Existing research

Although there has been a significant amount of research undertaken on flow within fractured rocks in both the oil industry e.g. Granet (1998), Habei (1990) and water industry e.g. (Becker (2000), Berkowitz (2002) there has not been the equivalent level of research for geothermal systems based in fractured aquifers. Allen (2003 and 2001) has looked specifically into the nature of thermal transport within fractured limestone and the potential for thermal breakthrough between wells. Indeed, she specifically highlights a case of early thermal breakthrough due to rapid thermal transport within fractures. Within the Chalk aquifer in London there has been a paucity of published papers to date on the relationship between a geothermal system and the aquifer. This is partly because the systems are new and little data has yet been made available. Notably over the last two years, namely 2009 and 2010 a small number of papers have been published that relate to geothermal systems and heat flow within aquifers, both of which have been published in the Quarterly Journal of Engineering Geology and Hydrogeology (2009 and 2010). For example, Gropius (2010) examines a number of different techniques for modelling groundwater flow and heat within the Chalk aquifer. Although this is a useful discussion on potential numerical codes it does not address the variability of the Chalk between sites and the important need for accurate hydrogeological data from a site in order for the numerical model to be fully validated. Clarkson et al (2009) present a very interesting case of a long term heat injection test into the Chalk beneath the Royal Festival Hall which shows the actual nature of heat flow between an injection and abstraction well. In this case the heat injected into the aquifer did not appear to travel unduly rapidly between the two wells, implying that fracture flow is not of overwhelming concern at the site. However, an important caveat is that the flow rate in this particular test was relatively low (<10l/s) and the distance between the wells relatively large (>100m) at the site.

The data presented thus far presented has definitely added to the knowledge base and it would be extremely useful if more data on operational sites were to be published and investigated in the forthcoming years. This would help to show the extent to which the Chalk varies beneath sites and how this impacts upon system performance.

4 THE GEOLOGY OF LONDON

Much research has been carried out on the geology of London and it is not proposed to repeat this work in its entirety in this thesis. This Chapter therefore summarises some of the key lithologies and geological events that have been instrumental in shaping (both literally and metaphorically) the development of London. The London district (which broadly encompasses the area of interest for this PhD) is covered by the British Geological Survey sheets 256, 257, 270 and 271 and is approximately contained by the M25 circular motorway.

4.1 Research history

The first geological survey of the district was carried out by Whitaker and others between 1861 and 1868 with the results being published in the first memoir of the district (Whitaker, 1872). Drift and superficial deposits were mapped later in a revised memoir (Whitaker, 1889). Large scale (1:10560) mapping was completed in 1922 based on geological work by Bromehead, Dines, Edmunds and Dewey with corresponding memoirs: Bromehead (1925), Dines and Edmunds (1925), Dewey and Bromehead (1921) and Dewey et al (1924). A partial resurvey of this data was made by Lawson and Moorlock in south London from 1973 to 1980. In 1992, a new project known as LOCUS (London Computerised Underground and Surface) was initiated to produce digital 1:10000 scale maps of the district and 3 dimensional models of the geology of London (Ellison et al, 1993). The most recent review of the current geological knowledge was published by the British Geological Survey in 2004 (Ellison et al, 2004).

4.2 Geological History

In early Palaeozoic times most of the district consisted of crystalline basement rocks of Neoproterozoic age overlain by a relatively thin cover (>3km) of early Proterozoic strata. The Palaeozoic cover rocks were deformed in early Devonian times by the Acadian phase of the Caledonide orogeny (Soper et al, 1987). The succeeding middle and late Devonian strata (mainly non-marine clastic sedimentary rocks) rest unconformably on the strata of the Arcadian fold belt. During Carboniferous times, the Devonian succession became part of a new stable high (Anglo-Brabant massif). Throughout much of the Mesozoic, the district continued to be a stable upland, now known as the London Platform. During the latter part of the Jurassic and early part of the Cretaceous, intense tectonic activity occurred in Europe, causing the gradual opening of the North Atlantic, uplift of the London district and extensive erosion of the Jurassic strata. However, in the early Aptian, the sea once again flooded the London basin depositing shallow marine sediments, beginning with the Lower Greensand Group and culminating with the deposition of the Gault and Chalk during a prolonged period of high sea level. For about 40 million years, between the late Eocene and Quaternary, the district was land, and pre-existing deposits were weathered and dissected. Rivers also flowed from the south and south-west towards a major river (the precursor to the Thames). About half a million years ago ice sheets advanced and altered the course of the river system and the Thames was diverted to its present day valley. The succeeding river deposits are well preserved. The most recent deposits (river alluvium and tidal river sediments), have been deposited in the last 8,000 years or so, during an interval of relatively low river discharge and periodic flooding.

4.3 Quaternary

Quaternary (drift or superficial deposits) were laid down in the London district during the last 1.65 million years or so and describe a river system that was a precursor to the river Thames. The chronology of the principal Quaternary deposits is shown in Figure 4-1. Also shown are oxygen isotope stages which have been tentatively related to climatic oscillations (Sumbler 1996).

The gravels are composed mostly of flints derived from the chalk and flint-pebbles from the Eocene deposits. The matrix of sand varies in the degree of its coarseness and the whole deposit may be between 9 and 12 metres in original thickness. Where the alluvial capping has not been subsequently removed by erosion or human activity it can reach a thickness of 6 metres or more and is a reddish-brown loamy clay. (This deposit was used in the Roman and subsequent historical periods as the raw material for brick making and has come to be known as "brickearth".)

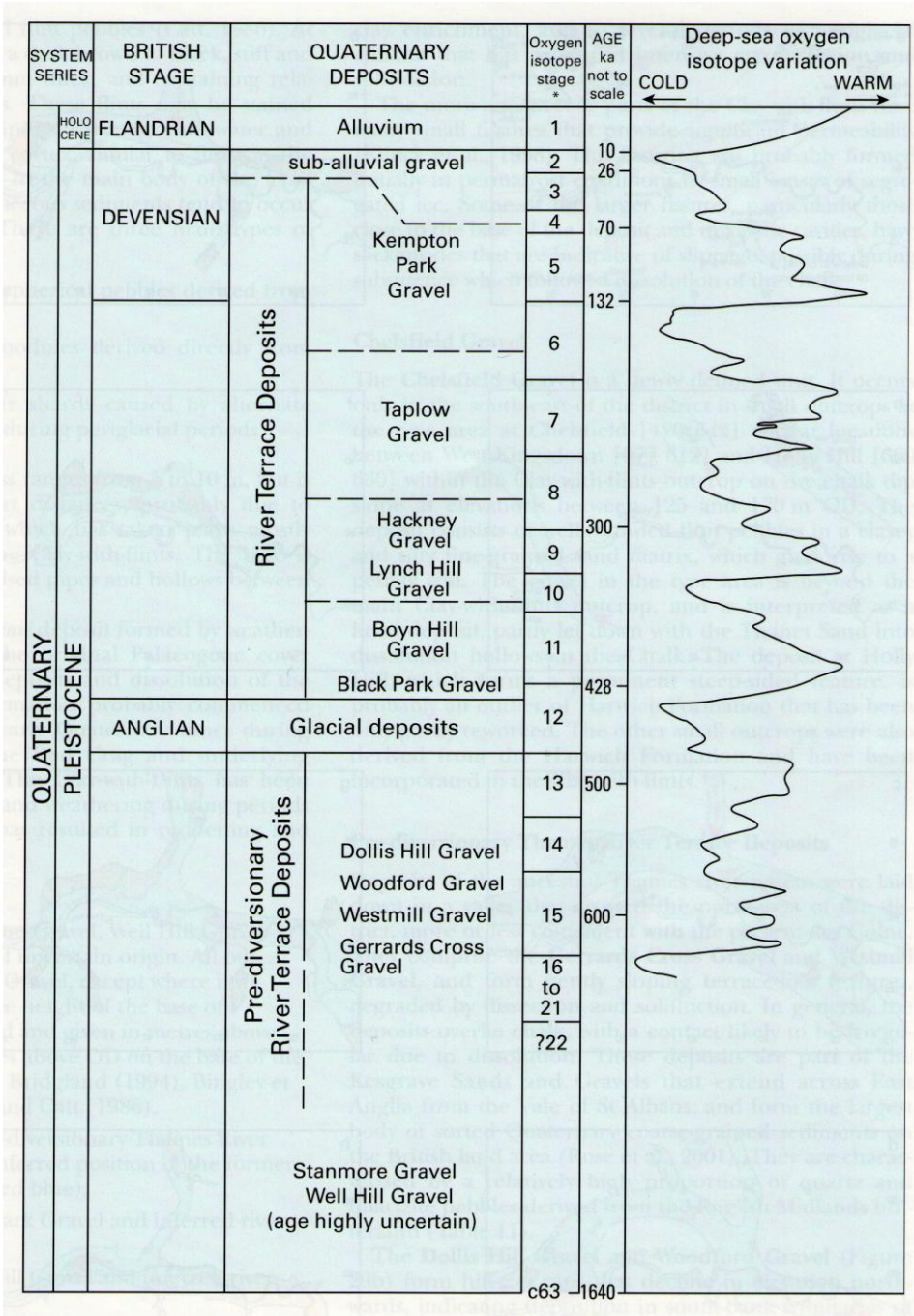


Figure 4-1 Chronology of principal Quaternary deposits and oxygen isotope stages (Sumbler, 1996) after Ellison, 2004.

4.4 Palaeogene-Eocene

This period is dominated by what is now known as the London Clay formation. Deposited in a tropical sea, it is a stiff, dark or bluish-grey clay which weathers to brown. As the name implies, the deposit is largely argillaceous and about 60% of the formation consists of bioturbated, slightly calcareous, silty clay to very silty clay. Although other lithologies are known to be present, notably calcareous concretions ('septarian nodules') within the London Clay, silcrete horizons in the Reading Beds (e.g. 'sarsens' and 'Hertfordshire Pudding Stone') and calcite cemented layers within the Woolwich Beds, their outcrops are too restricted to be reliably recorded. The main mass of the London Clay has been provisionally divided into 5 units by Ellison (2004). However, the boundaries between the units are gradational and are not clearly differentiated by gamma-ray logs. Further detail on these units can be found in the descriptions by Ellison (2004).

There is considerable variation in thickness in the London Clay. The maximum of 130 metres (430 feet) is seen at Wimbledon, Esher and Brentwood and on the north side it is about 106 metres (350 feet) at Highgate. In the centre, there has been considerable erosion so that it is between 26 and 40 metres (85 and 130 feet) in the City and only 19 metres (63 feet) in Tottenham Court Road (Davis, 1958). The formation has had an important influence on the development of the London infrastructure as it is a relatively homogenous and easy tunneling medium. It also gives rise to the relatively subdued topography in the Thames Valley.

4.5 Palaeogene-Paleocene

At the beginning of the Palaeogene time the London district lay on the edge of a sedimentary basin that included much of the present North Sea and extended eastwards, at least as far as Poland. To the West was the proto-Atlantic ocean. The Palaeogene deposits were laid down during alternating transgressions and regressions, driven by global sea level changes. The importance of understanding these units became apparent in the early 1970s, with the discovery of oil bearing strata of this age beneath the North Sea. The understanding of these units has also played a significant role in the development of major infrastructure projects in London. The most important lithographic units are shown in Figure 4-2.

The Thanet Sand formation is the oldest Palaeogene deposit in the London district. The base of this unit is unconformable on the eroded surface of the Chalk group. This unconformity is not caused by a single event but is attributable to erosion during reworking during two or more depositional sequences (Knox, 1996). The bulk of this unit is a coarsening-upward sequence of fine-grained sand (clayey and silty in the lower beds). Faint bedding planes can be seen but in general the sediments are intensely bioturbated.

The formal term Lambeth Group has been adopted in recent years (Ellison et al, 1994) to replace the Woolwich and Reading Beds of earlier authors. The group is divided into three formations and several informal units (Figure 4-2) and (Figure 4-3)

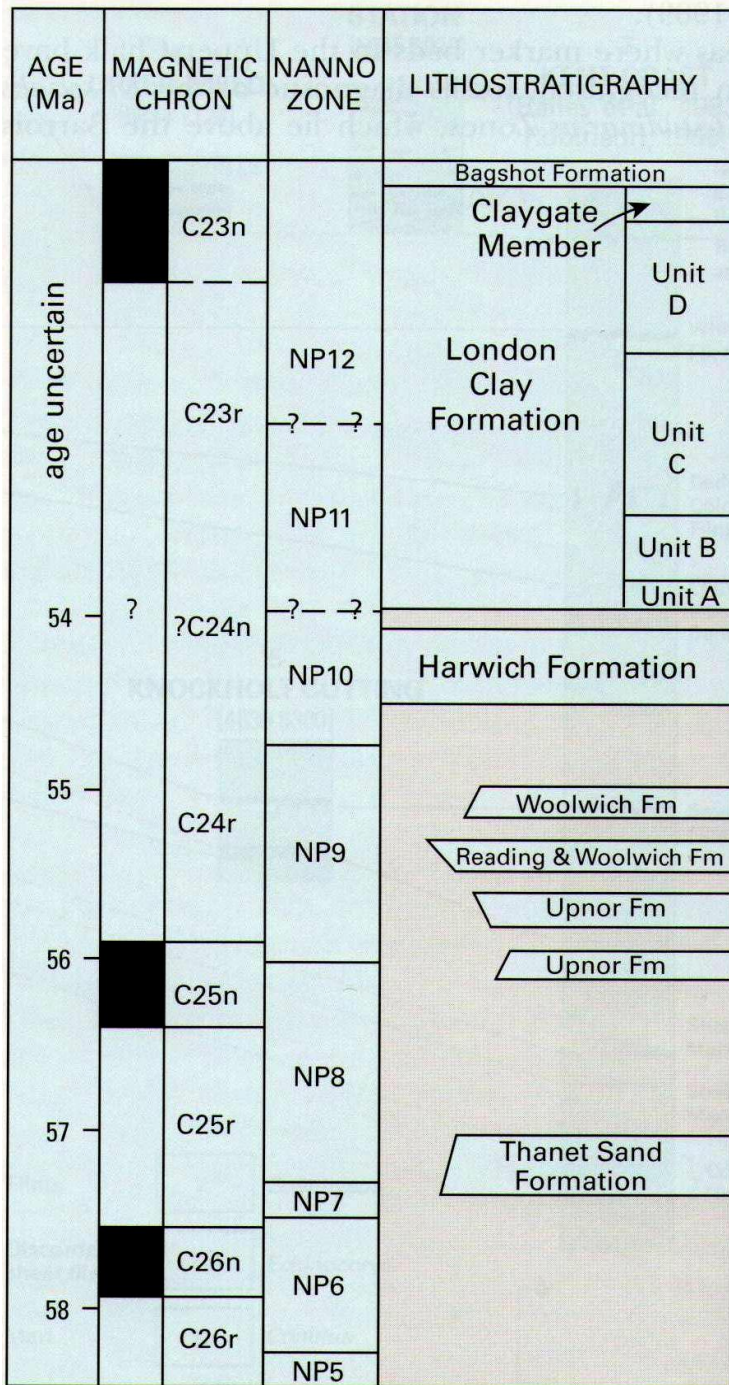


Figure 4-2 Palaeogene lithostratigraphy and chronology (after Knox, 1996)

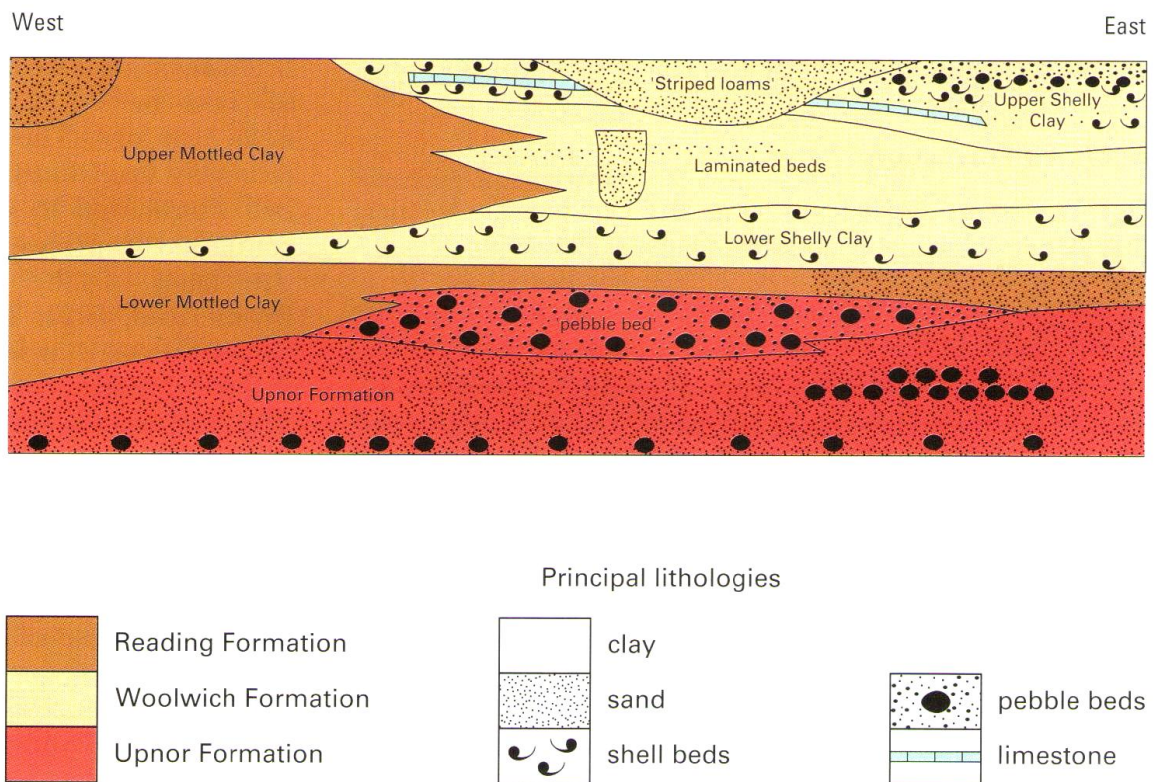


Figure 4-3 Schematic diagram showing the relationship between the informal lithological units in the Lambeth Group in central London (after Ellison, 2004)

The Upnor formation is present everywhere at the base of the Lambeth Group and sits unconformably on the Thanet Sand. It is a coarser grained sand than the Thanet Sand and is normally completely bioturbated. Pebble dominated units occur principally at the base and the top of the formation.

The Reading Formation rests on the Upnor Formation in the centre of the district and passes laterally into the Woolwich formation (a predominantly dark grey to black clay with abundant shells) in the central and south eastern outcrops of the Lambeth Group. The bulk of the formation consists of unbedded, colour mottled (pale brown, pale grey blue, dark brown, pale green and crimson) silty clay and clay.

The Harwich Formation was termed by Ellison et al (1994) to include sediments between the Lambeth Group and the London Clay formation. The unit has a sharply defined base and consists predominantly of fine grained sand and pebble beds of rounded black flints.

The main geological units and thicknesses of relevance to all geothermal systems are summarised in Table 4-1. The Chalk, which is the main aquifer beneath London, is used for both water abstraction and energy abstraction for open loop systems. It is therefore the most relevant unit for this PhD and is described in more detail in the subsequent Chapter.

Period	Stratigraphic Unit	Lithology	Thickness (m)
Recent and Pleistocene	Fill	Variable including man made debris	Up to 5
	Alluvium	Soft silt and clay with lenses of sand and gravel, some peat.	Up to 12. Generally 1 to 3
	Fluvioglacial (‘Terrace’ Gravel)	Generally loose sand and gravel	1 to 12
	Till (‘Boulder Clay’)	Stiff silty clay with sand and gravel fragments	Up to 12
Eocene	London Clay	Predominantly a firm to very stiff fissured dark blue/brown/grey silty Clay. Upper part is weathered and mottled orange/brown in colour at surface. Unweathered material locally contains vertical variations in particle size with occasional water bearing sand partings and claystone bands present	60 to 150

Period	Stratigraphic Unit	Lithology	Thickness (m)
	Lambeth Group (formerly Woolwich and Reading beds and Upnor Formation)	Highly variable material deposited in a series of layers in a marine environment. Undifferentiated pattern apart from upper beds being predominantly clayey and lower beds being predominantly sandy. Group generally comprises the following interbedded cohesive/granular units (after Skipper 2001): Upper Shelly Clay (USC) - laminated silt, sand, clays and shell beds; Lower Shelly Clay (LSC) - laminated clays with shells and silt/sand lignites; Upper Mottled Clay (UMC) - mottled clays, silts, sands and fluvial sands; Lower Mottled Clay (LMC) - mottled sands, clays and pebble beds Upnor Formations (UF) - pebbly beds, glauconitic sand with some conglomerate and clay matrix	Up to 50
	Thanet Sand	Relatively uniform sequence of silty sand (fine to medium grading).	Up to 30
Cretaceous	Chalk	Moderately weak porous very fine-grained limestone. Contains bands of gravel and cobble-sized masses of hard flint	Up to 200

Table 4-1 Geological units of relevance to geothermal systems (open or closed) in London (Arup, 2006)

5 THE CHALK

There is a significant amount of published material relating to the Chalk. A summary of properties, in particular permeability and transmissivity, is presented here.

Chalk as a deposit can be traced within continental Europe. It continues westwards from northern Germany and Denmark, to the British Isles where it outcrops in eastern and south eastern England, Ireland and small areas of Scotland. An extensive part of the North Sea is floored by chalk where deposition continued into lower Tertiary or Danian times. In central and southern Europe, Upper Cretaceous strata are represented by limestones within the Alpine mountain belt. Eastwards from Poland, chalk extends to the northern slopes of the Caucasus, with extensions to the Black Sea, Iraq, the Caspian Sea and south western Siberia.

Chalk is predominantly a soft, white biomicrite formation that accumulated under temperate to warm marine conditions in which water depths probably did not exceed 500 m. The outcrop within England is shown in Figure 5-1. The thickness of this unit displays considerable variation which, in part, reflects differences in the amount originally deposited but the effects of subsequent erosion are also important. The formation achieves its greatest thickness in England in Norfolk where, in some locations, it exceeds 400 m. It is generally a remarkably pure limestone, excluding flints and marl bands (Figure 5-2), the calcium carbonate content of the white chalk facies of England generally exceeds 98% and it does not usually fall below 96%. With the exception of southern England, which was affected significantly by Alpine tectonism, there is little evidence of compressional crushing of microfossils.

Consequently, the unit often retains a high porosity which is attributable to its predominantly fossil constituents, notably coccoliths (Bell et al., 1999).

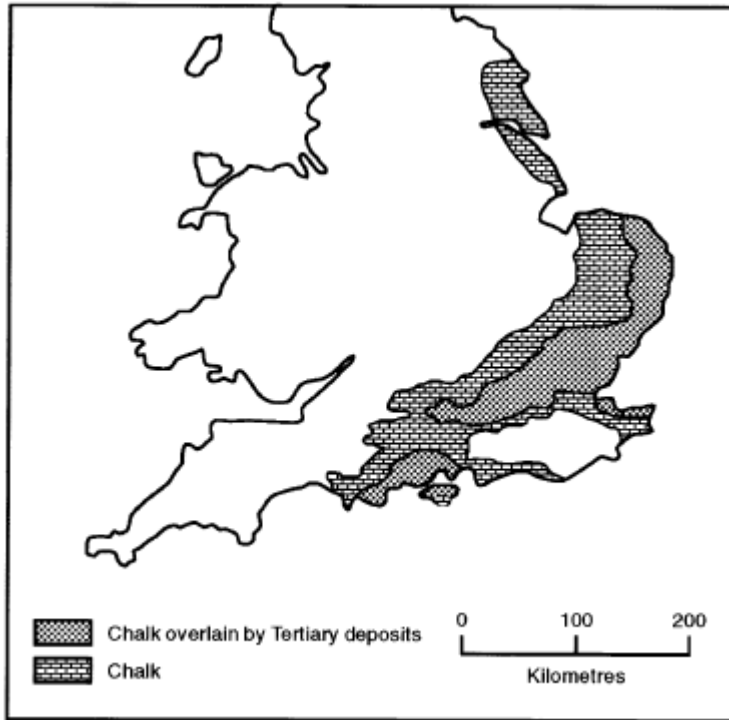


Figure 5-1 Sketch map of the extent of Chalk in England after Bell et al (1999)

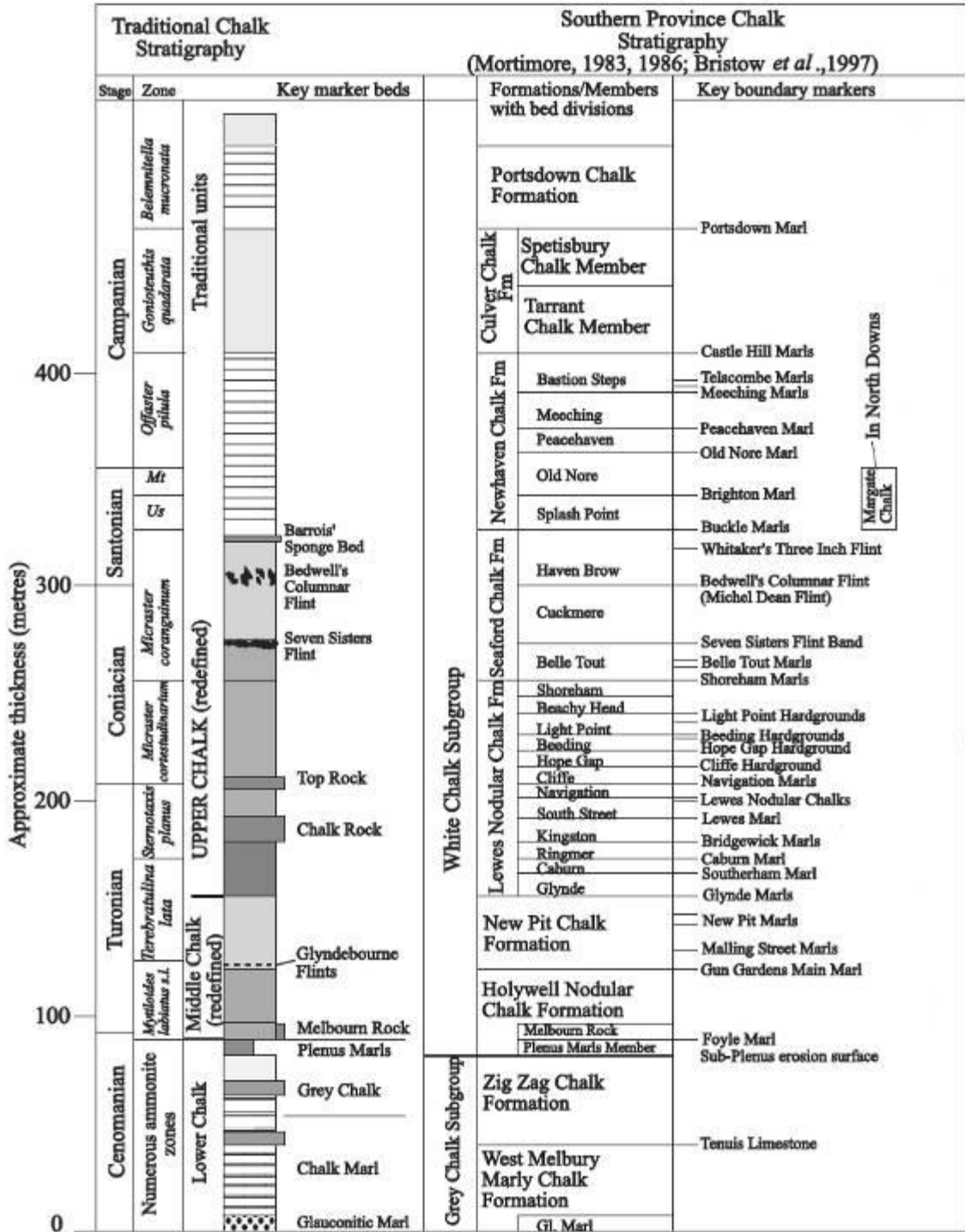


Figure 5-2 Typical stratigraphy of the Chalk after Mortimore 1983,1986.

5.1 Chalk matrix

Scholle (1977) pointed out that chalk may be deposited with as much as 70–80% porosity. Approximately half this pore space is lost by dewatering during the first tens to hundreds of metres of burial. Later diagenetic processes during consolidation and cementation can reduce this porosity to a value of <5%, although the average porosity is between 25 and 40%.

Although the matrix, porosity and permeability are crudely related, the hydrogeological properties are strongly dependent on fissures. Of particular significance are the shape, size and distribution of, and connections between, pores. In turn, these features are controlled by the grain size distribution, arrangement and packing of grains, as well as the presence of authigenic minerals.

Some of the highest values of porosity have been found in the samples of Upper Chalk from Kent and Norfolk where the porosity at times exceeded 40%, averaging above 35% (Bell et al., 1990). The average value of porosity of samples from Yorkshire tend to be <25%, and tends to be more uniform than in south east England. In the case of the North Sea, that is, Ekofisk Chalk, very high primary porosities of around 40% have been maintained, possibly due to the inhibiting of diagenetic cementation by hydrocarbon ingress.

5.2 Discontinuities and fracturing

Chalk is a material in which the mass hydrogeological and mechanical behaviour is largely controlled by fissure flow. The spacing, orientation, persistence and character of these features are all important controlling factors. The discontinuities in chalk

range in scale from microscopic grain boundaries and microfractures to major tectonic joint and fault structures. A complete appreciation of the hydrological and mechanical behaviour of chalk is possible only if the discontinuities are taken into account.

Price (1987) indicated that most of the English chalk is affected by three approximately orthogonal sets of joints, one of which is nearly parallel to the bedding. Near the surface in unweathered chalk at Mundford, Norfolk, the joints were approximately 0.2 m apart (Ward et al., 1968). In the South Downs of Sussex, Mortimore et al. (1996) found that in chalk with marl seams a high angle (60–70 degrees) conjugate fracture set was characteristic, whereas in homogeneous chalk without marl seams, vertical joint sets were typical. By contrast, at South Killingholme, South Humberside, between Norfolk and Yorkshire, at depths of 180–190 m, vertical fractures were several metres apart (Lake, 1990). On the other hand at this site, fracture spacings in vertical cores averaged five per metre, compared with four per metre in the Lower Chalk of the Channel Tunnel (Price, 1996).

Mortimore et al. (1990a) described the frequency of discontinuities and their tightness. Patsoules and Cripps (1990) studied the orientations of joints at various locations along the Flamborough coast from Sewerby to Little Thornwick Bay. These data provided a comprehensive and quantitative picture of the joint patterns that occur in these coastal exposures. In addition, the spacing data were obtained from five linear, horizontal scan lines measured on the Flamborough coast in east Yorkshire. The distribution obtained was similar to that obtained by Priest (1975) for the Lower Chalk at Chinnor, Oxfordshire. The results implied that the joints may be divided into the following sets:

“Set 1 (100–130°): joints with this orientation coincide with the orientation of the Westphalian - A (Carboniferous) uplift across Yorkshire. It seems likely that these joints have been formed by a reactivation of this structure. Set 2 (130–175°): joints belonging to this set are probably associated with a group of 130–160° trending faults identified by Glennie and Boegner (1981). Set 3 (175–190°): this group constitutes only a small proportion of the total discontinuities along the Flamborough Coast and inland locations. They probably reflect late Cretaceous and early Eocene subsidence of the North Sea central graben. Set 4 (10–65°): joints belonging to this set are associated with the Selwicks Bay contorted belt. Set 5 (65–100°): these joints have similar orientations to the major deformed belts in the Yorkshire Chalk and they correspond with faults that Glennie and Boegner (1998) suggested are responsible for the Cleveland Hills and Market Weighton structures. The set may be subdivided into a 65–80° subgroup which parallels the WSW-ENE contorted zones and an 80–199° subgroup associated with the Market Weighton structure, a positive area in Jurassic and early Cretaceous times with a trend that varied between WSW-ENE and WNWESE (Kent, 1980).” Priest (1975)

Similar trends to these were reported by Duval (1990) for jointing in the Ekofisk area of the North Sea.

5.3 Permeability and transmissivity

Although chalk has a high porosity, when the values are compared with intergranular permeability as obtained from laboratory testing, the two are poorly correlated. The reason for the poor relationship between porosity and permeability is the small size of

the pores and more particularly that of the interconnecting throat areas. Price (1987) showed from mercury porosimeter testing that the median throat diameters are smaller in chalk from the north of England than in those from the south. Owing to the operation of capillary and molecular forces, drainage of the 'larger' pores (according to Price their median diameter is approximately 5 μm) via such throats will not occur unless a suction of the order of 30 m head of water (300 kPa) is applied. Since gravitational drainage represents a suction of approximately 10 m, chalk has a very high specific retention.

Tests on samples of Upper Chalk from Yorkshire reported by Patsoules and Cripps (1982) indicated that permeability decreased with increases in confining pressure but it was more sensitive to changes in pore water pressure. In tests in which a constant confining pressure of 15 bars (1.5 MPa) was used, a relatively small increase in pore water pressure of 5 bar caused a large increase in permeability from values of about 2×10^{-9} m/s to ca. 5×10^{-9} m/s, a change of ca. 6×10^{-10} m/s per bar. On the other hand, for a constant pore water pressure of 4 bar, the permeability was reduced from a value of ca. 2×10^{-9} to ca. 1×10^{-9} m/s when the confining pressure was greatly increased from 15 to 250 or 300 bars. In this case the change in permeability expressed as a function of pressure change was 4×10^{-12} m/s per bar. Removal of the confining pressure did not result in complete recovery of the permeability to its former values since the high confining pressure had apparently brought about permanent structural modification to the chalk matrix. This included calcite dissolution and precipitation, grain deformation and material breakage.

A formation with fluid flow properties as characterised by the above values could not produce the groundwater yields that are normally encountered in the aquifer, it being the most important aquifer in England and also a significant source of hydrocarbons in the North Sea. Price (1987) pointed out that if chalk only possessed intergranular and primary fissure component permeabilities, then its transmissivity would be approximately 20m²/day or less, yet the yields of some larger wells indicate transmissivities in excess of 2000 m²/day. Hence, secondary fissures, enlarged by solution, are the features which produce the high permeabilities found in many areas. Toynton (1983) also showed that the transmissivities in Norfolk varied considerably according to the orientation of the discontinuity pattern. In addition, evidence is available that indicates primary fissures close with depth. For instance, investigations for an underground chamber at South Killingholme, Humberside, showed that at 180–190 m below the surface minor joints are closed by secondary calcite and the in situ permeabilities for the bulk were around 1.1×10^{-8} m/s.

Foster and Crease (1975), for example, maintained that the Chalk of east Yorkshire is a fissure flow, and largely fissure storage, formation with horizontal permeability in horizontal flow zones in the range 2×10^{-5} to 2×10^{-6} m/s. They suggested that under natural hydraulic gradients the velocities of through flow to discharge areas vary from 1×10^{-5} to 5×10^{-5} m/s.

A comprehensive study of existing borehole data was undertaken by McDonald (2001). Aquifer properties from over 2000 pumping tests in the Chalk were collated as part of a project undertaken by both the British Geological Survey and the Environment Agency. The median of the available data for transmissivity is 540 m²/

day with the 25th and 75th percentiles at 190 m²/ day and 1500 m²/ day respectively. Transmissivity is highest in the harder chalk of Yorkshire and Lincolnshire (median 1800 m²/ day). Throughout much of the aquifer a direct relationship is seen between transmissivity and storage co-efficient reflecting the importance of fractures in governing both storage and transmissivity. Pumping tests undertaken in unconfined areas consistently give higher values of transmissivity than those in confined areas probably as a direct result of dissolution enhancement of fractures in unconfined areas.

Area	Code	No. of localities	No. of tests	Transmissivity (m ² /d)			No. of tests	Storage coefficient		
				Median	25%	75%		Median	25%	75%
Dorset	Do	41	52	985	150	2580	27	0.0052	0.0020	0.016
Salisbury Plain	SP	13	23	1600	450	3300	22	0.01	0.001	0.016
Hampshire	Ha	29	63	2600	840	6100	53	0.009	0.005	0.017
South Downs	SD	28	45	440	230	1600	22	0.0022	0.00061	0.004
Kennet Valley	KV	74	117	830	380	1500	107	0.0075	0.004	0.017
Chilterns	Ch	44	62	860	276	2100	44	0.0029	0.0008	0.028
Thames	Th	81	88	230	44	990	41	0.0024	0.0004	0.0047
North Downs	ND	41	57	670	350	1600	35	0.0036	0.001	0.015
Hertfordshire	He	19	23	580	160	1000	23	0.004	0.0016	0.023
Cambridgeshire	Ca	81	125	800	323	1500	80	0.0058	0.0011	0.012
West Suffolk	WS	194	256	780	302	1750	134	0.0035	0.00087	0.011
West Norfolk	WN	40	45	1000	169	1880	22	0.004	0.002	0.0067
East Norfolk	EN	337	454	250	101	761	205	0.0022	0.00047	0.0078
East Suffolk	ES	84	110	315	69	868	61	0.0025	0.00093	0.011
North Essex	NE	207	415	400	180	1100	160	0.0013	0.0005	0.0037
Yorkshire	Y	68	87	1250	500	5970	28	0.005	0.0015	0.018
Lincolnshire	L	42	55	1640	895	3750	47	0.00023	0.000052	0.0023

	Transmissivity (m ² /d)			Storage coefficient		
	Confined	Semi-confined	Unconfined	Confined	Semi-confined	Unconfined
No. of tests	328	194	415	182	137	286
Median	217	279	923	0.00064	0.002	0.008
25 percentile	66	115	310	0.00027	0.00061	0.0028
75 percentile	620	720	2250	0.0035	0.011	0.017

Table 5-1 Transmissivity in the Chalk aquifer after McDonald, 2001

Transmissivity measurements also show a distinct difference between confined and unconfined pumping tests. Unconfined tests have an interquartile range of 310 to 2250 m²/ day (median 920 m²/ day), while confined tests have an interquartile of 66 to 620 m²/ day (median 220 m²/ day). Semi-confined measurements of transmissivity were marginally higher than those measured under confined conditions: interquartile range 115 to 720 m²/ day (median 280 m²/ day). These data indicate that transmissivity is significantly more developed in unconfined chalk than in confined or semi-confined chalk. This also helps to explain the regional trends detailed in Table 5-1. The areas with the lowest measurements of transmissivity (East Norfolk, East Suffolk and London) are also the areas where chalk is most heavily confined. Since transmissivity is largely governed by solution enhanced fractures, it is logical to conclude that in the confined (and probably semi-confined) areas of the aquifer, the solution enhancement of fractures has not developed to the same extent.

These data agree with Hiscock & Lloyd's (1992) study of permeability development in areas overlain by thick drift. They show that significant permeability development probably took place in the last 5000 years; however in areas covered by thick drift, or confined by younger deposits, permeability would not have been significantly enhanced. The origin of the solution enhanced fractures observed in deeply confined chalk is unclear. They may have developed in Eocene times, and enhanced with groundwater flow during glacial periods; slow groundwater flux may also help to enhance permeability. Local development of solution enhanced fractures may be related to discrete outlets through the confining cover. Some of these may have operated to greater effect during periods of lower sea level and glaciation.

5.4 Fracture geometry

It has been shown by Bloomfield (1996) that the structure of the Chalk can be observed to be made up of blocks of matrix defined by approximately parallel bedding planes (Figure 5-3). This was also observed by Price (1987).

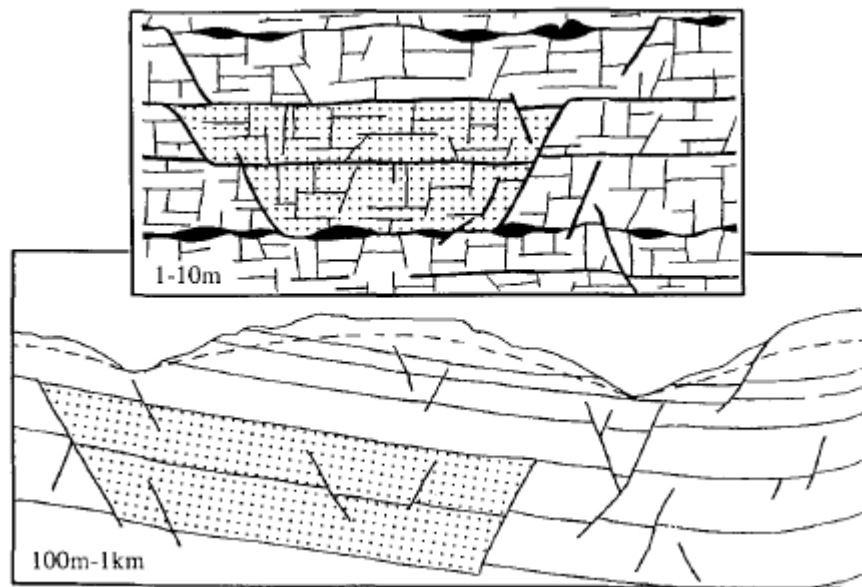


Figure 5-3 Conceptual model of fracture systems in the Chalk (after Bloomfield, 1996)

Although it is the case that these horizontal planes will have been subjected to some degree of tectonic disturbance they can still be observed in many outcrops (McDonald, 2001). The extent to which they remain in the horizontal plane will depend on the location of the observer and the extent to which the unit is folded. In the figure above, the planar features could be said to be dipping either toward the right of the image or to the left of the image depending on the position of the observer. However, it would seem fair to say that the major bedding plane features would be parallel, whatever position the observer occupied.

Summary

The range in transmissivity values of the Chalk (due to fissure flow) indicates the difficulties associated with predicting transport pathways. The structure of the Chalk and thus the transmissivity may vary between closely spaced locations affecting both borehole yields and by inference thermal transport. Predicting in advance, with any degree of accuracy, the expected flow rates for a borehole sited in the Chalk cannot be accomplished through literature research alone.

6 FRACTURE FLOW AND MODELS

Groundwater flow within the Chalk has been shown to be governed by fractures. Fracture flow has been the topic of much research and discussion in hydrogeology as it occurs in many different rock types. The main research fields in 2009 are those related to understanding how fracture flow affects leakage from long term nuclear storage plants and leakage of carbon dioxide from potential carbon storage reservoirs. Owing to the small scale changes in fracture orientation, structure and aperture, understanding and modelling fracture flow has proved to be difficult in all rock types. A number of different approaches to representing fracture flow have been developed and the most common methods, including their limitations are discussed below.

6.1 Treatment of single fractures

The starting point for a model of a fractured aquifer or reservoir has to be the representation of a single fracture. The most common approach to this has been to treat the fracture as a highly porous medium bounded by a pair of smooth parallel plates. This is the classical interpretation of a fracture, although it has been shown by both experimental (Pyrak-Nolte, 1987, Keller, 1995, Vandergraaf, 1995) and field studies (Rasmuson, 1986, Novakowski, 1995, Raven, 1988) not to be adequate for the description of flow. However, although more advanced conceptual models have been introduced in recent years (Berkowitz, 2002) a widely adopted alternative model for a single fracture has yet to be generally accepted.

One of the main stumbling blocks to the parallel plate model is the representation of the anisotropy of fracture wall roughness and its effects on flow. It has been

demonstrated (Meheust, 2001) that the orientation of the hydraulic gradient (relative to heterogeneities in wall roughness), can either enhance or inhibit flow in comparison to a parallel plate model. In addition, considering different aperture distributions with the same (measured) scale invariance property, these authors also quantify statistically how this phenomenon leads to a large variability in the fracture conductivity. In addition, fracture roughness affects the validity of the cubic law, which is a key feature in fracture flow conceptual models. The cubic law (Eq 6-1) states that the volumetric flow through a fracture varies as the cube of the fracture aperture. This then affects the velocity of the fluid:

$$v_x = \frac{b^2 \rho g}{12\mu} \frac{\partial h}{\partial x}$$

Eq 6-1

where:

v_x	Fluid velocity [m/s]
b	Fracture aperture [m]
ρ	Fluid density [kg/m ³]
g	Gravity [m/s ²]
μ	Viscosity [kg/m°C]

The definition of fracture aperture and the application of the cubic law affects quantitative analyses and interpretation of laboratory and field measurements on flow in fractures.

The extent to which the cubic law is adapted to rough geometries remains an unanswered question. Some recent simulations (Mourzenko, 1995, Brown, 1995) have suggested that the cubic law assumption might be incorrect in many cases. Even if the cubic law is accurate, it is not entirely clear how the aperture to be used should be measured. The general assumption is that the aperture should be measured orthogonally to the fracture plane but this definition becomes difficult when both surfaces of the fracture are significantly inclined relative to the global fracture plane. Alternatively, the aperture can be taken as being normal to the orientation of the centre line in the flow direction (Ge, 1997) or drawing a sphere around each point on the centre line and increasing the sphere until it touches both walls (Mourzenko, 1995)

The problem of trying to estimate flow velocities stems in part from a lack of knowledge of the actual flow fields in fractures. To try and improve the understanding of flow fields, nuclear magnetic resonance imaging (NMRI) has been used to directly and non-invasively measure flow patterns in natural, rough walled rock fractures (Dijk, 1999). Flow patterns were determined from 3D water density and flow velocity images. In contrast to the cubic law, which assumes parabolic and symmetric velocity profiles, the data showed asymmetry within the measured parabolic velocity profiles. Fracture wall roughness also accounts for flow channeling within individual fractures. Up to 90% of fluid flow has been observed to occur through 5-20% of the fracture exit plane (Rasmuson, 1986).

An additional issue, related to fracture roughness, is that of how the fracture walls are 'mated'. It has been demonstrated that even seemingly minor displacements of 0.5

mm of one wall relative to the other one (an unmated fracture) can change the fracture hydraulic conductivity by five orders of magnitude (Keller, 1995). What may often therefore be neglected as a small inaccuracy in the description of fracture wall geometry may be the major factor in controlling flow. At larger scales, which are of principal interest to geothermal applications, fractures with high conductivities can arise due to the presence of offsets in the mating or large scale wall roughness such as 'step' discontinuity, which are common in chalk fractures (Hakami, 1996).

The issue of defining, measuring and understanding the flow of fractures still remains a difficult and as yet, unresolved problem. The applicability of a single parallel plate representation has to be accompanied by all of the above caveats. However, until some form of universal agreement has been reached regarding a better model, the parallel plate approach for individual fractures remains valid.

6.2 Scaled conceptual models

Understanding the interaction between individual fractures to develop conceptual models at scales of interest to hydrogeologists is fraught with issues. Even if the flow within an individual fracture can be estimated there is a major leap to representing flow within multiple fractures at a larger scale. The scale of interest is of particular importance in determining what sort of model can best represent the flow within the aquifer. The most commonly accepted conceptual models are listed below and are illustrated in Figure 6-1. The models can account for a range of possible fracture distributions, densities and hydraulic characteristics, as well as different host rock properties, boundary conditions, and flow and transport processes. The modelling

approaches, all of which can be formulated in deterministic and stochastic frameworks, are traditionally divided into two rough classes:

1. Discrete fracture (to include channel networks)

It is assumed that only the components in the flowing voids (the fractures) are modelled, not the surrounding rock.

2. Continuum

Continuum refers to the averaging of flows over the solid and voids in the rock.

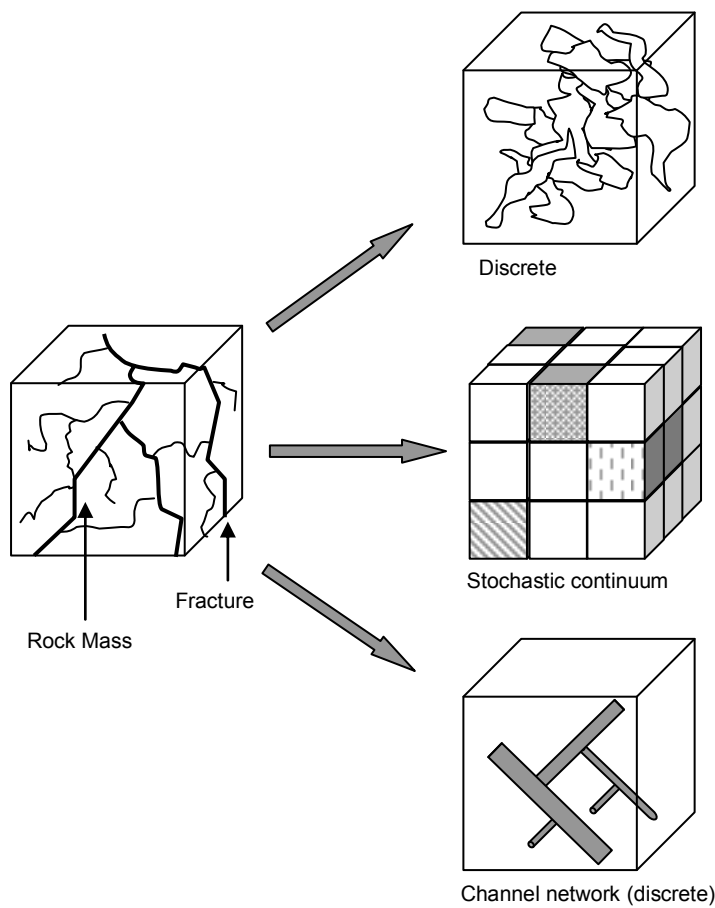


Figure 6-1 Fracture models

6.2.1 Discrete Models

Discrete fracture models encompass flow and transport phenomena that are not adequately captured by the use of continuum models. A major advantage of the discrete fracture approach is that it can account explicitly for the effects of individual fractures on fluid flow and solute transport. As a consequence, discrete fracture models have become popular for theoretical studies and for practical applications (Granet, 1998, Sahimi, 1995, National Research Council, 1996), in spite of their computational limitations for large-scale flow and transport.

Practical application of discrete fracture network models can be limited if detailed field data are not available for calibration. Such models also have the limitation that they demand more data than continuum models. Obtaining comprehensive data for discrete models is clearly not possible and there will always be some degree of approximation when considering a model of the scale of interest relevant to an open loop geothermal system.

The simplest discrete models consider flow and transport processes within a single fracture. In general for 2D and 3D fracture networks, computational intensity generally demands that fractures be treated as parallel plates although some commercial models adopt pipe flow representations (the fracture being treated as a cylindrical pipe). Fractures are often automatically generated in these models according to prescribed distributions governing length (2D) or diameter (or aspect ratio; assuming fractures are disks, ellipses or polygons in 3D), orientation, location, density, aperture, correlation and/or anisotropy. Alternatively, variable aperture

properties can be captured by mapping a 2D or 3D fracture network onto a regular, random, or correlated lattice network consisting of variable aperture segments.

6.2.2 Continuum models

Continuum models make use of spatial averaging based on the Representative Elementary Volume (REV) concept which can be useful for modeling flow and transport in ordinary porous media. In general, an REV approach can be justified if a formation contains a dense network of highly interconnected fractures. An REV approach will always be valid at a particular scale of interest. Whether that scale is of the order of metres or kilometres largely defines the validity of an REV model. If the REV can only be defined at a scale similar to the problem of interest, as is the case for poorly connected networks, and/or if a network clearly consists of fractures with no characteristic size limit then the REV approach is inappropriate. Continuum models follow naturally from the definition of the REV. These models can consist of single continuum, double continuum, or multiple interacting continua.

1. Single continuum, equivalent porous medium, models are applicable when either the fracture network (neglecting contributions from the host rock) is dense and highly interconnected, or when the interaction between the fracture network and the porous/permeable host rock allows a local equilibrium to be established.
2. Double continuum models have been suggested (Barenblatt, 1960) as a means of accounting for two interacting systems of fractures and porous blocks where each is conceptualised as a continuum occupying the entire domain. In this case, it is also necessary to define an exchange function accounting for

mass transfer between continua, which is not simplistic. Such models have seen particularly broad application in petroleum engineering (Bourbiaux, 1999, Ahmadi, 1996).

3. Multiple continua models can be considered if the overall fracture network consists of embedded fracture networks with different properties or scales (Kazemi, 1993). This often occurs when fractures have been caused by more than one process.

A distinction can also be made between double porosity and double permeability models. In double porosity models the flow is assumed to occur in either the fracture or the matrix but chemicals or heat can be stored. Double porosity models do not account for fluid storage changes in the rock matrix.

In double permeability models, the host rock forms an active part of the flow and transport system. The interaction between fractures and adjacent rock strongly determines the flow and transport through the entire system.

These continuum models are, generally speaking, deterministic, in that single values of hydraulic parameters, and resulting flow (and transport) properties, are defined at each point throughout the domain of interest.

A broad class of continuum models encompasses a range of hydraulic parameters and flow and transport properties in terms of probability distributions. Such stochastic frameworks are diverse, and include Monte Carlo analysis based on multiple

realisations of a fracture system, ‘black box’ formulations that use random fields and/or hierarchical conceptualisations that incorporate fractal and percolation concepts. Because of their flexibility and ability to provide quantified ranges of behavior, stochastic frameworks are generally considered to be of greater practical utility than deterministic frameworks (Berkowitz, 2002).

A site investigation does not often establish the presence of discrete fracture features and formation properties, although evidence presented later contradicts this to a degree. Analysis of flow and transport in real-world situations might best incorporate the use of so-called “hybrid” models, which combine aspects of discrete fracture and continuum models.

From a practical point of view, cut-off scales and truncations in measurements, as well as the finite scale of formations and problems of interest, can often permit reasonable (‘first-order’) approximation of flow and transport by hybrid continuum models, with appropriate conditioning to account for the large fracture features.

6.3 Scale of interest

The scale of interest is important and will, in conjunction with knowledge of the fracture network, determine the conceptual model. However, theoretical quantification of the scaling of effective permeability, as found from laboratory and field measurements, may discount this. Laboratory and field data have suggested growth in the permeability of fractured crystalline formations with increasing experimental scale (field length) (Clauser, 1992, Gelhar, 1993). Explanations for such

behavior usually rely on the argument that larger heterogeneities are likely to be encountered as the length scale increases.

To assist with the choice of a conceptual model, for both fracture networks and fractured porous media, various deterministic and stochastic formulations of transport equations are applied:

1. The very near field: thermal transport in a single well defined preferential flow path, possibly with transport into the adjacent porous matrix.
2. The near field: thermal transport in a set of well defined preferential flow paths is considered.
3. The far field: thermal transport is modelled by using two superposed continua, a mobile phase composed of a network of preferential flow paths and an immobile phase representing the rest of the system.
4. The very far field: entire medium is treated as a single continuum representing characteristics of both mobile and immobile phases.

The far field and the very far field approaches are more widely used than the other two approaches. This is appropriate if the scale of heterogeneities is much smaller than the scale of flow.

Open loop geothermal model

The above discussion highlights that there is some degree of choice for a conceptual model that represents the Chalk aquifer at a scale of interest relevant to an open geothermal system. The previously developed ideas about the geometry of the

fractures, the properties of Chalk and the known dimensions of common development sites will act as the constraining factors for the choice of conceptual model.

6.3.1 Fracture geometry

Accurately representing fracture geometry is difficult and will always be an approximation. The discussions above (6.1) suggest that the parallel plate model, with all its limitations, is still the most appropriate method of representing the geometry of individual fractures. This approach will therefore be used in this thesis and flow within fractures will be assumed to obey the cubic law (Eq 6-1). Moreover, field evidence, including that shown by Bloomfield (1996) implies that fractures within the Chalk are broadly located along bedding planes. Such planes are often horizontal and laterally extensive but they clearly do not display smooth parallel plate characteristics. However, adding an average friction factor to these fractures based on the discontinuities would be impractical for this thesis as not enough research has been undertaken on the geometry and structure of fractures in the Chalk. In addition, these properties are variable and representing them at the scale of interest for geothermal systems would be prone to error.

6.3.2 Porosity and permeability

Ward et al, 1968, suggest that fractures along joints are spaced at the scale of tens of centimetres. Bloomfield (1996) broadly concurs with this opinion. It can be safely assumed (Arup 2006) that not all the visible fractures (indeed, field evidence suggests that only a small minority of the fractures could actually be considered to be flowing) are connected over any appreciable distance and therefore that the observed fracture

network could not be described as 'dense'. This would rule out the possibility of treating the Chalk as a single continuum.

Price (1987) showed that the majority of the flow in the Chalk is controlled by fractures with little or no flow occurring in the matrix itself. Although little or no flow occurs in the matrix, the porosity of the matrix is relatively high (25 to 40%, Scholle (1977)). Any conceptual model must therefore allow for dual porosity to account for the high porosity and, by inference, high heat storage capacity of the matrix. The Chalk will be fully saturated and, as water has a much higher heat capacity than rock, the matrix will affect thermal transport rates through the aquifer. In addition, heat must be allowed to move between the fractures and the matrix. Further to this, the model must allow for a highly permeable fracture and a low permeability matrix. A dual porosity, dual permeability model would therefore seem appropriate.

Given the above arguments, possible options for a conceptual model could be:

1. Discrete fracture network

A discrete model, although often computationally demanding, can model the flow of individual fractures and perhaps more importantly, thermal exchange between the fractures and the surrounding matrix. However, to develop a discrete fracture model there must be a reasonable quantity and quality of field data.

2. Double continuum

A double continuum model would allow for the treatment of fractures and matrix as separate entities occupying the same domain. This would resolve any issues of

double porosity/ permeability but the exchange function for thermal transport between the two media will be difficult. The major problem with this approach is that, in reality, only a small proportion of the observed fracture networks are actually flowing (Arup, 2006) and flow within the Chalk aquifer is also often found in highly permeable zones. Although the thermal transport could be represented as a dual continuum model it would be inaccurate to suggest that flow was regularly distributed across the entire domain.

3. Multiple continuum

A multiple continuum model would again allow for the treatment of fractures and matrix as separate entities. In addition, it would allow for the representation of the multiple jointing sets observed by Patsoules and Cripps (1990). However, like the double continuum model, there is a problem in estimating a term for the distribution of flowing fractures.

The path of least resistance would be to adopt a discrete fracture model, provided that the computational demands can be controlled and that sufficient information on the fractures can be gathered from the field to justify the additional time spent creating such a model.

6.3.3 Scale of interest and the conceptual model

The scale of interest for geothermal systems will be defined by the distance between the injection and abstraction boreholes. This distance is governed by the building dimensions which places some broad limits on the model. The majority of new buildings in central London rarely exceed 100m in the horizontal plane and this can

been taken as the principal scale of interest for the conceptual model. As discussed above, the most common scales of interest are the ‘far field’ and ‘very far field’. The discussion here is whether a distance of 100m in the horizontal plane can be considered as ‘far’ or ‘very far field’. The very far field approach would steer the model towards the idea of treating the entire aquifer as a single continuum (there would therefore be no need for a discrete model). The ‘far field’ would treat the Chalk as two continua, a mobile network of preferential flow paths and an immobile phase representing the rest of the system.

One property that can help resolve the far field/ very far field problem is the measured value of transmissivity for the Chalk. The range in transmissivity values recorded by McDonald (2001) suggests that on a scale of tens of kms the Chalk could be treated as a single continuum model, displaying a broadly similar value of transmissivity. On the scale of hundreds of metres, such as those of interest to designers of geothermal systems, the range of transmissivity values would imply that a ‘far field’ approach would be more appropriate.

Further to this discussion is the thermal transport. Although the fluid transport within the Chalk may be best represented (at the scale of 100s of metres) by discrete fractures, the thermal transport may actually be equivalent to a single continuum. The nature of the thermal transport will be dependent upon the fracture spacing, the thermal properties of the matrix and the flow rates of the geothermal system. This is further discussed in the following chapter.

6.3.4 Summary

The above discussion suggests that despite the stated limitations, a parallel plate model will be the most appropriate method of representing the geometry of the individual fractures in the Chalk. The most suitable conceptual model is that of a 'far field' discrete fracture network, despite its potential computational problems. An additional control will be whether the thermal transport, under the flow rates generated by a geothermal system and at the scale of interest of a geothermal system, will actually warrant the development of a discrete model.

7 THERMAL TRANSPORT IN FRACTURES

7.1 Background

The movement of energy through homogenous porous material is fairly well understood from both theoretical studies (Lauwerier, 1955, Lippmann et al, 1980) and experimental evidence. The movement of heat through fractures is less well understood and has been of interest to both the oil industry (Cappetti, 1995, Stefansson, 1997, Sinha, 2004) and the geothermal power industry (Chasteen, 1975). Both industries produce waste water or brine. In the case of the geothermal industry the water can often contain heavy metals or arsenic. The waste water is usually re-injected into the formation both as a convenient form of waste disposal and to maintain pressure in the reservoirs. As this waste water is normally cooler than the formation there is potentially a problem with thermal breakthrough of the cooler water in the abstraction borehole. For the geothermal power industry this would mean a reduction in the power output, for the oil industry this can result in reduced production. The issue of thermal breakthrough in these two industries is directly analogous with that for open loop geothermal systems with the only exception that the scale of interest for open loop geothermal systems is considerably smaller than that of the oil industry or the geothermal power industry.

The experience gained from large scale re-injection experiments indicates that the advancement of the thermal front depends to a great extent on the geological conditions at the site; (Horne, 1982) found thermal interference in four of the five Japanese geothermal fields where re-injection is practiced. However, at the Otake site, where re-injection has been employed since 1972, no thermal effects were

observed. The geology therefore strongly influences the speed of thermal transport beneath a site.

7.2 Conceptual model (thermal breakthrough)

Building on the discussion in the previous chapter, the open loop geothermal system can be described in its most simple form as a number of parallel plate fractures linking the abstraction and injection boreholes. The number and separation of these fractures will be the principal factor controlling the thermal transport between the two boreholes and will need to be determined before any numerical model for a planned site can be developed. Figure 7-1 shows some possible thermal transport patterns for the Chalk:

Figure 7-1 (a) Fracture dominated thermal transport; a single fracture links the injection and abstraction borehole. Thermal breakthrough is expected to occur rapidly at the abstraction borehole.

Figure 7-1 (b) Fracture dominated thermal transport; multiple fractures link the injection and abstraction boreholes. The fractures are separated by sufficient vertical distance to ensure that no vertical thermal interference occurs between them. Thermal breakthrough is still expected to be more rapid than for an equivalent homogenous medium.

Figure 7-1 (c) Fracture thermal transport leading to homogenous thermal breakthrough. If multiple fractures link the injection and abstraction boreholes and are vertically separated by a small enough distance to allow thermal interference to

occur between the fractures, thermal breakthrough will occur at approximately the same rate as that of a homogenous medium.

Figure 7-1 (d) High permeability zone. A high permeability zone will cause thermal breakthrough to occur at a faster rate than for a homogenous medium. Flow rates will be higher and the volume of rock exposed to energy would be less than if the water was flowing through the entire aquifer.

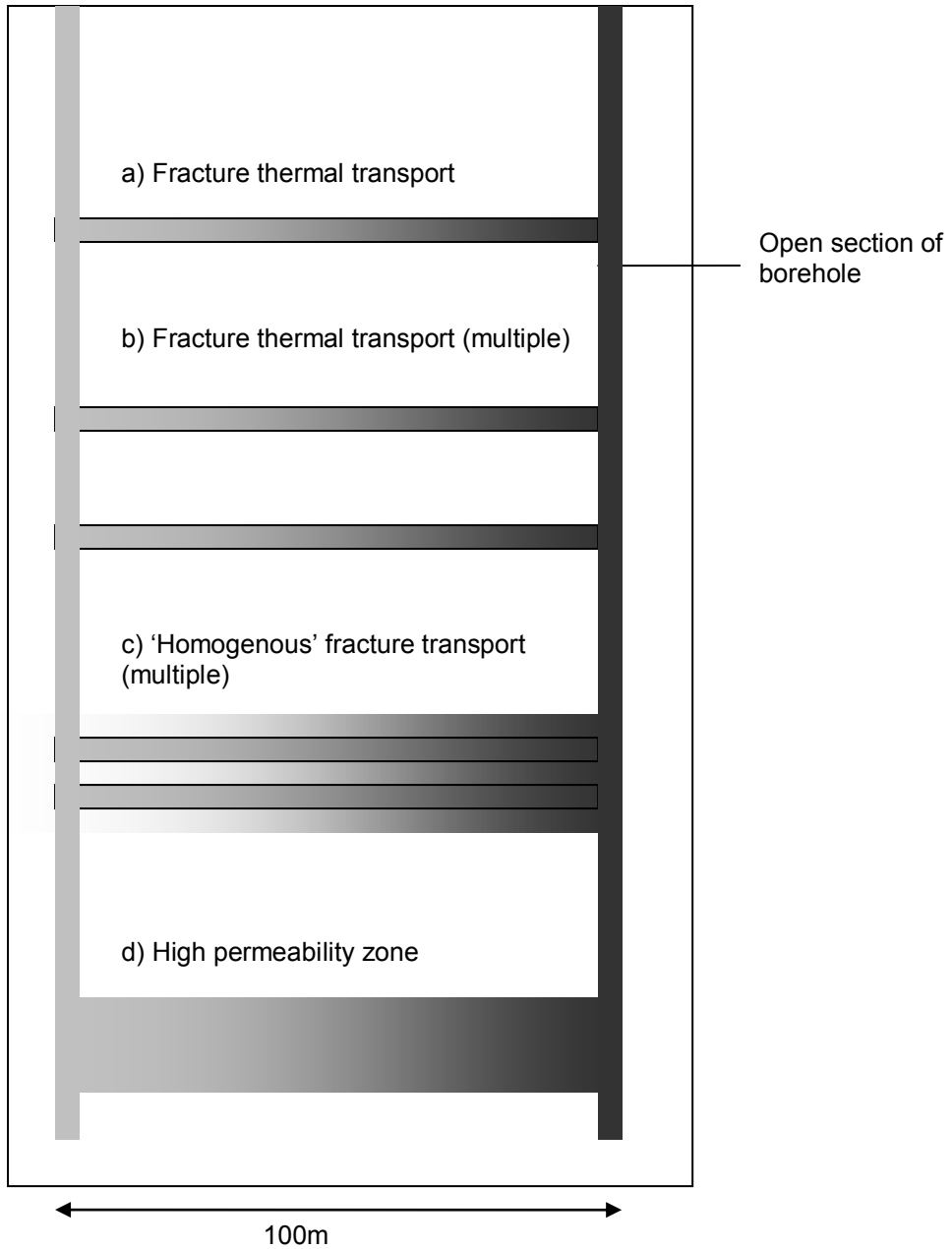


Figure 7-1 Different representations of thermal transport

To develop the conceptual model, it is important to understand, at the scale of interest of an open geothermal system and the flow rates generated by such a system, which of the patterns shown in Figure 7-1a best represent the thermal transport through the aquifer.

If some broad approximations about the fracture characteristics of the Chalk are made, it should be possible to develop an analytical solution that illustrates, over a transport length of 100m, with a variety of fracture apertures and spacings, which of the above patterns are appropriate. This result can then further inform the conceptual model to be used for a particular site.

An analytical model for the type of problem shown in Figure 7-1 was developed by Bodvarsson (1982) to understand thermal breakthrough between boreholes used for a geothermal power plant. The solutions he developed can also be used for shallow open loop geothermal systems, with the caveat that the flowing fractures are uniformly spaced throughout the aquifer. Although this is clearly an oversimplification of reality it does at least allow an initial understanding of thermal transport to be developed. Provided that the fractures are uniformly spaced, the aquifer can be reduced to the simple geometry shown in Figure 7-2.

The injection rate q is assumed to be evenly distributed throughout the fractures over the entire length of the borehole, with D representing half the vertical spacing between fractures. The aperture of each fracture is therefore the same b (Figure 7-2). The flow into the fractures is considered to be steady and radial with the injection well located at $r = 0$.

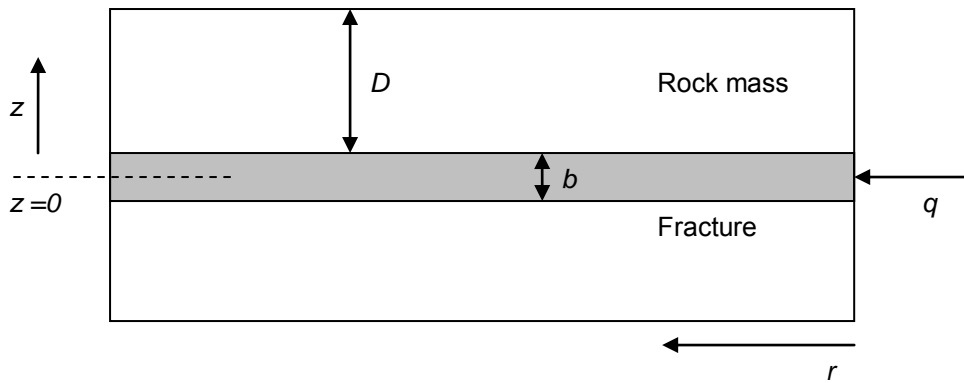


Figure 7-2 Reduced geometry for the analytical model

The fracture is located at an elevation of $z = 0$ with the rock mass extending vertically to $z = \pm D$. Initially the temperature is T_0 throughout the system but at t (time) = 0 the temperature of the injected water is fixed at T_i . The fracture itself can contain some proportion of solids, that is to say that the porosity of the fracture is less than or equal to 1 and any solids within the fracture are to have instantaneous thermal equilibrium with the fluid in the fracture. In the fracture, horizontal conduction is neglected (the thermal transport is deemed to be dominated by convection). In addition, a uniform temperature in the vertical plane of the fracture has been assumed (infinite vertical thermal conductivity).

The rock matrix above and below the fracture is considered to be impermeable and horizontal conduction within the matrix is ignored, heat conduction only occurring in the vertical plane. Heat flow boundaries at $\pm D$ are assumed to be no flow (i.e. they are reflective boundaries caused by lines of symmetry). At the interface between the matrix and the fracture an infinite heat transfer coefficient is assumed and therefore the fracture temperature is assumed to be equal to the matrix temperature at the

contact points. The density and heat capacity of all solids and the fluid in the fracture is assumed to be constant. The temperature range of an open loop geothermal system (0°C to 30°C) allows this statement to be applied. Whether this can be applied to a geothermal electricity generation system with temperatures above 100°C is debatable as both the density and heat capacity of the fluid will change.

The differential equation governing the fluid temperature in the fracture can be derived from the energy balance in a control volume of the fracture. This was reported by Lauwerier (1955) and developed further by Bodvarsson (1969).

The equation for the fracture is as follows:

$$\frac{1}{2\pi r} \frac{\rho_w C_w q}{b} \frac{\partial T_f}{\partial r} + \rho_f C_f \frac{\partial T_f}{\partial t} - \frac{2\lambda}{b} \frac{\partial T_r}{\partial Z} \Big|_{z=0} = 0$$

Eq 7-1

And for the matrix

$$\frac{\partial^2 T_r}{\partial z^2} = \frac{\rho_r C_r}{\lambda} \frac{\partial T_r}{\partial t}$$

Eq 7-2

The derivation of these equations is discussed in the following chapter. The additional parameters not mentioned in the above discussion are:

λ	Thermal conductivity of the rock matrix. (also assumed to be the thermal conductivity of any material in the fracture). [W/m°C]
ρ_w	Density of water [kg/m ³]
C_w	Specific heat capacity of water [J/kg°C]
T_f	Temperature of the fluid in the fracture [°C]
T_r	Temperature of the fluid in the rock matrix [°C]
ρ_f	Bulk density of fracture [kg/m ³]
C_f	Bulk specific heat capacity of fracture [J/kg°C]
ρ_r	Density of rock matrix [kg/m ³]
C_r	Specific heat capacity of rock matrix [J/kg°C]

The initial and boundary conditions can be expressed as:

$$\begin{aligned}
 T_f(r,0) &= T_r(r,z,0) = T_0 \\
 T_f(0,t) &= T_0 \quad t < 0 \\
 T_f(0,t) &= T_0 \quad t \geq 0 \\
 T_f(r,t) &= T_r(r,0,t) \\
 \left. \frac{\partial T_r}{\partial z} \right|_{z=D} &= 0
 \end{aligned}$$

To assist with the solution and the interpretation of Eq 7-1 and Eq 7-2, Bodvarsson, (1982) developed the following dimensionless parameters.

$$\xi = \frac{\pi r^2 (2 + \theta)}{\rho_w C_w q D}$$

$$\tau = \frac{\lambda t}{\rho_r C_r D^2}$$

$$\eta = \frac{z}{D}$$

$$\theta = \frac{\rho_f C_f b}{\rho_r C_r D}$$

$$T_D = \frac{T - T_0}{T_i - T_0}$$

Substituting the above parameters into Eq 7-1 and Eq 7-2 gives:

Fracture

$$(2 + \theta) \frac{\partial T_{Df}}{\partial \xi} + \theta \frac{\partial T_{Df}}{\partial r} - 2 \frac{\partial T_{Df}}{\partial \eta} \Big|_{\eta=0} = 0$$

Eq 7-3

Rock

$$\frac{\partial^2 T_{Dr}}{\partial \eta^2} = \frac{\partial T_{Dr}}{\partial \tau}$$

Eq 7-4

The initial and boundary conditions become

$$T_{Df}(\xi, 0) = T_{Dr}(\xi, \eta, 0) = 0$$

$$T_{Df}(0, \tau) = 0 \quad \tau < 0$$

$$T_{Df}(0, \tau) = 1 \quad \tau \geq 0$$

$$T_{Df}(\xi, \tau) = T_{Dr}(\xi, 0, \tau)$$

$$\frac{\partial T_{Dr}}{\partial \eta} \Big|_{\eta=1} = 0$$

Eq 7-3 and Eq 7-4 form a coherent, self sufficient set of equations which can be solved using the Laplace transformation. The derivation of the solution is not shown

here but can be found in Bodvarsson, (1982). Inverting the solution proved to be difficult and a numerical inverter was used. The resulting type curves are extremely useful in that, given some known parameters such as flow rate and injection temperature, the nature of the thermal front (homogenous or discrete fracture) can be determined at any distance from the injection borehole.

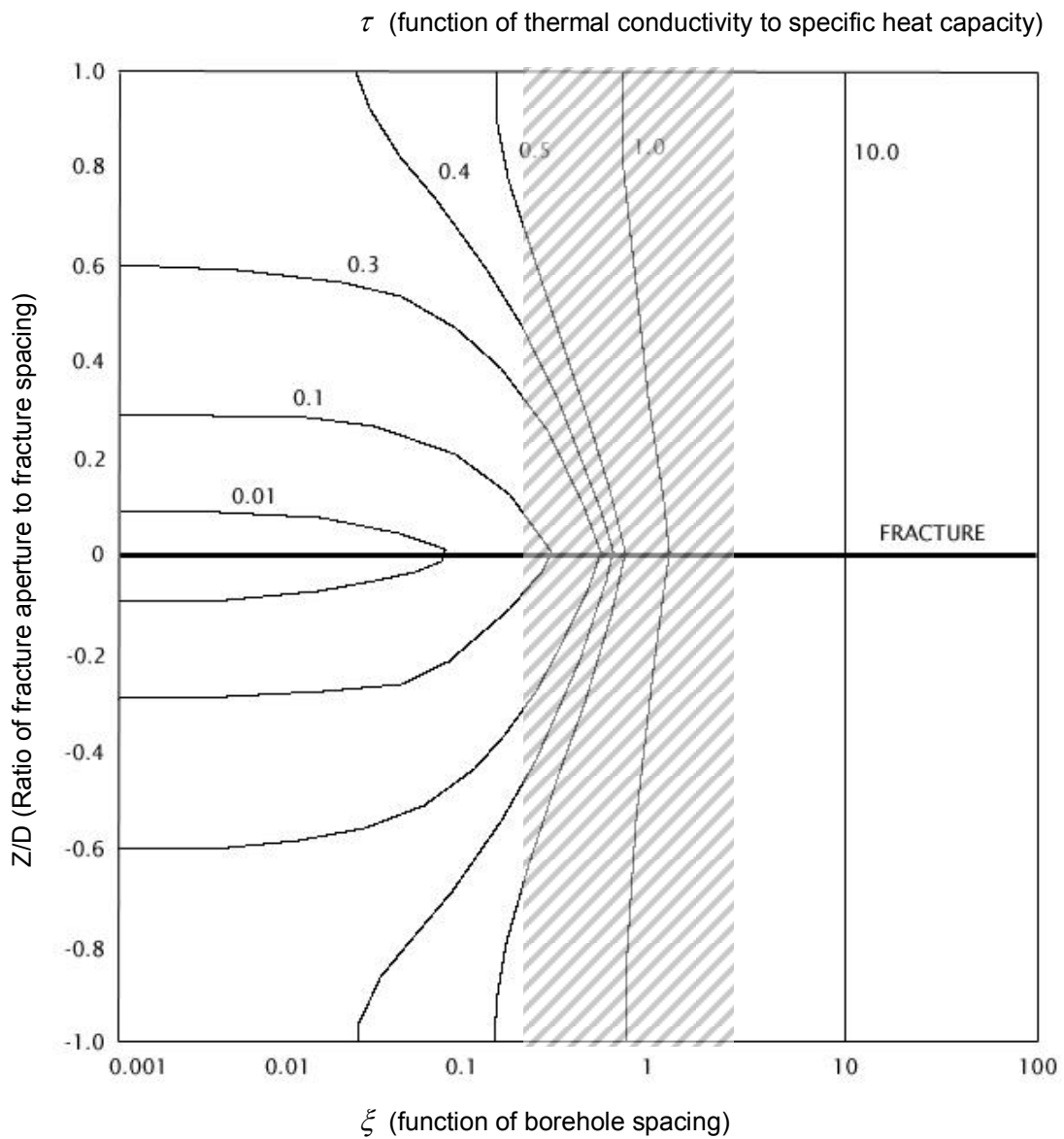
To decide which of the type curves produced by Bodvarsson is the most appropriate for an open geothermal system within the Chalk a value of θ needs to be derived. θ represents the ratio of the bulk thermal capacity of the fracture to the bulk thermal capacity of the rock:

The parameters for the Chalk (Table 7-1) and the fracture need to be used to calculate θ . The porosity of the fracture has been estimated at near to unity (0.98). The porosity and density of the Chalk have been taken from reference values (see previous chapters for properties of Chalk). Estimation of the fracture aperture is not simple (see previous chapter). To calculate plausible values of θ for the Chalk a range of fracture apertures and spacings have been used, based on both previous site investigations (Arup, 2006) and those reported in the literature. The fracture aperture is assumed to be the hydraulic aperture.

Porosity of fracture in the Chalk	0.98
Porosity of Chalk	0.30
Density of Chalk	2,400 kg/m ³
Density of water	1,000 kg/m ³
Specific heat capacity of water	4,182 J/kg°C
Specific heat capacity of Chalk	900 J/kg°C
Fracture aperture	0.5mm (min) to 2mm (max)
Fracture spacing	1m (min) to 30m (max)

Table 7-1 Parameters used for the Chalk

Inserting the above range of parameters gives θ a minimum of $3e-5$ ($b=0.5\text{mm}$, $D = 15\text{m}$) to a maximum of $3e-3$ ($b=2\text{mm}$, $D = 0.5\text{m}$). For both of these cases it is important to note that $\theta \leq 0.01$. This identifies a specific series of type curves generated by Bodvarsson. The curve for $\theta \leq 0.01$ is shown in Figure 7-3.



Zone for the majority of shallow geothermal systems in the Chalk

Figure 7-3 Type curve for $\theta \leq 0.01$ (After Bodvarsson, 1982). The zone of interest for a geothermal system with typical flow rates and borehole spacings is highlighted

The above diagram (although not necessarily intuitive) can best be viewed as representing a single horizontal fracture at the abstraction well. The horizontal line (FRACTURE) is the central axis of a horizontal fracture. The curves in the figure are

potential thermal fronts for a variety of flow rates, fracture apertures, fracture spacings and borehole spacings. If, for example $\frac{Z}{D}$ (y-axis) is low (small aperture, large fracture spacing) and ξ (x-axis) is also low (distance between injection and abstraction borehole) then (reading from the above figure) the nature of the thermal front at the abstraction borehole is likely to be dominated by fracture flow for most of the timescale of interest. Conversely, if $\frac{Z}{D}$ is large and ξ is large the thermal transport is likely to appear homogenous at the abstraction well.

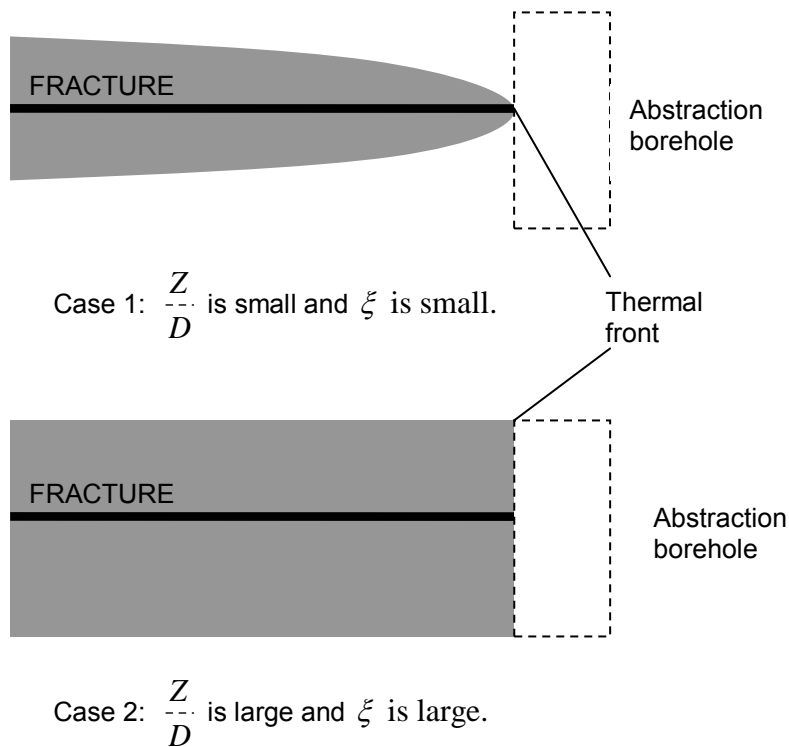


Figure 7-4 Representation of Figure 7-3 showing the thermal front for two different conditions

To interrogate the type curve the variables τ and ξ need to be determined for the specific conditions likely to be encountered at a site. These variables relate primarily to the time of interest, flow rates and spacings between boreholes.:

In order to calculate ξ the following additional parameters were defined

R	100m (scale of interest)
Thermal conductivity of rock matrix	2.2 W/m°C (reference parameter for Chalk)
q (flow rate)	15 l/s ('typical' sustainable flow rate for a borehole in the Chalk)

Using the previously calculated maximum and minimum values of θ a maximum and minimum value of ξ can be calculated: 2.006 and 0.067 respectively. These values have been plotted on Figure 7-3, and the shaded portion represents all plausible values of aperture and fracture spacings that are likely to be encountered in the Chalk beneath a site. Without yet adding the variable τ (time dependence) it can be seen that for greater than 60% of the plausible Chalk fracture geometries and spacings the thermal front and thus the nature of the thermal breakthrough at the abstraction borehole will be fracture dominated (for flow rates of 15 l/s and upwards). The parameter τ is important however in that it defines what could be called a timeframe of interest.

Back calculating τ will help to understand how much time would need to elapse before the thermal front resembles one of the patterns in Figure 7-3. Reading off from

Figure 7-3 for the previously stated parameters, τ has a minimum value 0.05 and a maximum of 2. Time t will therefore range in value from 8 hrs to 32 years depending on the fracture aperture and spacing used. The larger values of t are derived from the portion of the type curve with high values of ξ , illustrating that, for the case of a small number of fractures, separated by larger vertical distances within the aquifer, homogenous thermal transport would not occur throughout the aquifer beneath a site until many years had passed. At the other end of the spectrum, when fractures are more frequent and closely spaced, equivalent homogeneous thermal transport will occur within approximately eight hours.

This last result has interesting implications for an open loop geothermal system. It proves that, for the majority of geothermal systems sited within the Chalk aquifer, the thermal transport, and thus the thermal breakthrough in the abstraction borehole will be determined by fracture flow. It should be remembered that the above models are conservative in that they assume an equal distribution of fractures throughout the depth of the aquifer. In practice, flowing fractures will not be evenly distributed, increasing the heterogeneity of flow. In some extreme cases, when the flowing fractures are frequent (1 every 0.5m) the thermal transport could be modelled by representing the Chalk as a homogenous medium. However, for the vast majority of cases the thermal transport will have to be modelled using dual porosity / permeability or discrete fractures. A unique case may arise however if the flowing fractures are all located within a relatively narrow high permeability zone. In this case it may be possible for the zone be treated as a homogenous medium. However, this could only be determined by sufficient field data.

7.3 Numerical models

A further aspect to the above discussion is that open loop geothermal systems do not operate at constant injection/ abstraction rates and will fluctuate between heating and cooling through the year, affecting the energy inputs and outputs to any model. The time dependent nature of this flow dictates that a numerical model rather than an analytical model needs to be used to predict the thermal footprint of an open loop geothermal system. At the time of writing this thesis (2008) there are only a small number of numerical codes capable of coupling transient groundwater flow and thermal transport. The three most appropriate codes are:

TOUGH2 (Berkeley National Laboratory)

TOUGH2 is a general-purpose numerical simulation program for multi-phase fluid and heat flow in porous and fractured media. It has applications in geothermal reservoir engineering, nuclear waste disposal, unsaturated zone hydrology, and geologic storage of CO₂ (carbon sequestration). It is a well proven code and is used extensively in the field of geothermal reservoir modelling.

FEFLOW (DHI-WASY GmbH)

FEFLOW is a finite element code that has some design features which are well suited to the representation of open loop geothermal systems. In particular, there is a module that automatically feeds the calculated temperature at the abstraction borehole back in to the model as an injection temperature. This saves the user time and effort. However, FEFLOW has been primarily designed for homogenous material and is difficult to adapt to a 3 dimensional discrete fracture flow model.

SUTRA (United States Geological Survey)

SUTRA 3D was released by the USGS in September 2003 and employs a 3D finite-element and finite-difference method to approximate the governing equations that describe the processes of fluid-density-dependent saturated or unsaturated groundwater flow in conjunction with transport of thermal energy in the ground water and solid matrix of the aquifer. The code is not commercial and there is therefore no licence fee associated with this code. In addition, as the program suite is not a 'black box' it is easier to manipulate to model discrete fractures.

Both TOUGH2 and SUTRA would be the most suitable codes to model thermal transport in fractures. As TOUGH2 requires a licence to be paid and, from personal experience, is the more difficult to code to be made to work correctly, it was decided to use SUTRA 3D for the numerical model construction.

7.3.1 Representation of thermal transport in SUTRA

As discussed in previous sections, fractures will be represented as parallel plates. It is important to understand how thermal transport from the water in the fracture to the matrix of the surrounding material will be represented in the numerical model.

Ground-water flow in SUTRA is simulated through the numerical solution of a fluid mass-balance equation. Fluid density may be constant, or vary as a function of fluid temperature. For the temperature range of an open loop system the change in density caused by changes in fluid temperature will be minimal.

The transport of heat (energy) is simulated through the numerical solution of an energy-balance equation. The simulation of energy transport provided by SUTRA is actually a calculation of the time rate of change of the amount of energy stored in the solid matrix and fluid. In a unit volume of solid matrix plus fluid, the amount of energy contained is:

$$(\phi S_w \rho_w e_w + (1 - \phi) \rho_s e_s)$$

Eq 7-5

where:

- e_w Energy per unit mass of water [J/kg]
- e_s Energy per unit mass of solid matrix [J/kg]
- ρ_s Density of solid grain in matrix [kg/m³]
- ρ_w Density of water [kg/m³]
- S_w Saturation []
- ϕ Porosity of the material []

The stored energy in a volume may change with time due to: ambient water with a different temperature flowing in, injected well water of a different temperature, changes in the total mass of water in the block, thermal conduction (energy diffusion) into or out of the volume, energy dispersion in or out, and energy production or loss due to nuclear, chemical or biological reactions.

This balance of changes in stored energy with various energy fluxes is expressed as follows:

$$\frac{\delta}{\delta t} [\phi S_w \rho_w e_w + (1 - \phi) \rho_s e_s] = -\nabla(\phi S_w \rho_w v) + \nabla[\lambda \nabla T] + \nabla[\phi S_w \rho_w C_w D \nabla T] + Q_p C_w T^* + \phi S_w \rho_w \lambda_0^w + (1 - \phi) \rho_s \lambda_0^s$$

Eq 7-6

where:

$\lambda(x, y, z, t)$ Bulk thermal conductivity of solid matrix plus fluid (W/mK)

I Identity tensor (in 3D a 3*3 matrix of values)

C_w Specific heat of water (J/kg°C)

$D(x, y, z, t)$ Dispersion tensor (in 3D a 3*3 matrix of values)

$T^*(x, y, z, t)$ Temperature of source fluid (°C)

$\lambda_0^w(x, y, z, t)$ Energy source in fluid (J)

$\lambda_0^s(x, y, z, t)$ Energy source in solid grains (J)

S_w Saturation

Q_p Fluid mass source (kg/s)

The time derivative expresses the total change in energy stored in both the solid matrix and fluid per unit total volume. The term involving v expresses contributions to locally stored energy from average-uniform flowing fluid (average energy advection). The term involving bulk thermal conductivity, λ , expresses heat conduction contributions to local stored energy and the term involving the dispersivity tensor, D , approximately expresses the contribution of irregular flows and mixing, which are not accounted for by average energy advection. The term involving Q_p accounts for the energy added by a fluid source with temperature, T^* . The last

terms account for energy production in the fluid and solid, respectively, due to endothermic reactions, for example.

While models that are more complex are available and may be implemented if desired, SUTRA employs a volumetric average approximation for bulk thermal conductivity,

$$\lambda_A = \phi S_w \lambda_w + (1 - \phi) \lambda_s$$

Eq 7-7

where:

λ_w Fluid thermal conductivity (W/m°C)

λ_s Solid thermal conductivity (W/m°C)

The specific energy content (per unit mass) of the fluid and the solid matrix depends upon temperature as follows:

$$e_w = C_w T$$

$$e_s = C_s T$$

where:

C_s Solid grain specific heat (J/kg°C)

An expanded form of the solid matrix fluid energy balance is therefore obtained by substitution:

$$\frac{\delta}{\delta t} [\phi S_w \rho_w C_w + (1-\phi) \rho_s C_s] T + \nabla(\phi S_w \rho_w C_w v T) - \nabla \{ [S_w \lambda_w + (1-\phi) \lambda_s] I + \phi S_w \rho_w C_w D \} \nabla T$$

$$= Q_p C_w T^* + \phi S_w \rho_w \lambda_0^w + (1-\phi) \rho_s \lambda_0^s$$

Eq 7-8

The solid grains of the aquifer matrix and the fluid are locally assumed to have equal temperature, and fluid density and viscosity may be affected by temperature. Again, for the temperatures involved in an open loop geothermal system the viscosity and density of water will show little change. However, the assumed local equilibrium between the solid matrix and the fluid may over-represent the thermal conductivity of the matrix when the fluid is moving quickly. As an example, in the initial moments when heated or cooled water enters a fracture in an aquifer, there will not be temperature equilibrium between the solid grains in the fracture wall and the fluid moving through the fracture. Although equilibrium will be quickly established, the SUTRA code, by assuming instantaneous local equilibrium, will over exaggerate the thermal conductivity of the material in the fracture walls. The thermal conductivity of the matrix material may therefore have to be decreased in the model to account for this effect.

7.4 Summary

The most accessible method of modelling water flow through the Chalk is to represent the Chalk as discrete horizontal, planar fractures. The theoretical work undertaken by Bodvarsson has proved to be a useful first step in understanding the extent to which thermal transport for open loop geothermal systems sited in the Chalk, given known constraints of flow rate, borehole spacing and a likely range of fracture apertures and spacings is governed by fractures. Using a plausible range of fracture apertures and

spacings, data on flow rates from boreholes in the Chalk, average site dimensions for an urban building in central London and the timescale over which a geothermal system operates in one direction (heating or cooling cycle) it can be seen that in most cases the aquifer will need to be modelled as discrete fractures, not as a an equivalent continuum. To model a system successfully, a code needs to be used to allow for the above characteristics and transient energy inputs and outputs as the system provides heating and cooling energy to the building.

A small number of numerical codes are available with the capacity to model discrete fracture planes coupled with combined flow and transport solutions. The numerical code chosen to model the geothermal systems was SUTRA 3D (developed by the USGS).

8 SUTRA TEST

To model thermal transport for different configurations of open loop geothermal systems in the Chalk, discrete fractures need to be constructed within the SUTRA code. There is no previous documentation in the literature regarding the use of SUTRA to construct discrete fracture networks. Therefore, the method of constructing the fractures in the model (geometry, discretisation, time steps, dispersion coefficients) needs to be tested against a known analytical solution for thermal transport in a single fracture. This is a useful method of determining the accuracy of assumed parameters and detecting user error.

The theory underlying the prediction of thermal transport in fractures dates back to the work of Lauwerier (1955). Lauwerier derived equations for the movement of heated fluid and its subsequent loss of energy between two infinite confining oil boundaries. This theory can be adapted to fractures and the surrounding matrix by treating the matrix as the infinite confining boundary. Indeed, the equations used previously to further the discussion of the nature of thermal transport in evenly spaced multiple fractures were derived from the original work by Lauwerier. The derivation of the equation thermal transport in a single fracture is shown here for the sake of completeness and to enable the development of the analytical solution used to test the construction of the numerical model in SUTRA.

The single fracture theory is based on the representation of a fracture as a plane of highly permeable material with a high porosity. If the value of porosity chosen is close to 1, it follows that the thermal properties of the fracture will be almost equal to

that of the injected fluid. These thermal properties can be represented as a combination of the thermal properties of the injected fluid (in this case water) and the fracture ‘matrix’ – material within the fracture. At the assumed porosity of the fracture the contribution of the fracture ‘matrix’ will be minimal.

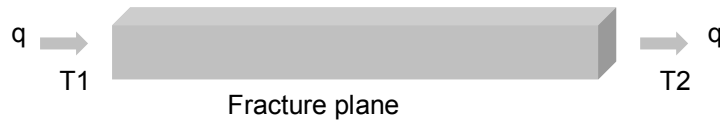


Figure 8-1 Fracture model (1D)

To develop the theory, the fracture can initially be considered in thermal isolation (Figure 8-1), effectively ignoring any effects of the rock matrix and thermal conduction (1 Dimensional model). Fluid is injected at a rate q (kg/s) from time $t=0$ into a horizontal ‘reservoir’ (thickness h (m) and constant cross sectional area A (m²). In this case the system has a very simple geometry and associated governing equation for heat flow. The temperature of the injected fluid is T_2 and the initial temperature of the reservoir is T_1 . The porosity of the ‘reservoir’ is ϕ . To define temperature as a function of time and distance from the injection point the following differential equation needs to be solved.

$$(C\rho) \frac{\partial T}{\partial t} + \rho_w C_w V \frac{\partial T}{\partial x} = 0$$

$$\text{With } T(x,0) = T_1 \text{ and } T(0,t) = T_2$$

Eq 8-1

Where $(C\rho)$ represents the average volumetric heat capacity of the ‘reservoir’:

$$(C\rho) = \rho_w C_w \phi + (1 - \phi_f) \rho_r C_r$$

And $V =$ the true velocity of the injected fluid:

$$V = q/(\rho_w A \phi)$$

As the porosity of the fracture is close to 1 the velocity is essentially the flow per unit area of the ‘reservoir’.

Solving Eq 8-1 for the given conditions (Zabarny, 1998) gives the step function:

$$T_{(x,t)} = T_1 \text{ if } x > \frac{C_w \rho_w}{(C\rho)} Vt$$

or

$$T_{(x,t)} = T_2 \text{ if } x < \frac{C_w \rho_w}{(C\rho)} Vt$$

where $x = \frac{C_w \rho_w}{(C\rho)} Vt$ defines the location of the thermal front at any time for the reservoir.

If the confining beds and heat transfer from the confining beds by conduction are considered (Figure 8-2).

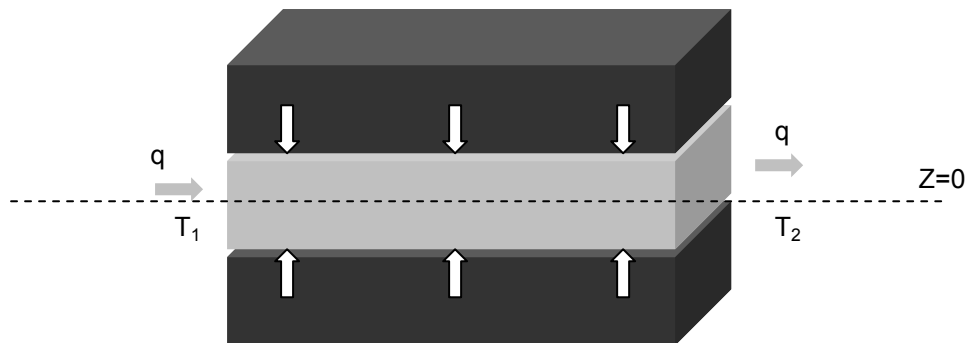


Figure 8-2 Matrix model geometry

If $T(x,t)$ defines the temperature within the ‘reservoir’, $T_m(x,z,t)$ is the temperature of the confining beds and $T(\infty, \infty, t) = T_2$ and $T(x, y, 0) = T_1$. The heat transfer between

the reservoir and the confining beds is given by Eq 8-2 and within the ‘reservoir’ by Eq 8-3.

$$(C\rho) \frac{\partial T}{\partial t} + \rho_w C_w V \frac{\partial T}{\partial x} = \frac{\lambda_m}{h} \frac{\partial T_m}{\partial z}$$

Eq 8-2

$$(C\rho) \frac{\partial T}{\partial t} + \rho_w C_w V \frac{\partial T}{\partial x} = (\lambda) \frac{\partial^2 T}{\partial x^2}$$

Eq 8-3

Where $(\lambda) = \lambda_m \phi + \lambda_r (1 - \phi)$ is the average thermal conductivity in the ‘reservoir’.

8.1.1 Analytical solution

If boundary conditions for the system are set as follows,

$$T(x,0) = T_1$$

$$T(0,t) = T_2$$

$$T_m(x, z, 0) = T_1$$

$$T_m(x, z, t) = T_1; x \rightarrow \infty, z \rightarrow \infty$$

Solving the problem defined by the above equations using these conditions (Zabarnay, 1998) gives:

$$\theta_{(x,t)} = \operatorname{erf} \left(\frac{\frac{\lambda_m x}{C_w \rho_w V}}{h \sqrt{\frac{\lambda_m}{C_m \rho_m} \left(t - \frac{(C\rho)_f x}{C_w \rho_w V} \right)}} \right) \text{ when } t > \frac{(C\rho)_f x}{C_w \rho_w V}$$

Eq 8-4

And

$$\theta_{(x,t)} = 1 \text{ when } t < \frac{(C\rho)_f x}{C_w \rho_w V}$$

Eq 8-5

Where

$$\theta_{(x,t)} = (T_{(x,t)} - T_2)/(T_1 - T_2)$$

Eq 8-4 can be solved using a spreadsheet for different values of x (distance from the injection point). The results can then be used to check against those produced by the numerical model that represents the same geometry and flow rates.

8.1.2 Analytical solution parameters

Literature values (Table 8-1) for the thermal characteristics of the Chalk were used in the analytical solution. A fracture plane with an arbitrary aperture of 1mm was chosen for the test. An injection rate of 1.5 l/s was chosen to reflect a total injection rate of 15 l/s into a theoretical borehole with the flow being carried by a total of 10 equal aperture fractures. An injection rate of 15 l/s would be typical for a geothermal borehole in the Chalk. To calculate the velocity of the water in the fracture it has been assumed that the fracture has a width of 1m. The cross sectional area of the fracture is therefore 0.001m. With the given flow rates and fracture dimensions the velocity of the water in the fracture is 1.5 m/s.

Porosity values for the Chalk matrix are known to be in the region of 30% (Bell, 1999, Bloomfield 1996) although this value does often decrease with depth. Chalk matrix density of 2800 kg/m³ (McDonald, 2001) and a thermal conductivity of 2.2

W/mK (Blackwell, 1989) have been assumed. The fracture has been assumed to be almost without matrix and has been assigned a porosity of 0.99.

The geothermal system is assumed to be running in cooling mode with a delta T of 10°C. The injection temperature T_2 is therefore ten degrees greater than the abstraction temperature. If it is assumed that the groundwater temperature in the Chalk T_1 is 13°C the injection temperature T_2 is therefore 23°C.

Parameter	Symbol	Value	Units
Specific heat of water	C_w	4182	J/kg°C
Density of water	ρ_w	1000	kg/m ³
Density of the rock material	ρ_r	2400	kg/m ³
Thermal conductivity of the rock material	λ_m	2.2	W/m°C
Specific heat of rock	C_r	900	J/kg°C
Injection rate	q	1.5	l/s
Porosity of matrix	ϕ_m	0.3	
Porosity of 'reservoir'	ϕ	0.99	
Time of injection	t	variable	seconds
Height of fracture	h	0.001	m

Table 8-1 Parameters used in the analytical solution

The analytical model was then run in Microsoft Excel and the temperature at various distances from the injection point (1 to 75m) was calculated.

8.1.3 Analytical Solution Results

The results from the analytical solution for the injection period are shown in Figure 8-3.

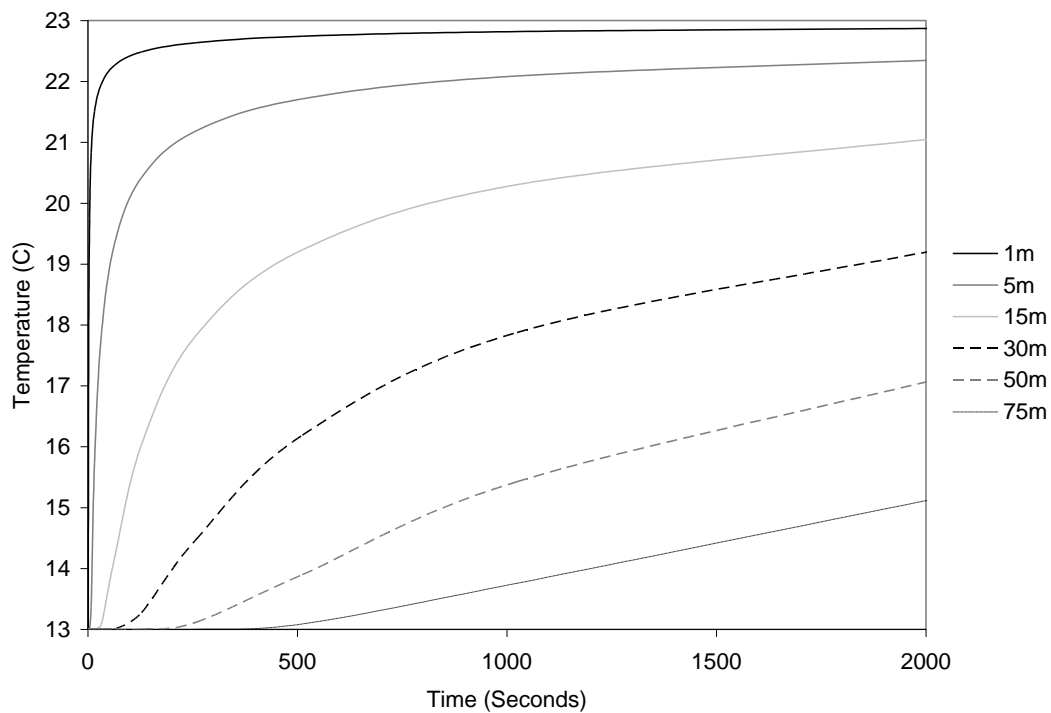


Figure 8-3 Results from the analytical solution

The results indicate a rapid rise in temperature at distances nearer to the injection point, as would be expected. At further distances from the injection point the increase in temperature is less abrupt.

The model results seem logical as they show that the heat transfer into the matrix affects the rate of migration along the fracture. If no perpendicular heat transfer occurred there should be a step function response. Strong perpendicular heat transfer should produce effectively zero longitudinal transport.

8.2 Numerical modelling

The numerical model to be calibrated is a replica of the analytical model. It therefore does not allow for radial flow or transient energy input.

8.2.1 Geometry

The geometry of the model used to replicate the analytical solution uses the principle of symmetry to split the fracture in the horizontal plane. This method of reducing the size of a numerical model is commonly used. Although this approach is valid for testing the single fracture model, the actual system models are likely to have more randomly distributed fractures and this line of symmetry may no longer be valid. The numerical model represents a single fracture within a vertically extensive chalk block. The fracture runs along the base of the model. The depth of this fracture is 0.0005 m (Figure 8-4) which represents half of the 1mm analytical model fracture depth. The horizontal dimension of the model has been set at 100m (the largest value of x in the analytical model is 75m)

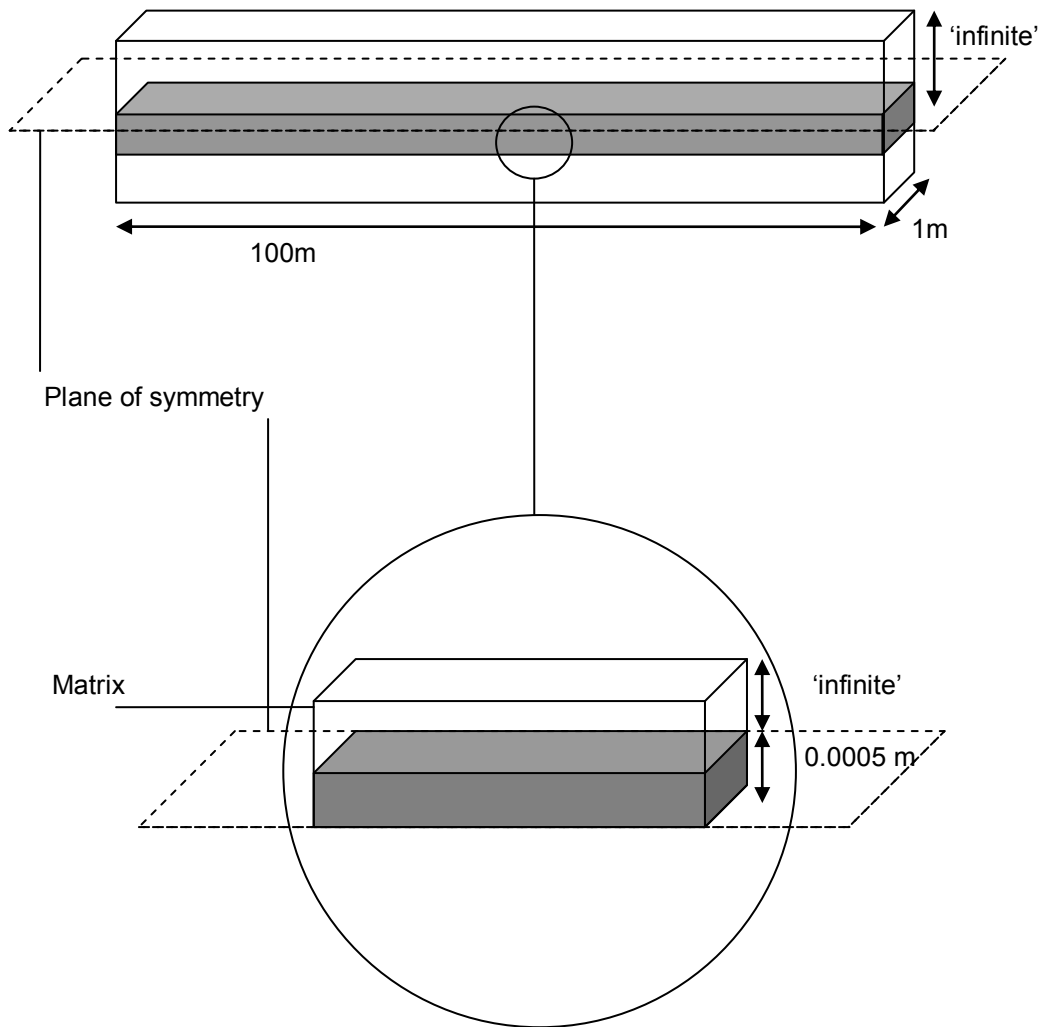
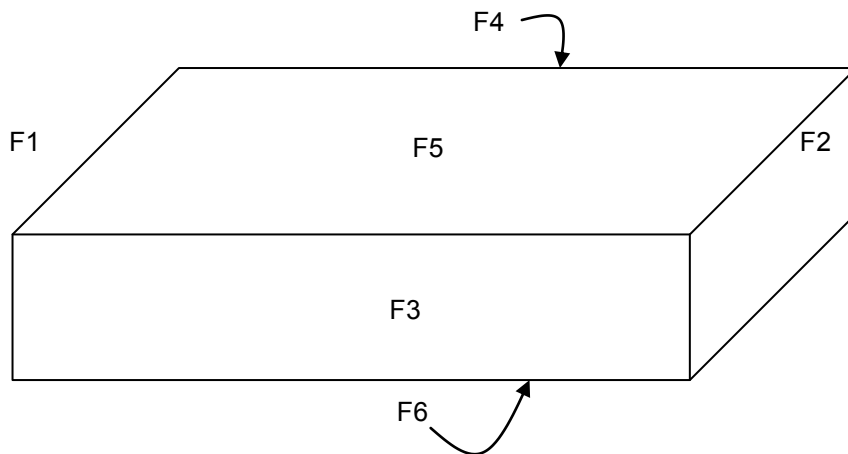


Figure 8-4 Representation of the geometry used in the numerical model

The parameters used for the numerical model were the same as those listed in Table 8-1. The only difference between the two is that the injection rate for the numerical model is half that used in the analytical solution (to reflect the horizontal symmetry used in the model).

8.2.2 Boundary conditions

The boundary conditions were allocated to the model on a face by face basis. The faces are shown in Figure 8-5 whilst the values / conditions added to each face are given in Figure 8-5.



Face	Pressure	Temperature
F1	No fluid movement across boundary except through the nodes that represent the fracture.	No flow except for nodes that represent the fluid injection temperature.
F2	No fluid movement across boundary except through the nodes that represent the fracture.	No flow except for nodes that represent the fluid abstraction.
F3	No flow.	No flow.
F4	No flow.	No flow.
F5	No Flow	No flow.
F6	No flow.	No flow.

Figure 8-5 Boundary conditions for numerical model

8.2.3 Grid

Horizontal Spacing

Determining the correct grid size for numerical models is always a tradeoff between computer power (the time taken to run a model) and the definition required to prevent numerical errors from occurring. The greater the definition, the larger the model and thus the more time it takes to run the model. In regions of the model where the temperature gradient is large the grid size and time steps must be small enough not to cause the model to create spurious values. The transition points presented between these tradeoffs can be quantified numerically using the Mesh Peclet number and the Courant Number.

The spatial stability of the numerical approximation of the unified transport equation in SUTRA (Section 0) depends on the value of the mesh Peclet number, Pe_m , given approximately by:

$$Pe_m \approx \frac{\Delta L}{\alpha_L}$$

where ΔL is the local distance between element sides along a streamline of flow and α_L is the dispersion coefficient (see note at end of this section). Spatial instability appears as one or more oscillations in concentration or temperature. Stability is guaranteed in all cases when $Pe_m < 2$, which gives a criterion for choosing a maximum allowable element dimension, ΔL , along the local flow direction. This criterion significantly affects discretisation. Spatial stability is usually obtained with SUTRA when $Pe_m < 4$ which gives a less-stringent criterion. Mesh design according to the criterion is critical when temperatures change significantly along streamlines,

such as when a front is propagated in the direction of flow. When concentrations or temperatures exhibit small changes along streamlines, then the criterion may safely be violated, even by a few orders of magnitude, without inducing spatial instability.

The value of dispersion chosen for this numerical model is different to that normally assigned to a homogenous medium (approximately one tenth of the model size in the direction of transport). There will be no dispersion in a fracture with a porosity of unity and little or no dispersion in a fracture with a porosity close to unity. In addition, the analytical model, against which the results of the numerical model will be tested, does not take dispersion into account. For this numerical model, dispersion within the fracture portion of the model was assigned to close to zero (1e-9). An absolute value of zero will cause errors in the model code. The dispersion in the matrix (which is effectively impermeable to flow) was set to one tenth of horizontal transport length, in this case 10m. If the value of dispersion applied to the fracture is used to calculate the Mesh Peclet number, ΔL will have to be impractically small. The value of dispersion applied to the matrix (10) was used to ensure that ΔL (1m) was sufficiently small.

The Courant number relates the time stepping and velocity to the size of each element direction ΔL . It becomes important when the velocity of the fluid is of a similar order of magnitude to the element size divided by the time step. The Courant number is represented numerically as follows:

$$C_o = \frac{\delta t |U|}{\delta x}$$

Where

C_o = the courant number

$|U|$ = the velocity of the fluid

δt = the timestep

δx = element dimension or ΔL

To avoid spurious numerical results it is important to keep the Courant number below 1. For this model, the velocity of the fluid is 1.5 m/s and the grid size (ΔL) is 5m. A timestep δt value of 1 second would lead to a Courant number C_o of 0.3, well below the defining limit of 1. The model was therefore run with a δt of 1 second.

Vertical Spacing

The vertical grid spacing is dictated primarily by the aperture of the fracture to be modelled. The aperture of the fracture will be relatively small compared to the vertical extent of the model. To construct a model with a uniform vertical element size equivalent to the fracture aperture would be impractical, requiring an extremely large number of elements. A principle of doubling the grid size for every element was therefore adopted. The fracture, with an aperture of 1mm, is represented in the model by an initial grid size of 0.5mm (vertical symmetry has split the fracture in half). The next vertical element size is 1mm and so on until the correct vertical model dimension was obtained.

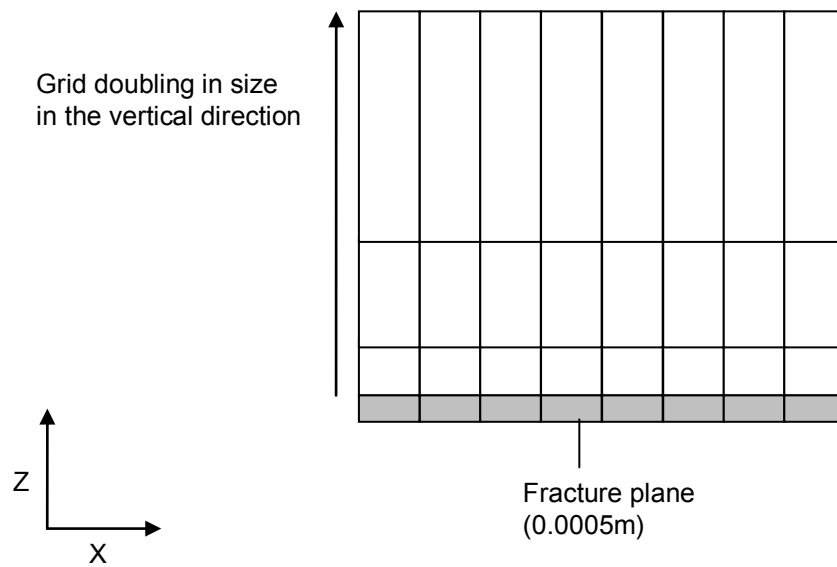


Figure 8-6 Representation of grid used in the numerical model

8.2.4 Fluid injection

Fluid injection to the model is represented as a positive injection through the nodes that represent the fracture face open to flow. The fluid injection used in the analytical model corresponds to an injection rate through the numerical model of 0.75 l/s (1.5 l/s divided by two to account for symmetry).

The fracture plane is represented in the SUTRA code by a single plane of elements with a permeability that corresponds to the fracture aperture (vertical height). The SUTRA code uses intrinsic permeability and not hydraulic conductivity to represent the resistance of blocks to flow. The two are related according to the following relationship.

$$K = \frac{k\rho g}{\mu}$$

Where:

K = hydraulic conductivity

k = intrinsic permeability

γ = fluid viscosity

ρ = fluid density

As, from the cubic law, fracture hydraulic conductivity is:

$$K = \frac{b^2 \rho g}{12\mu}$$

It follows that the intrinsic permeability value used as an input to SUTRA as a function of fracture aperture is:

$$k = \frac{b^2}{12}$$

Where b is the fracture aperture.

The fluid is inputted into the model through the nodes that effectively represent the central line of the fracture, Figure 8-7. The nodes on the outside edge of the model will represent half again of the total injection rate. Example flow rates are listed in Table 8-2.

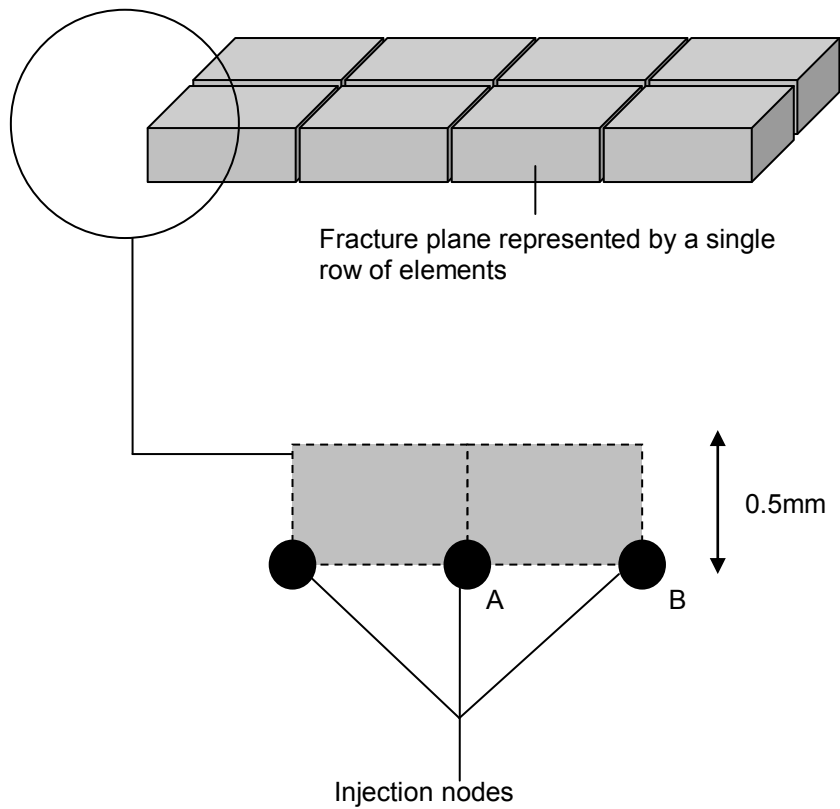


Figure 8-7 Block representation of a fracture plane and injection nodes

Total rate of injection into fracture	1.5 l/s
Model uses horizontal symmetry. Total injection through model	0.75 l/s
Injection rate A	0.375 l/s
Injection rate B	0.1875 l/s

Table 8-2 Example injection and abstraction rates

8.2.5 Model Operation

The model was run for a total injection time of 2500 seconds with an observation result recorded every second. Observation results show, for every node selected, pressure, temperature or any other variable selected as an output.

8.2.6 Model Results

The results for the numerical modelling and analytical modelling can be seen in Figure 8-8. As in the analytical modelling there is a rapid rise in temperature nearer the borehole followed by a slower increase at distances further from the borehole.

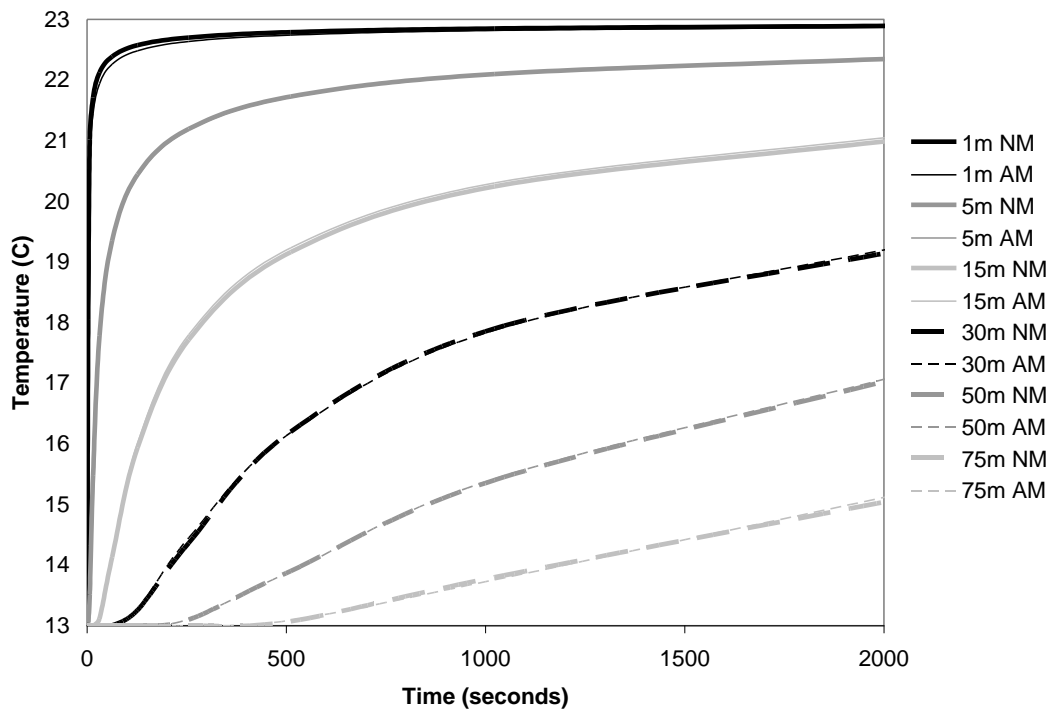


Figure 8-8 Numerical modelling (NM) results using SUTRA 3D and analytical results (AM)

The numerical results closely match those of the analytical solution. For comparison, both results have been plotted on the same graph (Figure 8-8). The numerical model results have been plotted as thick lines, the analytical as thin lines. The results are well matched at all distances from the injection point. For the purposes of verifying the model construction therefore, the similarity of predicted results was deemed to be sufficient proof of the method of construction and the use of suitable time steps.

8.3 Summary

It can be seen from Figure 8-8 that predictions of temperature distribution over time using the analytical model are well matched to the numerical model developed using the SUTRA code. It is apparent that the modelling approach (geometry, discretisation, time-stepping) for a single fracture plane in SUTRA and the parameters used to represent that plane and run the model do not produce spurious results. This method of representing planar fracture flow has therefore been applied subsequent numerical models.

9 SITE INVESTIGATION TECHNIQUES

The previous chapters have summarised both the nature of fluid and thermal transport in the Chalk and how to best represent them in models. To be able to construct a discrete numerical model in SUTRA that accurately represents the Chalk beneath a proposed site, field data on the Chalk structure need to be obtained. The most important parameters will be the number of fractures that are flowing, their distribution over the length of the open section of the borehole and the fracture hydraulic apertures.

To assist in determining these parameters a suite of standard and non-standard site investigation techniques is proposed. Some of these techniques would routinely be used when a borehole is drilled into the Chalk. The combination of the standard techniques, coupled with a tracer test and thermal test (devised for this thesis) should help to characterise the Chalk, at least to the extent that it can be represented with some degree of accuracy in a discrete numerical model. The proposed tests were carried out at a site in central London and the tests, results and interpretation are presented here.

The proposed tests require at least one and, in the case of the tracer test, two boreholes to be drilled at a site. The drilling/ casing of boreholes and the testing are expensive and this represents something of a Catch-22 situation. Drilling and testing implies that a client is already committed to a geothermal system, even though no tests have been undertaken at the site. However, the client can only finally commit once the tests have been undertaken and an assessment of the performance of the aquifer

completed. In some senses there is no way to resolve this. The only approach that can be taken pre-testing is to use 'typical' values for boreholes within the Chalk during the initial appraisal of proposed system. If the geothermal system, as planned, looks plausible then the decision to test and drill follows.

9.1 Suite of tests

It is proposed that the following tests be carried out a site to categorise the Chalk:

1. CCTV survey
2. Flow logging
3. Pumping tests
4. Tracer test
5. Thermal test

A brief description of each and the reasons for choosing the test follow:

CCTV survey

A Closed Circuit Television (CCTV) survey is routinely carried out over the entire length of a borehole that has been drilled in the Chalk. The survey normally serves two purposes: a method of checking the way in which the borehole has been drilled and cased and, which is of more importance to this thesis, as a method of locating subsurface structures such as fractures. Fractures can often be identified from CCTV images. The fracture depth beneath ground level and its aperture can be recorded. A CCTV survey can therefore provide information on fracture spacing (regular/irregular) and fracture apertures (dimensions, similarity over the depth of the borehole). The images provided by the CCTV survey do not indicate whether a

fracture is flowing or whether the fracture is laterally extensive. The fracture aperture measured during the CCTV survey may also be misleading as the fracture face at the borehole may have been damaged during drilling. It is more than likely that the hydraulic fracture aperture will be smaller than that measured during a CCTV survey.

9.2 Flow logging

A flow log should be conducted in both static and pumped conditions in a borehole. An impeller is lowered into the borehole and the flow rate of the impeller is recorded. Flow can, therefore, be measured at all points throughout the depth of the borehole. Flow rates in the borehole increase where fractures occur, this is particularly apparent when the borehole is pumped. If the increase in flow is fairly regular over the entire depth of the borehole then it can be assumed that many fractures are carrying the flow. Conversely, if the flow rate jumps at certain points along the borehole then only a few fractures are likely to contribute to the flow. The information from the flow log can be linked to that of the CCTV survey to identify which of the fractures recorded by the CCTV survey are flowing. The results do not however give an indication of the lateral extent of the flowing fractures. However, if flow logging and CCTV surveys are undertaken in both the abstraction and injection boreholes (if two boreholes have been drilled at the site) it may be possible to match flowing horizons and therefore by inference estimate whether fractures extend laterally between the two boreholes.

9.3 Pumping tests

Pumping tests are routinely used to prove the flow rate for a borehole. In addition, constant rate pumping tests enable the transmissivity of the aquifer to be calculated.

The transmissivity calculated from a pumping test in the Chalk is important because it provides an indication of the extent to which the Chalk displays anomalous properties. A higher than expected transmissivity may be evidence of increased fracturing or larger than expected fracture hydraulic apertures. Previous chapters have presented data on the expected transmissivity values for the Chalk. It can be assumed for the central London area that the median transmissivity is $250 \text{ m}^2/\text{day}$ (Monkhouse). If the results of pumping tests indicate transmissivity values significantly above this then it may be an indication that significant fractures exist. The transmissivity value from the pumping tests can also be used to determine approximate fracture apertures throughout the aquifer. If the results of the flow tests are used to estimate the number of flowing fractures then the approximate average aperture can be determined using the cubic law. This aperture can then be checked against the results of the CCTV survey.

9.4 Tracer test

Tracer tests are a method of measuring the velocity of water as it travels through an aquifer. The most effective test requires two boreholes to be drilled; one injection and one abstraction. At the injection borehole a known quantity of tracer (often fluorescein) is fed into the borehole. A detector is placed in the discharge line at the abstraction borehole and the time that the tracer takes to travel from the injection borehole to the abstraction borehole is measured. This can be used to estimate the velocity of the water, which allows the transmissivity of the aquifer and a range of possible fracture numbers and apertures to be deduced. See Barker (1985) for a full description of the method of interpretation. The results, used in conjunction with those of the pumping tests, narrow down the number and thus the aperture of fractures

that actually connect the injection and abstraction boreholes. The fracture apertures calculated using the tracer test can be checked against the images from the CCTV survey and the number of fractures checked against the results of the flow logs.

9.5 Thermal test

A thermal test is proposed here as part of the above suite. The test has been designed to understand the interplay between heat transport by conduction and convection. The ideal thermal test would be similar to the above tracer test – a heat pulse injection followed by detection at the abstraction borehole. However, the quantity of heat required to ensure detection at the abstraction borehole (over 100m away) would be impractical. There is a case to be made at sites where the heating and cooling equipment is still in place (a retrofit or during demolition) to connect the existing equipment to the boreholes. The existing system should be able to supply sufficient energy to ensure detection at the abstraction borehole. There is one example in London where this has occurred, although the results have not yet been officially published (Clarkson, 2009).

A more practical, although limited test is proposed here. It consists of heating a specified volume of water at the surface to a temperature sufficiently higher than the aquifer. A zone of high flow in the borehole is identified from the flow logs and isolated using packers. The heated water is then pumped into the packered section of the borehole. Once all of the heated water is injected, the flow is reversed and the same volume of water is abstracted. Throughout the test the temperature in the packered section of the borehole is recorded. The temperature of the packered section of the borehole during the abstraction period should correspond to the amount of heat

absorbed by the aquifer and therefore the extent to which the aquifer is behaving as a homogenous or fractured medium. The simplistic theory is that the greater the quantity of heat absorbed by the aquifer, the more homogenous the thermal transport characteristics.

9.6 Application to a proposed site

A large development is currently (2008) under construction in central London. An open loop geothermal system is planned to provide a significant quantity of energy for heating and cooling. Ove Arup & Partners (Arup) were appointed as consulting engineers to provide structural and geotechnical advice for the redevelopment.

In October 2005 Arup prepared, on behalf of the Client, a specification for the installation and testing of a single abstraction borehole and a single recharge borehole. WJ Groundwater (WJG) were appointed as Contractor to undertake this work. Arup was further appointed to provide site supervision of key site activities during construction of the wells, including grouting, acidisation and specified testing.

All the above tests were conducted at the site. The thermal test was to be conducted on a portion of the borehole that showed the highest flow rates, as detected by the flow meter.

9.7 The site

A geotechnical site investigation was carried out by Soil Mechanics in 2006. A factual report was prepared by Soil Mechanics on completion of the fieldwork, laboratory testing and groundwater monitoring.

The ground investigation confirmed that the downward geological sequence comprise Made Ground, River Terrace Deposits (clay and gravel) and London Clay. Further information on the downward geological sequence was obtained during the drilling of groundwater boreholes. This confirmed beneath the London Clay that the downward geological sequence comprised of the Lambeth Group, Thanet Sands and Chalk. A summary of the geology is provided in Table 9-1.

Stratum	Thickness (m)	Depth to base (m)
Made Ground	3.0	3.0
Black clay, contaminated	8.5	11.5
Terrace gravels	2.0	13.5
London Clay	15.0	28.5
Lambeth Group and Thanet Sands	27.0	55.5
Chalk	54	109.5

Table 9-1 Summary of ground conditions at the site

Two aquifers generally exist in the geological profile of the London Basin as discussed in previous chapters. The upper aquifer exists in the granular drift deposits and Made Ground that overlie the tertiary clays (London Clay and Lambeth Group). The lower aquifer includes the Chalk and the Thanet Sands, as well as the predominantly granular deposits towards the base of the Lambeth Group.

9.8 Borehole specification

The borehole was drilled using a rotary method previously used in exploiting the Chalk Aquifer. The drilling muds, additives and foams used were degradable and approved for use in potable water wells. Bentonite was not used as a drilling mud for drilling through the Chalk. Any water introduced into the well was to be potable water from the Thames Water plc supply.

The borehole was drilled to provide a minimum finished internal bore of lined and unlined sections of 350 mm. The drilling of the section through the Thanet Sand and into the Chalk was carried out in one shift. The top of the Chalk was identified and permanently cased to 5m.

The borehole was lined with minimum 350mm internal diameter bitumen enamel coated steel casing to API 5L standard. The open hole section was drilled to 55m into the Chalk. At the intended target depth, the borehole was flushed with clean water until there was no visible sediment in the return flow. Figure 9-1 illustrates a typical configuration for a borehole sited in the Chalk.

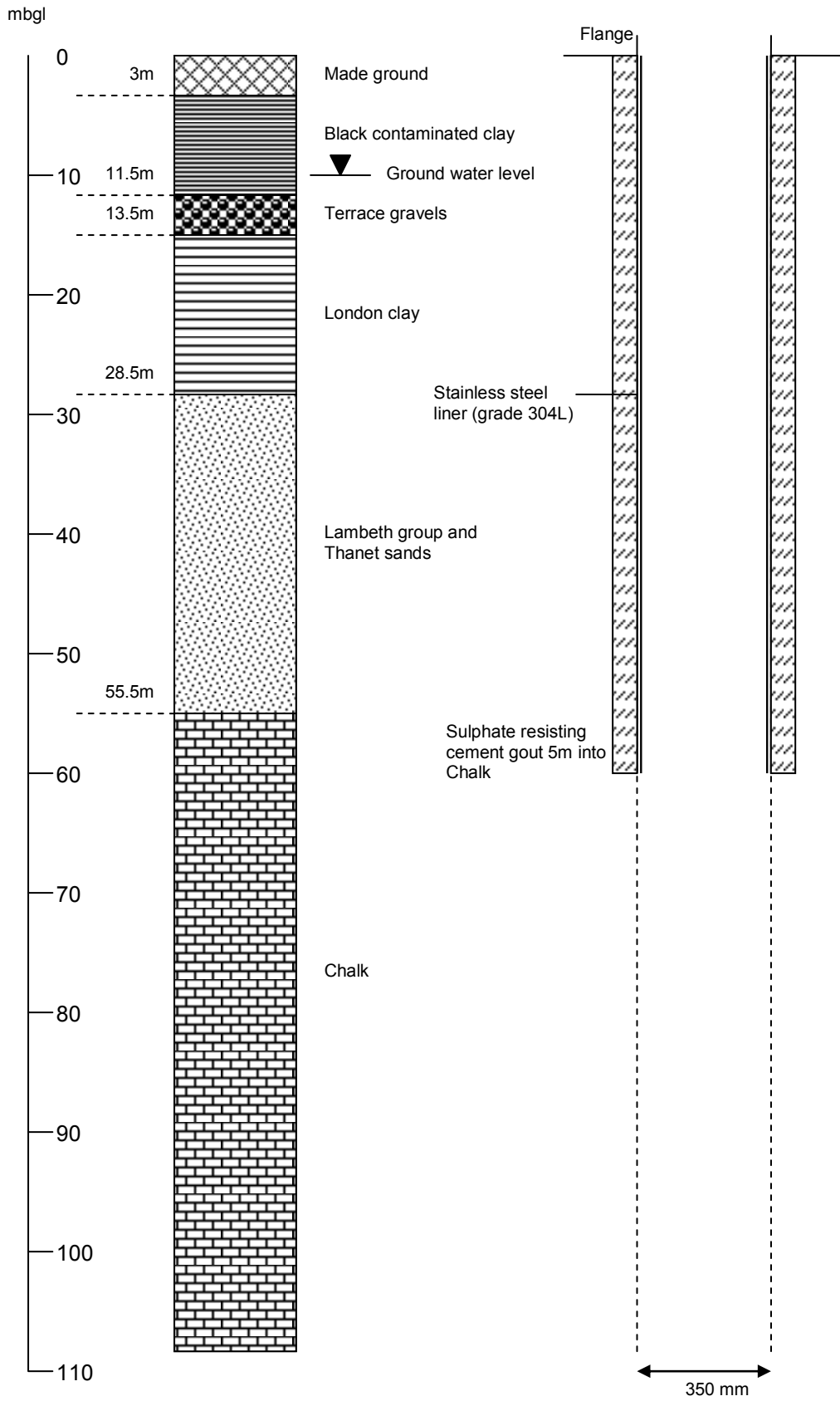


Figure 9-1 Borehole configuration

9.9 Initial Development and Geophysical Logging

Following completion of drilling, the borehole was developed by the following methods:

- High pressure water jetting of the open hole section to remove any disturbed Chalk residue
- Airlift pumping of the borehole to remove any sediment with flow rate measurement to allow crude estimation of the unacidised yield

Following initial development and geophysical logging the borehole was to be acidised.

9.10 Geophysical surveys

The following geophysical logging was undertaken by European Geophysical Services (EGS) following drilling of the well:

- CCTV
- Caliper
- Natural Gamma
- Fluid conductivity
- Temperature
- Flow

The later three items were undertaken for both static and pumped conditions. The results of the geophysical surveys undertaken in both boreholes are presented in Figure 9-2 and Figure 9-3.

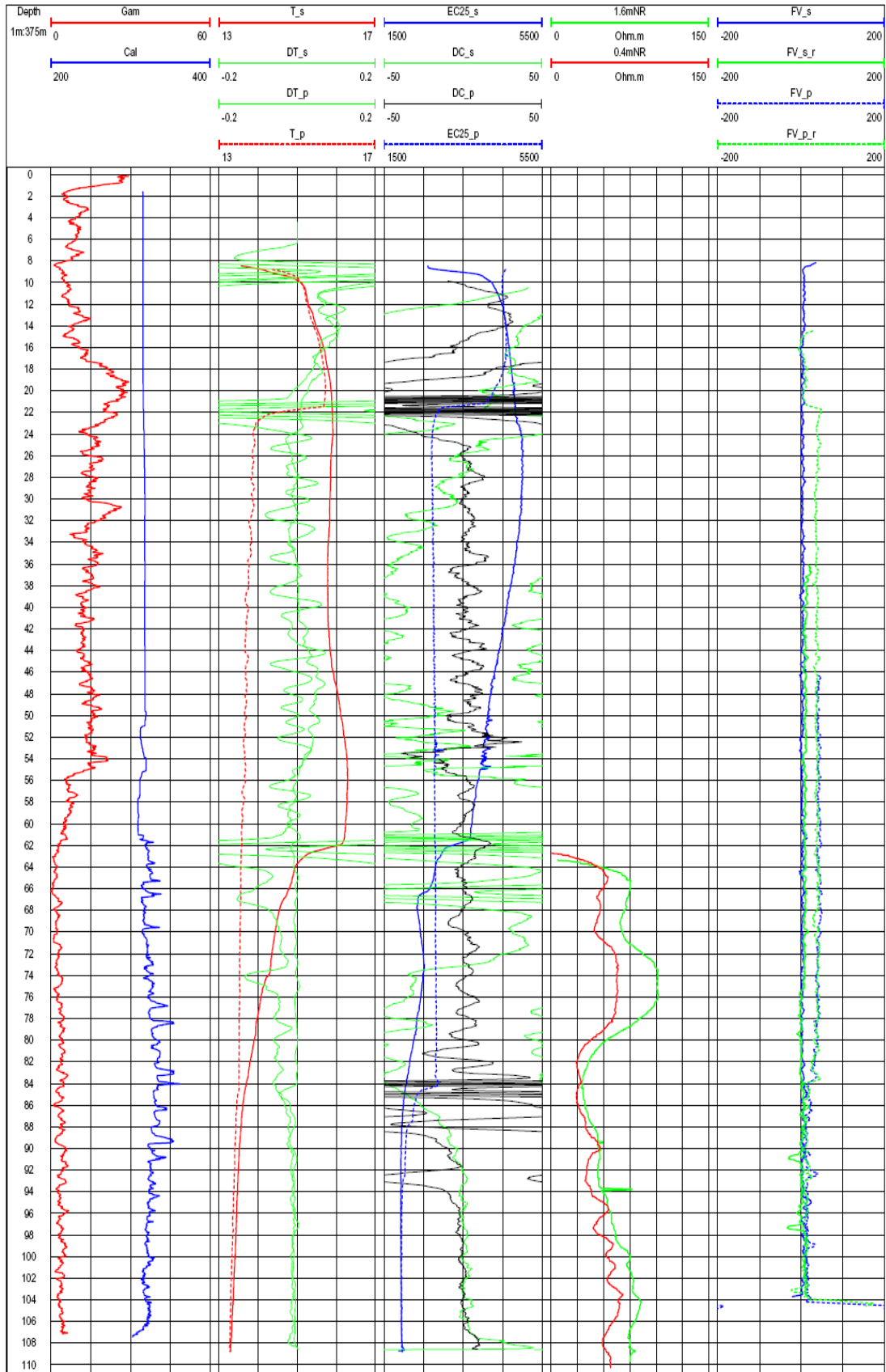


Figure 9-2 Geophysical survey – borehole 1

The trace shows that the casing diameter is typically approximately 310mm diameter. This diameter narrows between approximately 51m to 54m bgl and 55.5m to 61m bgl. This is thought to be a grout smear (also identified during the CCTV survey). The calliper traces show that the borehole is cased to approximately 62m bgl; this correlates with the CCTV survey and the installation records.

The trace shows that the open borehole diameter typically varies between 310mm and 360mm. Widening of the borehole, which could be related to presence of fractures, is noticeable at 78.5m, 83m, 84m and 89.5m bgl. The differential geophysical logs for fluid conductivity, temperature and fluid velocity show variation under pumped conditions are indicative of an area of flow into the borehole. This suggests that inflow horizons exist between 83m and 88m bgl.

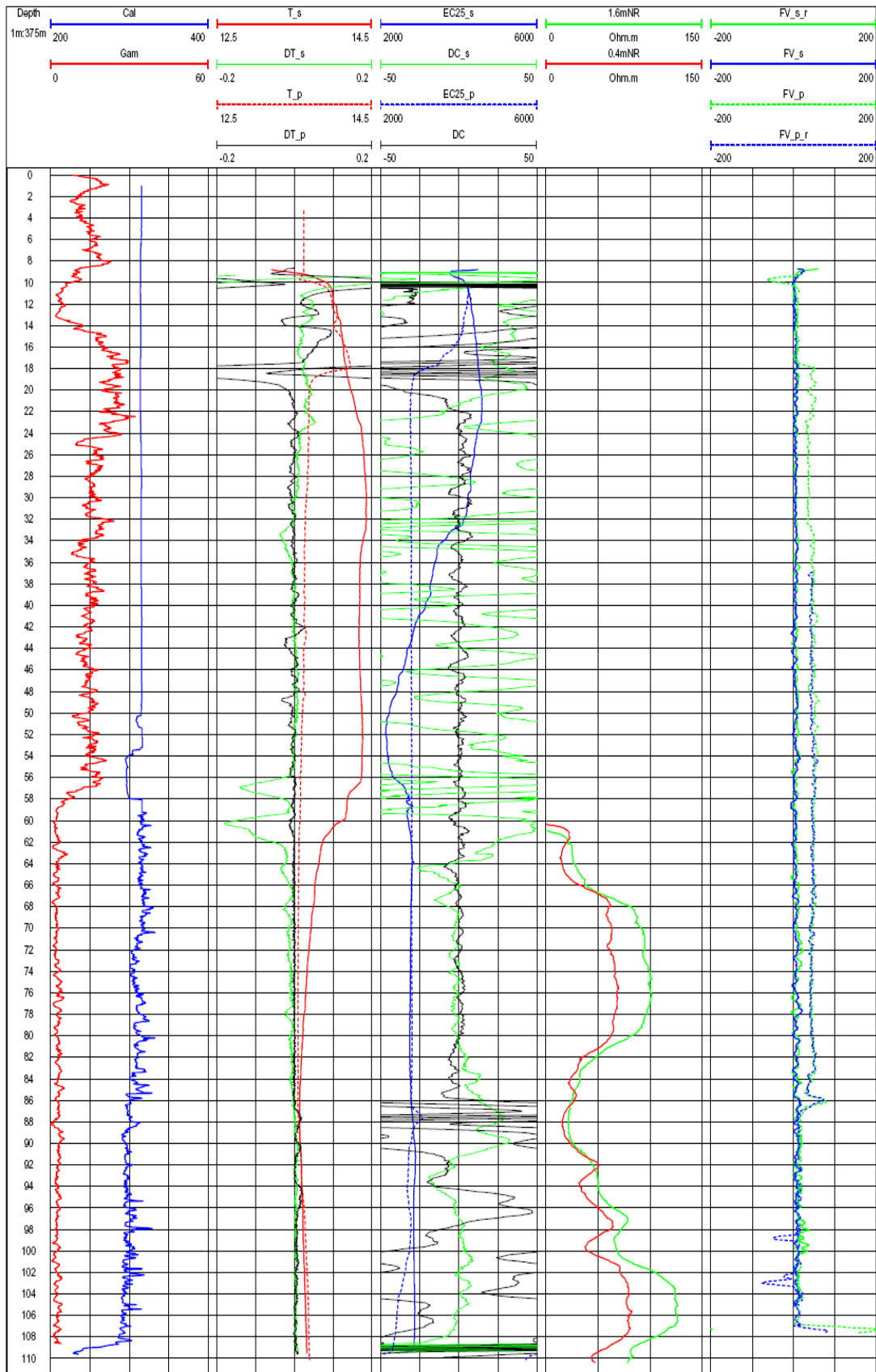


Figure 9-3 Geophysical survey – borehole 2

The trace shows that the casing diameter is typically approximately 310mm diameter. This diameter narrows significantly between approximately 50.2m to 57.5m bgl and 53.5m to 58m bgl, in some places to less than 300mm. This is thought to be a large grout smear up the borehole (also identified during the CCTV survey). The caliper traces show that the borehole is cased to approximately 60m bgl; this correlates with the CCTV survey and the installation records.

The trace shows that the open borehole diameter typically varies between 280mm and 330mm, generally becoming progressively narrower with depth. Widened areas of the borehole, which could be related to presence of fractures, are noticeable at 70.5m, 80m , 84.5m, 85.5m and 98m bgl.

9.11 CCTV Survey

A CCTV survey was undertaken in both boreholes following the initial development of the well. Observation of the CCTV images confirmed the integrity of the installed casing and the integrity of the joins between segments of casing.

At approximately 86m bgl a dark feature was observed in the wall of borehole 2, potentially a fracture (Figure 9-4).



Figure 9-4 CCTV survey, potential fracture at 86mbgl – borehole 2

Fractures were also identified in borehole 1 at a depth of approximately 84mbgl and further fractures at 80mbgl (Figure 9-5, Figure 9-6).



Figure 9-5 CCTV survey, potential fracture at 84mbgl – borehole 1

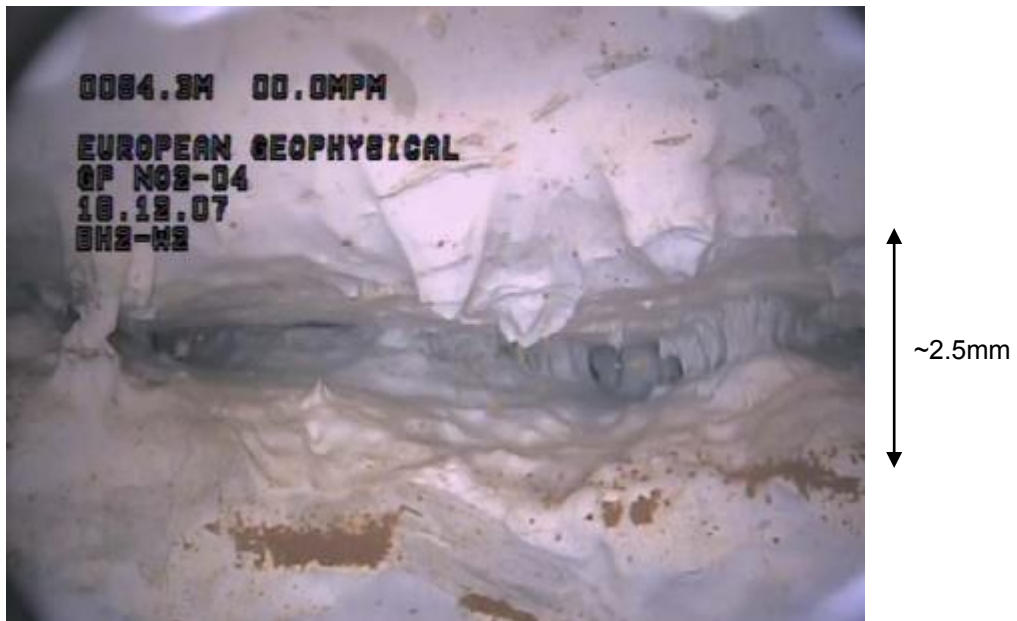


Figure 9-6 CCTV survey, potential fracture at 80 mbgl – borehole 1

9.12 Flow logs

Figure 9-7 is a close up of the flow logs for both boreholes during pumped conditions, at a depth of between 68 and 98 mbgl. There would appear to be a clear influx horizon where the flow rate increases, at approximately 86 mbgl. This is particularly apparent on the logs for borehole 2. This corresponds to the fracture detected at this level by the CCTV survey and helps to confirm that this particular fracture is not only flowing but carrying a significant quantity of the flow. Indeed, looking at the extended flow log over the whole depth of the borehole it could be said that this fracture is carrying almost all the flow.

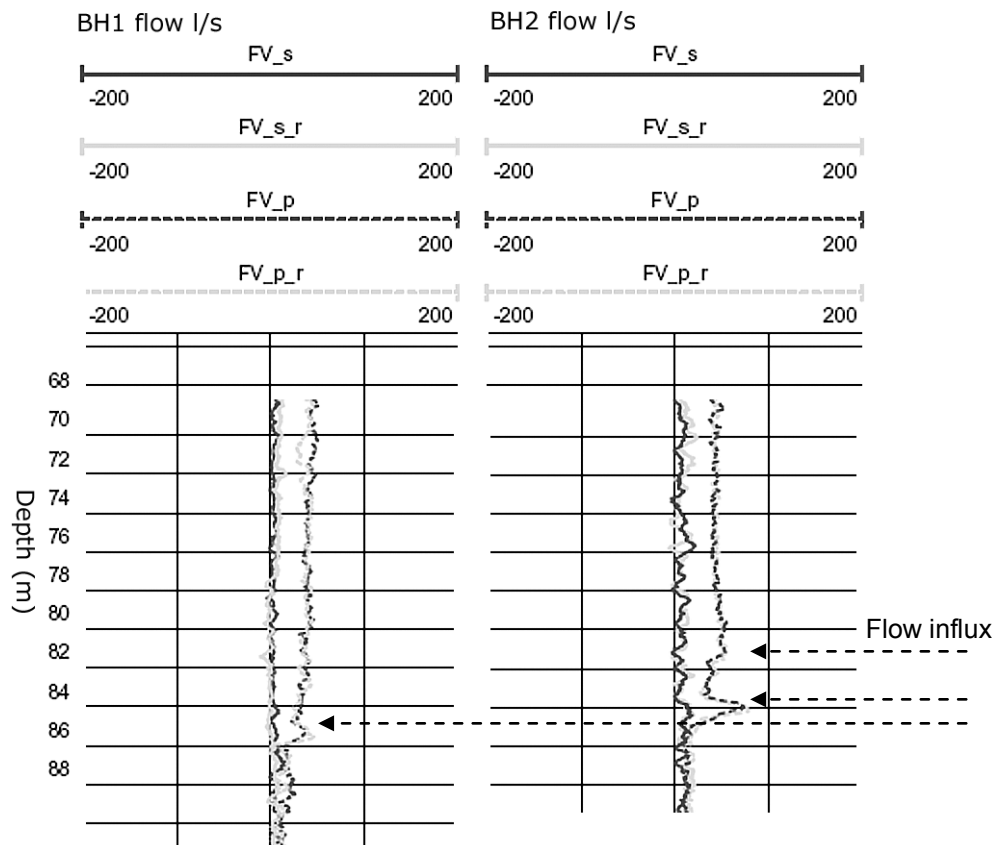


Figure 9-7 Close up of results from the flow logging (_s_ unpumped conditions; _p_ pumped conditions; _r_ recharge)

9.13 Pumping tests

9.13.1 Correction of groundwater level data

Due to tidal influence on the groundwater pressure in the Chalk aquifer, it was necessary to apply a correction to some of the data in order to analyse it. This correction was made to data collected during the step test to allow a more accurate analysis to be conducted. A baseline groundwater level was taken by calculating the average level between the high and low tide. The difference between this baseline level and the recorded level was calculated and this produced a correction factor for every 10 minutes. This correction factor was then applied to the step test data and resulted in either a deduction or addition, depending on the time since the last high or low tide.

9.13.2 Step drawdown tests

A step drawdown test was undertaken on each of the water wells, starting at a flow rate of 5l/s and finishing at 30l/s. Each stepped increase was 5l/s. Analysis of the data was undertaken using the Eden-Hazel method to establish the head loss in the borehole during abstraction (details in following chapter)

9.13.3 Constant rate tests

Two constant rate tests were undertaken, one on each of the boreholes at 20l/s. The 20l/s flow rate was selected as this proved (from the step drawdown tests) to be the maximum sustainable rate for the borehole. The maximum sustainable rate being defined as the maximum possible flow rate for an acceptable (minimum pumping cost) level of drawdown. Each test was run for 24 hours. The results of the tests were interpreted using Jacob's straight line analysis (details in following chapter).

9.13.4 Combined abstraction and recharge trial

The abstraction and recharge trial comprised abstracting from Borehole 1 whilst simultaneously recharging to Borehole 2 at a constant flow rate of 20l/s. Once the trial had commenced, the measured water level in the abstraction borehole (B1) was drawdown by 2.2m whilst the measured water level in the recharge borehole (B2) rose by 1.4m, giving a head difference between the two boreholes of 3.6m. The boreholes are positioned 106m apart. The linear hydraulic gradient between the abstraction and injection borehole is therefore 0.034 m/m.

9.13.5 Tracer test

The tracer test was undertaken by the British Geological Survey. 52 grams of fluorescein, dissolved in 20 l of water, was injected at a depth of 90 mbgl. The 20 l of tracer was flushed in with 30 l of water. The injection was complete over a period of 5 minutes. An in-line recording fluorometer was installed on a take off from the discharge line from the abstraction borehole. This instrument records tracer concentration (measured in millivolts) at pre-determined intervals, from 15 seconds to 1 hour. The millivolt readings are converted to a concentration using calibration carried out in the laboratory with known tracer concentrations. The conversion also takes into account the turbidity of the water, which is simultaneously measured by the instrument.

The background readings were very low, ranging from 0.1 to 0.9 ppb. This was considered to make the site suitable for use of fluorescein as a tracer.

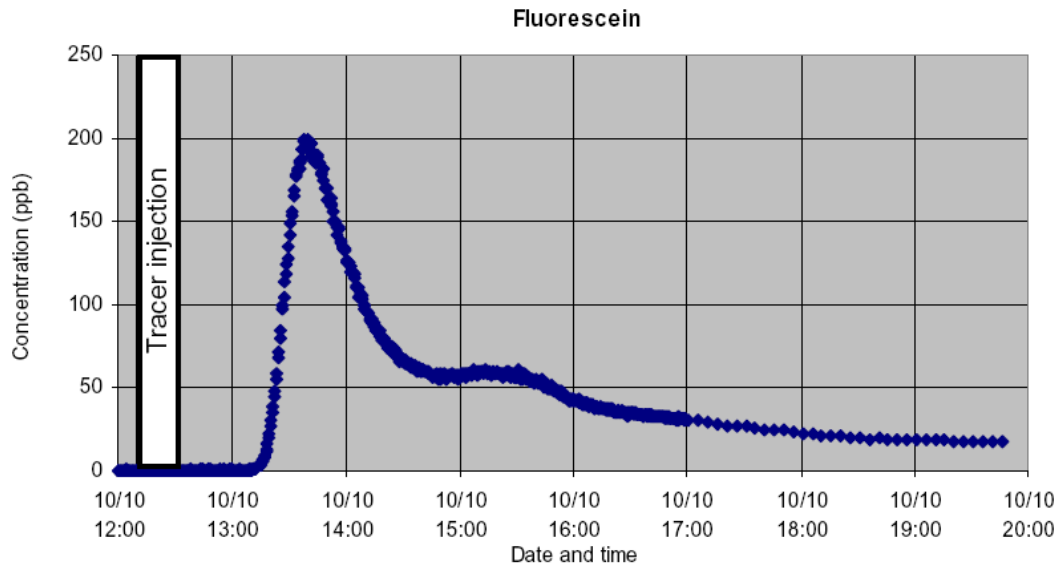


Figure 9-8 Tracer test response (courtesy of the BGS)

The results (Figure 9-8) show three interesting features. First, a clear rapid early breakthrough curve at the abstraction borehole. The first breakthrough occurs at 65 minutes after the start of injection, which is approximately 60 minutes after the tracer is first injected to the aquifer (as a result of the delay in transmission down the borehole in the injection pipe). The second is the apparent secondary breakthroughs at later times. Closer inspection of the secondary breakthroughs shows a periodic pattern with decaying amplitude. The secondary breakthroughs imply the recycling of the tracer around the injection/discharge loop. The third, and somewhat surprising result, is the smoothness of the breakthrough curves. A fracture network would be expected to give a ‘noisier’ response and this suggests flow in continuous and relatively uniform planes or channels. The data from this test are subject to interpretation in the following chapter.

9.13.6 Thermal test

The thermal test procedure was designed to be as simple as possible to install and operate. The test consisted of injecting heated water (upwards of 25°C) into a packered (3.66m) section of borehole. The packered section of borehole was chosen to correspond to the point in the borehole where the highest flow rates were recorded by the flow meter (9.2). In addition, the packered section length was chosen to ensure that the volume of water heated for the test would be significant enough to penetrate the rock to some degree and not just simply fill the borehole with heated water. Once the supply of heated water had been exhausted the pump would be reversed and an equivalent volume of water abstracted. The heated water for the test was stored within specially constructed, thermally isolated plastic containers with a total volume of approximately 6 m³ (Figure 9-9). The total injection time, based on an expected flow rate of 5 l/s was therefore 20 minutes.

The pump was placed within the packered section along with three thermistors; one at the base, one at the middle and one at the top of the section (Figure 9-10). Figure 9-11 shows the equipment and packer being lowered into the borehole.

During the test, the temperature of the injected fluid was monitored in the packered section of the borehole by means of the three thermistors. In addition, the flow rate was monitored and maintained at a constant rate.



Figure 9-9 Plastic insulated containers for heated water storage

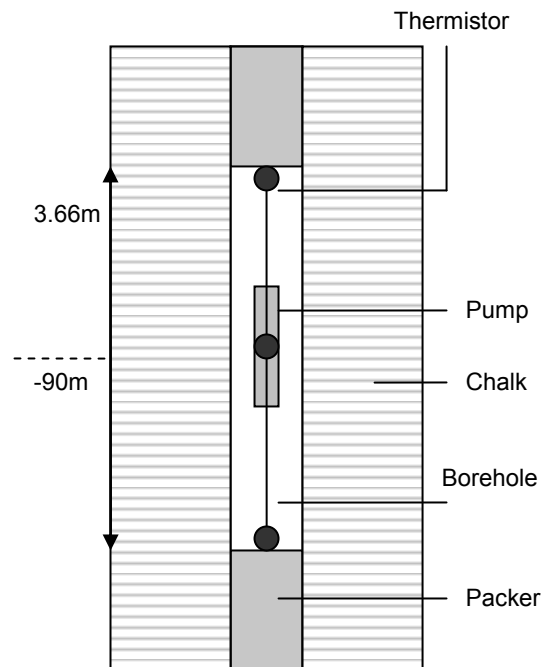


Figure 9-10 Schematic section of thermal test equipment



Figure 9-11 Equipment being lowered into the borehole

The results of the thermal test are presented in Figure 9-12. The flow rate was approximately constant at 5 l/s before and after the flow was reversed. The background temperature of the Chalk aquifer is 13.56°C. It is often the case that an aquifer temperature of 12°C is assumed for groundwater in the United Kingdom. However, at the depths involved for open geothermal systems in central London, temperatures are likely to be higher than 12°C due to the effects of the background geothermal gradient. In this case the temperature is 1.56°C higher.

The graph shows that after injection commenced, the temperature in the packered section of the borehole was not uniform with depth. This was also true during abstraction. The thermistor positioned in the centre of the packered section of the borehole recorded the highest temperature. The thermistor at the top of the packered section of the borehole recorded higher temperatures than that positioned at the base of the packered section.

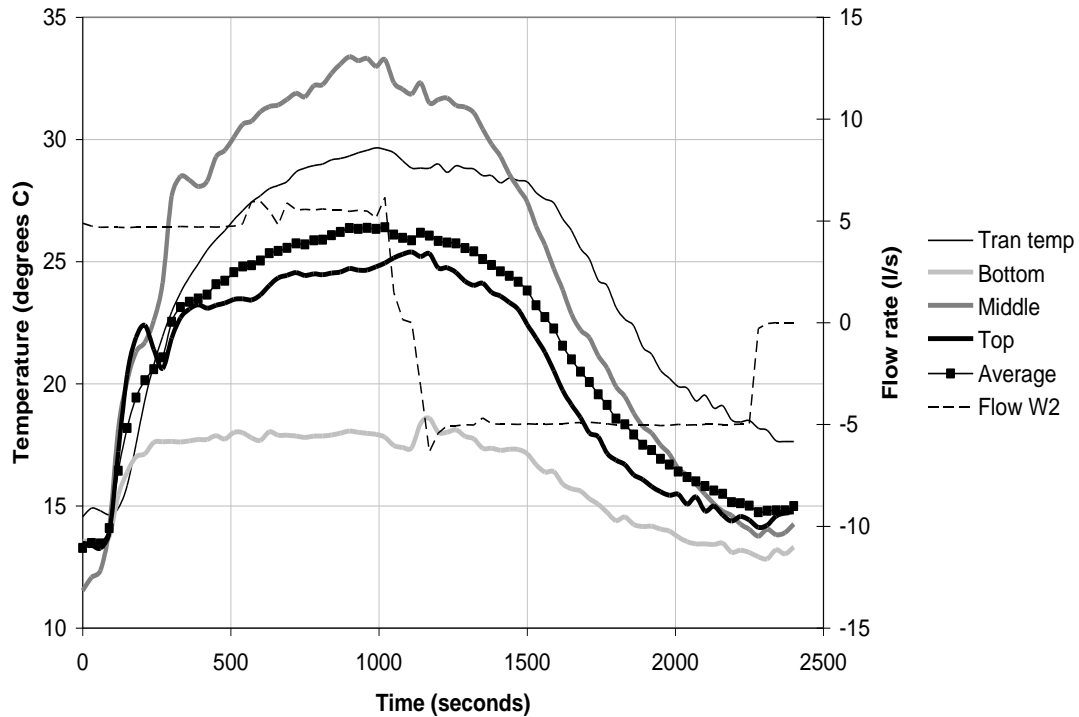


Figure 9-12 Results of the thermal test

A second thermal test was also undertaken over a different section of the borehole. Unfortunately this test recorded anomalous flow rates and the results had to be discarded. It was later discovered that there had been problems with the packer. A full interpretation of the successful test is presented in the next Chapter.

9.14 Summary

A suite of site investigation techniques were developed to help determine the fracture characteristics of the Chalk beneath a site in central London. These tests were then carried out at a site where a geothermal system was proposed. The results suggest that a small number of fractures carry the majority of the flow. The fractures identified by the CCTV correspond well to flow influxes recorded by the flow meter. In addition, it appears as though a flowing fracture links both the abstraction and injection borehole which would not necessarily have been expected before the tests

were undertaken. The smoothness of the tracer test response also indicates some degree of channel flow. The majority of the flowing fractures appear to be located over a small section (10m) of the open borehole at a depth of between 85 and 90 mbgl.

10 SITE INVESTIGATION INTERPRETATION

10.1 Flow logging and CCTV

The results of the flow logs show that most of the water flows into the boreholes at a depth of between 80 and 90 mbgl. This is indicated by a clear jump in the recorded flow rate. At other depths in the boreholes there is no evidence of significant water ingress, implying that a significant proportion of the total flow is occurring through the fractures located between 80 and 90 mbgl. This pattern is visible in both boreholes which suggests that the zone of flow or fracture is laterally continuous over a distance of 106m (the separation between the boreholes). The CCTV data tend to back up this theory, as the larger visible fractures occur at a depth of between 81 and 88 mbgl. Although these fractures are flowing, the apertures recorded by the CCTV survey (2 to 3mm) are unlikely to be the flowing apertures. A single fracture with an aperture of 3mm would have a hydraulic conductivity sufficient to carry 20 l/s (the flow rate of the test) with little head difference between the injection and abstraction borehole. The observed head difference between the injection and abstraction borehole during constant rate testing was 3.6m, implying that fractures with a hydraulic aperture less than 3mm are carrying the flow.

10.2 Pumping tests

The results of the pumping tests were interpreted using two methodologies:

1. Eden-Hazel's method for confined aquifers for step-test data.

Eden-Hazel's method uses short-term yield-drawdown data from the step tests. Therefore, the estimate of transmissivity is most applicable to the immediate vicinity of the boreholes where the relative transmissivity of the Chalk is increased due to the acidisation during borehole development. The Eden Hazel interpretation is shown in Figure 10-1.

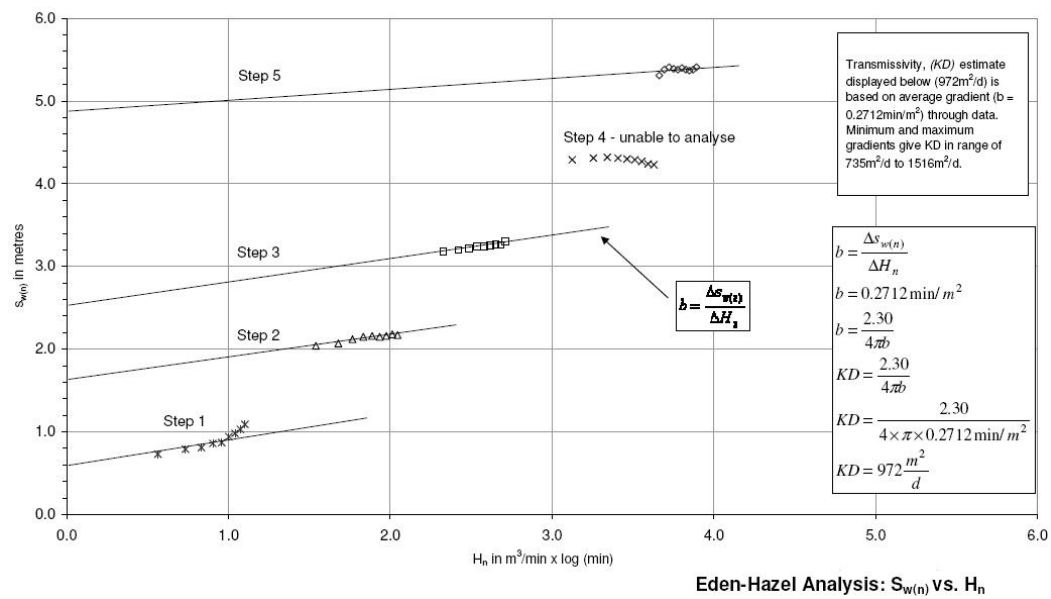
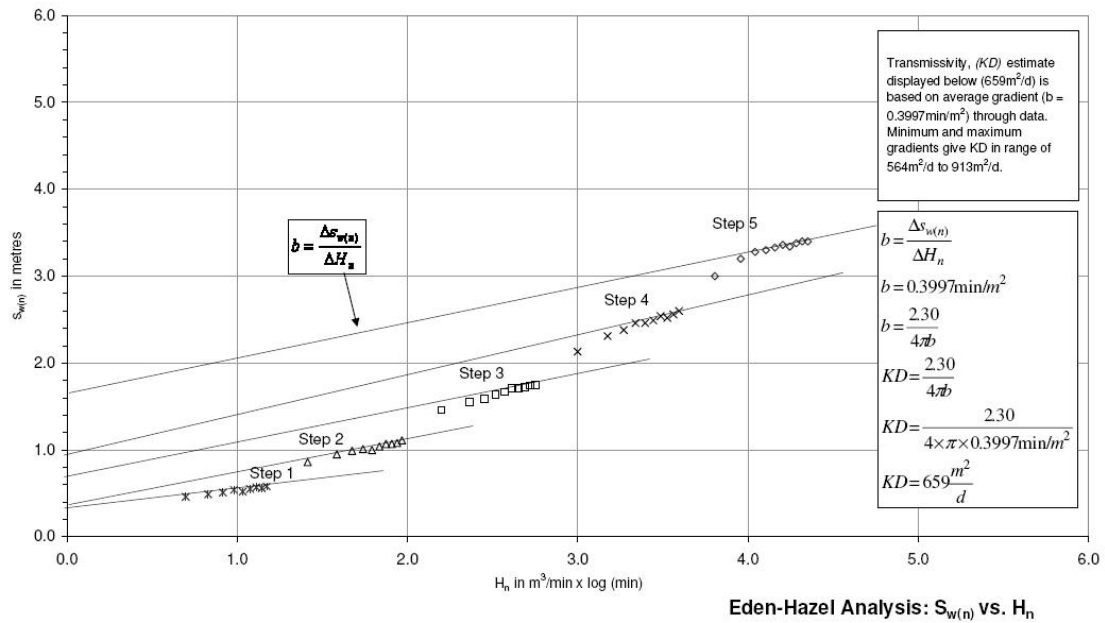
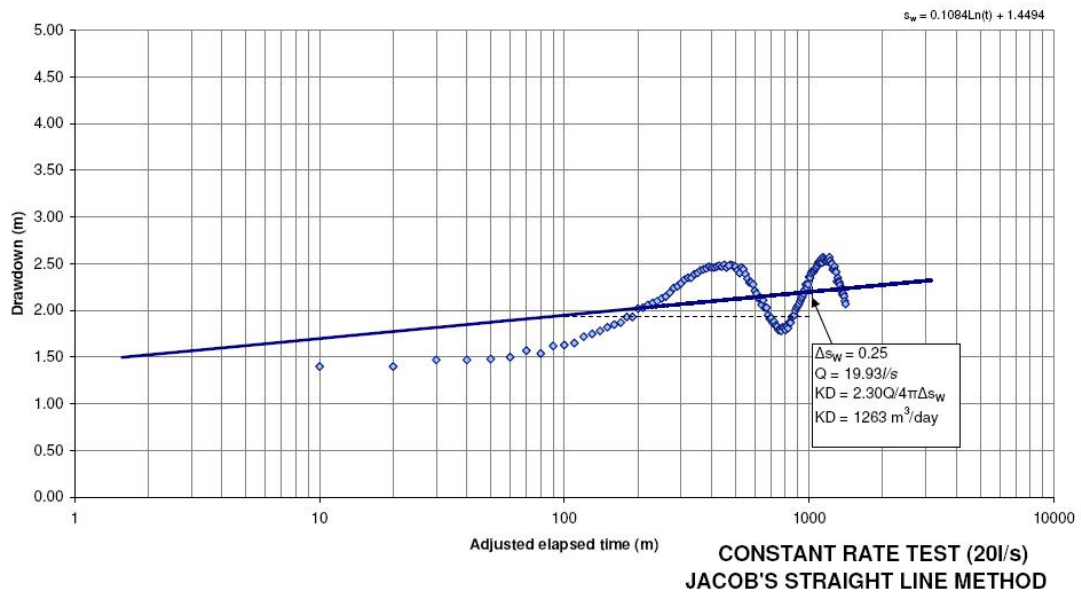


Figure 10-1 Eden Hazel Analysis for Borehole 1 and Borehole 2

2. Jacob's Straight-line method for data from single-boreholes constant discharge tests.

Jacob's straight line method uses late-time data from the constant rate tests from the pumped borehole. This method gives results which are considered to reflect the transmissivity close to the borehole. The Jacob's straight line interpretation is shown in Figure 10-2.



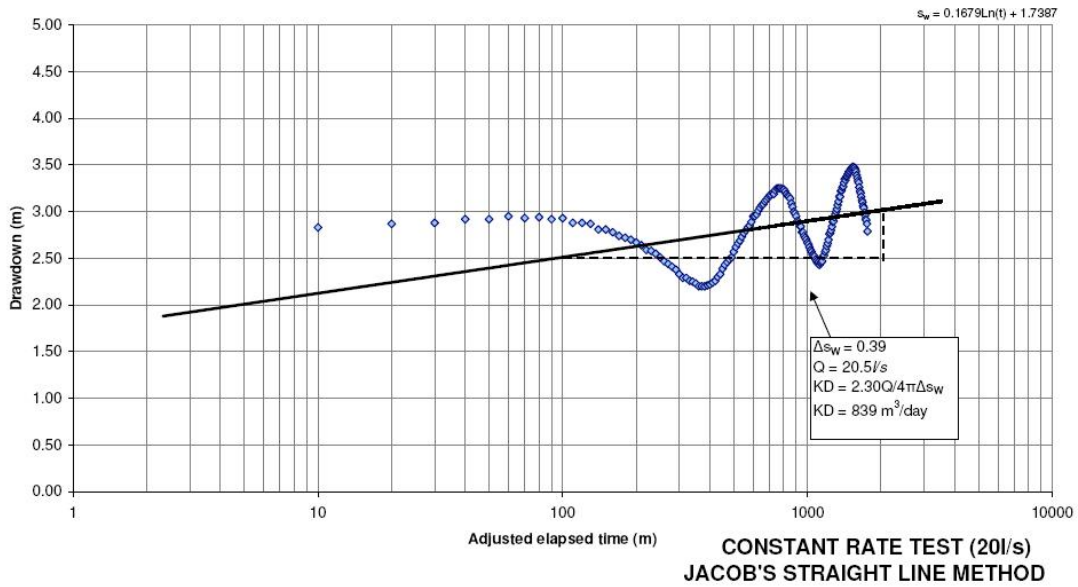


Figure 10-2 Jacob's straight line interpretation for Borehole 1 and Borehole 2 respectively

A summary of both interpretations is presented in Table 10-1.

Pumped borehole	Estimate of transmissivity (m ² / day)	
	Jacob's straight line method (data from pumped borehole)	Eden Hazel's method (data from pumped borehole)
B1	1263	659 to 913 Average 564 m ² / day
B2	839	972 to 1516 Average 735 m ² / day

Table 10-1 Summary of calculated transmissivity

The upper values of calculated transmissivity (1,000 to 1,500 m² / day) from the Jacob and Eden-Hazel methods are high when compared to those suggested by Monkhouse (2001) for the confined Chalk (250m²/day). There will be some exaggeration of the

far field transmissivity by both methods. However, the data still points towards a higher than expected transmissivity for the Chalk at this site implying a greater degree of fracturing than would normally be expected (either larger apertures or more fractures than expected carrying the flow).

10.3 Tracer test

The formula for the first breakthrough time across a doublet borehole system with constant rate injection/discharge of Q with no mechanical dispersion and separation distance L in a homogeneous medium is (Muskat, 1937):

$$t_b = \frac{\pi \phi b L^2}{3Q}$$

Eq 10-1

where ϕ is the porosity of an aquifer of thickness b . For clean fractures the porosity can be interpreted as unity and b as the aperture. The first breakthrough occurs about 1 hour after initial injection of the tracer to the aquifer (note injection time to the aquifer has been adjusted from start of injection at ground surface to account for the injection procedure adopted). Using equation 1 yields an apparent aperture of 5.8mm.

A transmissivity of about 1000 m²/d has been calculated based on the interpretation of the head differences between the boreholes during pumping. To satisfy the combined transmissivity and aperture constraints presented by the pumping and tracer tests implies that about 4 equal fractures of approximately 1.5mm would yield the appropriate breakthrough.

This calculation assumes that the hydraulic aperture and the mechanical aperture for the fractures are the same. Whilst this condition is not confirmed, it has been adopted as an appropriate initial working hypothesis for the modelling interpretation.

This calculation also assumes that the fractures are planar rather than channelled. To test these assumptions it is necessary to do more than simply investigate the first breakthrough time, it is necessary to model the full breakthrough curve. This has been carried out using a particle tracking model to model conservative tracer breakthrough to the discharge borehole in steady-state flow conditions (analytically modelled) around a doublet borehole in an infinite aquifer. The adoption of a steady-state approximation for the flow geometry should be sufficiently accurate given the low storage coefficient for confined fractured chalks and the lateral extent of the Chalk.

Breakthrough curve analysis was undertaken assuming no rock matrix diffusion. Dispersion, the potential for flow loss down the borehole to the deeper flow horizons and recycling of the fluorescein was allowed. The modelled properties obtain a good calibration (Figure 10-3) assuming that there is a flow loss of about 30% to the lower horizons of the injection well (this is consistent with the flow data shown earlier). The calibrated model presents the following features:

1. The shape of the first breakthrough curve is well matched to the observation data.
2. The timing and amplitude of the secondary breakthrough curves is well matched to the observation data.

3. The decay of the secondary breakthrough curves is only slightly lower than the decay rate observed in the actual tracer response but the total loss of tracer is less than indicated in the observations.

The results indicate that the assumption of Darcian flow in homogeneous planar fractures is a good approximation of the real conditions for this particular site. The required magnitude of the longitudinal dispersivities indicates that the fracture apertures show some heterogeneity but that this is most likely not derived by large scale channelling features. The results also indicate that the tracer lost to the lower borehole section does not reach the discharge borehole during the first 7 hour period of the tracer test. Feature 3 suggests a further net loss of material that is not identified by the model. During calibration it was not possible to increase the downflow loss of 30 percent further without underestimating the magnitude of the first breakthrough peak. Two possible causes for this are rock matrix diffusion and possible regional scale heterogeneity increasing the lengths of some flow paths between the boreholes during pumping.

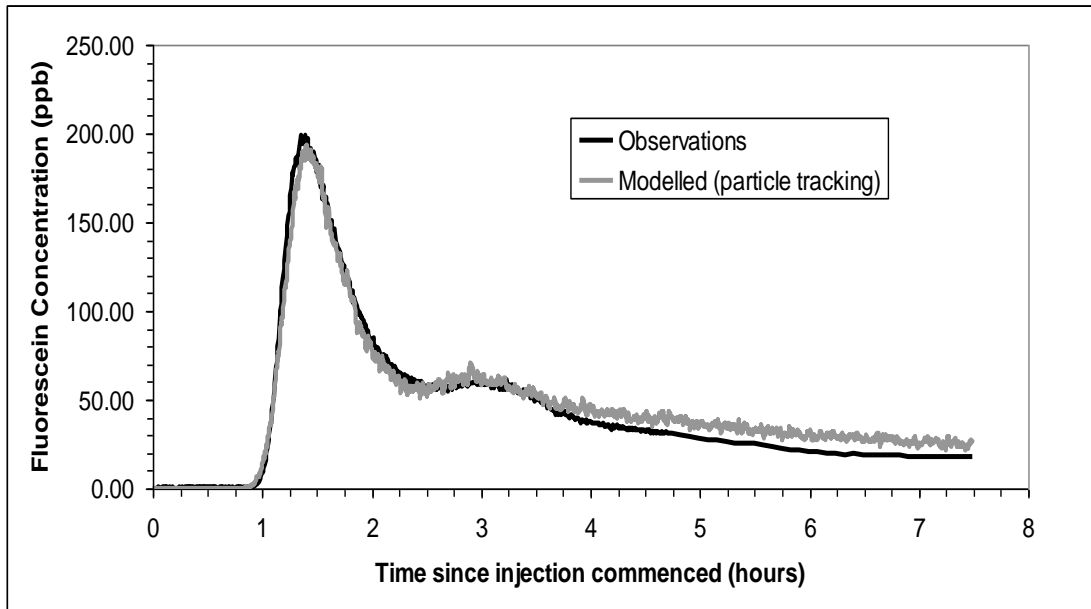


Figure 10-3 Calibrated versus observed breakthrough tracer concentrations at the outlet of the doublet discharge borehole.

The results of the modelling indicate that about 70% of the injected water is travelling through the fractures in the upper section of the Chalk. The model suggests a total aperture of 7 mm and, therefore, assuming that 70% of the transmissivity (i.e. 666 m²/d) is provided by the upper section and uniform fracture properties, then roughly 7 fractures of aperture 1.1mm are required to meet both the transmissivity and fracture porosity constraints. This figure is rather different from the first breakthrough time analysis (ignoring the full tracer response) and will have the effect of increasing the time to thermal breakthrough under the operation of the doublet borehole for thermal energy storage.

Typical values for rock matrix diffusion at fracture walls for limestone have been estimated in a study by Greswell et al. (1998) to be around 3×10^{-6} m²/d. Based on

this value, it is possible to estimate the maximum amount of tracer that could be lost by this process over the duration of the test if 7 fractures are assumed. When calculated this amounts to about 28 percent of the injected volume after 7 hours. A figure of 30 percent is needed to explain the apparent loss and therefore rock matrix diffusion could provide a possible explanation for the enhanced decay.

Whilst each of these results must be considered cautiously, the tracer test has provided potentially very useful information for the determination of the physical system that controls thermal breakthrough.

10.4 Thermal test

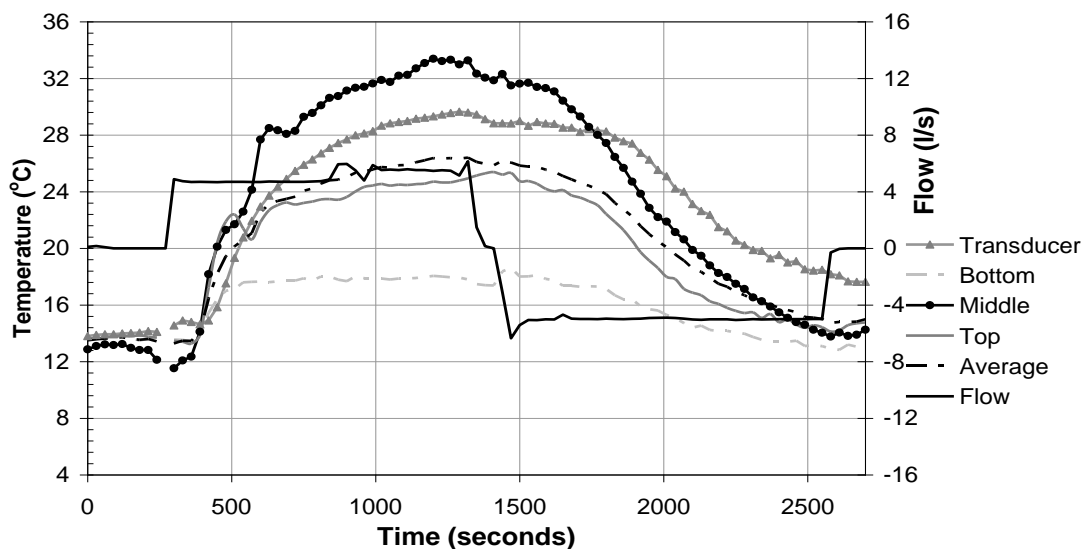


Figure 10-4 Results of the thermal test

The results for the 3 thermistors are interesting in so far as they show remarkably different magnitudes of response. The highest temperatures are recorded in the mid section, while the lowest are recorded at the lower section with the upper section showing a rise in temperature intermediate between the other two. The heated water

was injected at the midpoint of the packered section. In addition, the temperatures only gradually increase towards the injected water temperatures during the test and on cessation and reversal of flow, they show a gradual response to the reversal that is rather different from the typical recovery shape as would be expected for simple heat injection and withdrawal in a single fracture. The gradual rise in temperature cannot be explained by thermal losses in the injection pipe and as there is apparently little mixing in the open section of the packered borehole and the volume of the open section is much smaller than the injected volume, it cannot be explained by manifold type mixing. Another explanation is required to resolve the apparent thermal behaviour of the experiment.

Figure 10-5 shows the arrangement of the packers, pipework and the pumps in the borehole. This figure provides the information to the processes controlling the form of the temperature observations. If it is assumed that flow is to one or a few localised fractures below the inlet to the pump, then the water in the borehole between the packers will be effectively stationary other than between the outflow from the pump and the fractures. It is important to note that this interpretation ignores local thermally driven flow cells, which may play a role in determining the temperature distribution within the packered section. The pipework transmitting the inflow down to the midpoint of the packered section permits heat to be transmitted by thermal conduction to the stationary water in the annular space surrounding it. Thus, during injection the upper half of the packered section will be heated. As the pump has a larger diameter than the pipework above and because heat transmission of metals is high relative to water (and the annular space around the pump is smaller), the water in the annular space around the pump will be heated more quickly than the

water above the pump, leading to higher temperature rises. At the base of the packered section, a similar heat source is not present and the temperature rises will therefore be much lower. To test whether the concepts identified here explain the results, a highly simplified model (excluding thermal convection in the annular space) was built to include the main elements of the borehole as shown in Figure 9. The thermal properties used are presented in Figure 10-4. The data used in this Table are taken from standard values presented in the literature and on the web (The Engineering ToolBox, 2005). The modelling results are shown in Figure 10-6.

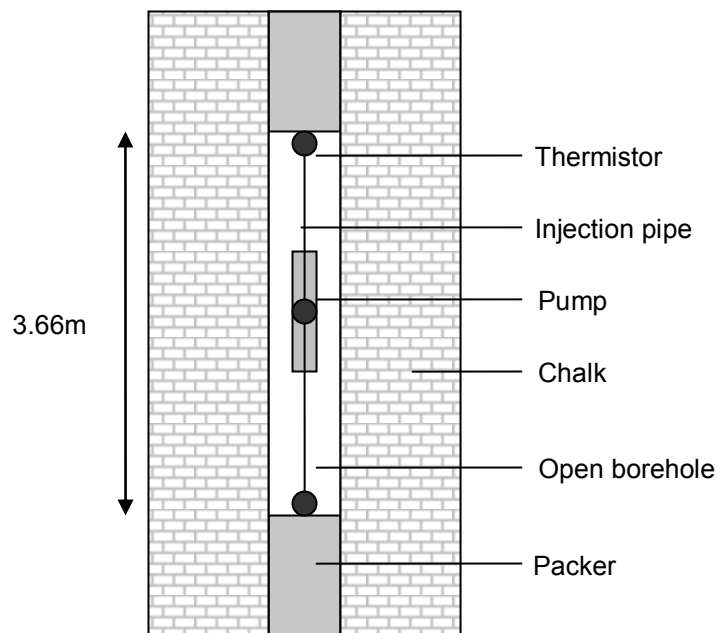


Figure 10-5 Basic elements of the thermal test

Material	Thermal Conductivity kJ/m/s/°C	Thermal Capacity kJ/m³/°C
Water	6.1×10^{-4}	4.18×10^3
Limestone matrix	2.0×10^{-3}	1.56×10^3
Steel	9.2×10^{-2}	3.62×10^3

Table 10-2 Material properties used to model the thermal injection test

Whilst the results are imperfect, as the model does not account for convective processes, the similarity in the response of the upper and middle temperature sensors to the model results suggests that the explanation given here for the observed results is probably correct. The model failed to reproduce the lower temperature profile suggesting that either a part of the internal construction of the packer/pump system is not properly represented in the model or alternatively there is a very slow discharge to the aquifer close to the base of the packered section. Neither will have a strong influence on the use of the model results.

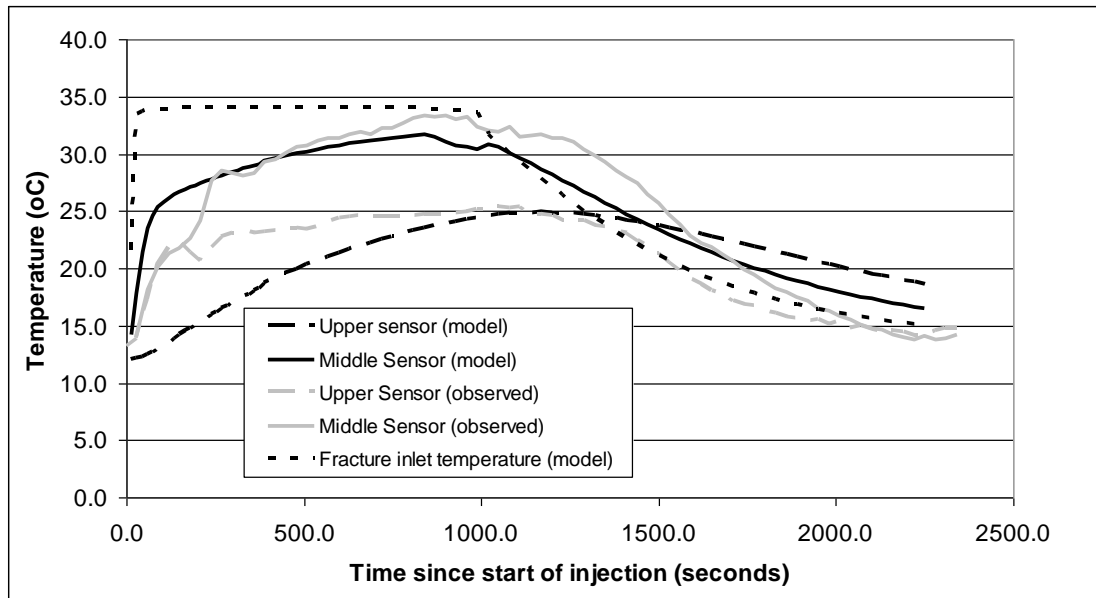


Figure 10-6 Modelled versus observed response for the thermal test.

The thermal modelling analysis carried out here illustrates two rather important points and areas of caution. First, the sensitivity of the modelled temperature variations to sensor location in the annular space and to the modelled processes taking place that drive heat flow in this region is very large and therefore caution is needed when drawing inferences from the modelling for the interpretation of thermal properties. For fractured rock masses, the adoption of within packer monitoring is essentially inappropriate under these circumstances. Second, the recovery of the temperature in the borehole provides some evidence for the degree of fracturing in the packered section only if the thermal properties of the rock are known.

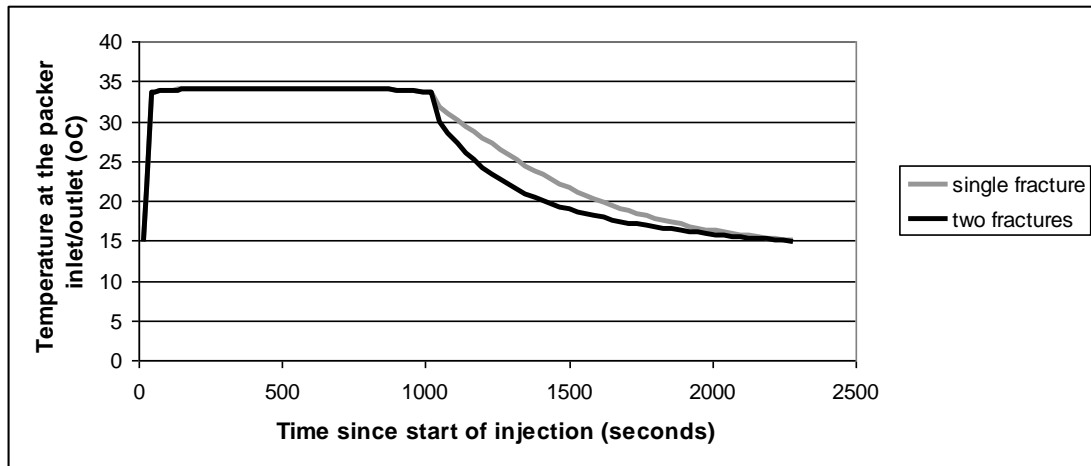


Figure 10-7 Modelled results for a single fracture and two fractures.

The different responses during recovery for one and two fractures is shown in Figure 10-7. There is a marked increase in the thermal losses to the matrix from the two fractures compared with the single fracture case, indicating that this test can support the assessment (at least locally to the injection well) of the frequency of fracturing. However, for a valid interpretation of the fracture frequency, the modelling does require *a priori* knowledge of the rock thermal properties. Such knowledge does appear to be available and the current experiments show that in this case, the adoption of standard literature values for the thermal properties of chalk and the borehole construction materials yield similar results to those observed. Nevertheless, the full results suggest that thermal heating tests are most useful when they are accompanied by a tracer test to acquire an initial appraisal of the fracture frequency and property data. Thus, the thermal test does provide a valuable confirmation of the applicability of the literature derived values for thermal conductivity and heat capacity once an understanding of the flow geometry is available. It is also reasonable to infer from the combination of the tracer and thermal test results that an adequate understanding of the fracture systems is essential to prove the value of a fractured rock site for

geothermal energy storage and recovery. Moreover, it appears from the present results that a combination of tracer and thermal testing supported by use of existing data on thermal properties for many of the UK rock types is sufficient to provide the required information for assessment of both the short term risks and the longer term behaviour of the aquifer under an applied cyclical thermal loading.

10.5 Summary

The testing has identified that a small number of fractures carries the majority of the flow. CCTV and flow logging identified the approximate location of some of the fractures. Tracer testing (fluorescein) proved to be the most successful method of categorising the fractures.

Two methods were used to interpret the results of the tracer testing. The first method used a simple interpretation based on the breakthrough time. This interpretation concluded that 4 fractures, each of 1.5mm would be a good approximation for the flow. The second interpretation, that modelled the full breakthrough curve, concluded that flow was carried by 7 fractures, each of 1.1mm.

The interpretation of the results of the thermal test showed that for such a test to provide conclusive results, observations of the integrated thermal outputs during recovery (i.e. the temperature of the recovered discharge) would be needed. The results suggest that a thermal heater test of the type described would on its own provide insufficient evidence for assessing the risk of adverse thermal breakthrough and that the combination of the tracer and thermal testing is the most effective testing regime for a fractured rock such as the Chalk.

11 APPLICATION OF A NUMERICAL MODEL TO A PROPOSED SITE

The preceding chapters have shown that there is a need to understand the interactions between an open loop geothermal system and the Chalk aquifer. The principal areas of discussion have focused upon the representation of fracture geometries, fluid flow, thermal transport, the appropriate application of numerical models and the development of site investigation techniques to provide suitable parameters for use in numerical models.

This chapter uses the results of the suite of site investigation techniques as the basis for a numerical model that represents, as much as is realistically possible, the thermal transport in the Chalk beneath a proposed site. The intended heating and cooling loads for a planned building for the site are then applied to the numerical model to investigate both the short term and long term sustainability.

11.1 Parameters

11.1.1 Building heating and cooling demands

For most new buildings, the heating and cooling demands are calculated using one of a number of available codes, most notably IES (Integrated Environmental Solutions). The output of these codes is used to size the equipment for heating and cooling the building. Outputs are often in the form of electrical loads (based on standard performance figures used for the equipment to be used in the building) or thermal loads, to which system performance figures must be applied to determine the quantity of energy that is eventually taken from or rejected to the ground.

Heating and cooling loads for the proposed building were calculated using IES and the output provided by the building Mechanical and Electrical engineers. These were then re-calculated using an estimated Seasonal Performance Factor (SPF) for the geothermal system (the SPF is the expected COP of the geothermal system throughout the year). The building loads are therefore transformed into quantities of energy rejected to the ground and energy abstracted from the ground. For this building, an SPF of 4.0 was chosen as the system. The example calculation below shows how the building loads alone can be misleading and that an annual bias towards heating in the building does not necessarily correspond to a net withdrawal of energy from the ground.

Example building:

Annual heating: 30,000 kWh.

Annual Cooling: 20,000 kWh.

Imbalance in building: 10,000 kWh heating

Applying an SPF of 4.0:

Annual energy supplied by ground for heating ($30000 / (SPF / SPF - 1)$): 22,500 kWh

Energy rejected to ground by cooling ($20000 * (SPF / SPF - 1)$): 26,667 kWh

Imbalance to ground: 4,167 kWh rejected to ground during cooling

In the above example, the building has a net demand for heating. This suggests that there will be a net withdrawal of energy from the ground over the year. However, re-calculating the data using the SPF shows that, in fact, the building energy loads result in a net rejection of heat to the ground. This is because during cooling, the system is

rejecting both the energy from the building and the electrical energy that has been used by the heat pump during cooling. The above calculation assumes that there is no direct cooling provided by the system. With direct cooling only the energy from the building is rejected to the ground.

For the proposed site, the preliminary design was for a cooling dominated system with a net heat rejection (taking the COP of the system into account) of 1,500 MWh/ year. If complex hydrogeology is ignored, it is possible to make an initial estimate of the long term sustainability of the proposed design based on the thermal storage capacity of the ground beneath the site and the following broad assumptions:

1. The thermal conductivity of the rock is sufficiently low to ensure that energy is not transmitted by conduction further than 20m from any boundary of the site.
2. The background hydraulic gradient is sufficiently low as not to transport energy further than 20m from the boundaries of the site
3. The depth of aquifer exposed to energy input or output is the equivalent of half the open section of the borehole (flow is therefore not uniform throughout the aquifer)
4. The rock is fully saturated

For the given site dimensions and proposed heat rejection therefore:

Site area (site + 20m border)	14400	m ²
Depth of aquifer accessed	30	m
Volume of aquifer accessed	432,000	m ³
Porosity	30%	%
Volume of water	129,600	m ³
Volume of rock	302,400	m ³
Volumetric heat capacity water	2.16	MJ/m ³
Volumetric heat capacity rock	4.12	MJ/m ³
Total volumetric heat capacity	1,525,824	MJ/°C
Annual building rejection to ground	1,500	MWh
	(5,400,000)	(MJ)
Annual temperature change	3.54	°C
<i>Suggested building rejection to ground</i>	<i>200</i>	<i>MWh</i>
Recalculated annual temperature change	0.47	°C

Table 11-1 Estimation of ground temperature changes

The estimated annual temperature change in the ground (+3.5°C) could not be regarded as sustainable. Even if the proposed system rejected heat to the entire volume of available aquifer (the full depth of the borehole) the annual temperature rise would still be unsustainable. The designers of the system were therefore asked to re-visit the design to achieve a lower level of heat rejection to the aquifer. Using the

above method of calculation it was suggested that an annual heat rejection of approximately 200 MWh would prove to be sustainable.

The revised loads for the proposed building are summarised graphically in Figure 11-1. The data shows two trends:

- There is still a continual cooling demand (rejection to the ground) throughout the year. This is increasingly common in new buildings in the United Kingdom and reflects the combination of efficient insulation and the internal heat gains from computers and other electronic devices.
- The annual energy abstracted from the ground (including domestic hot water) is less than the amount rejected to the ground during cooling. This imbalance has been reduced to approximately 200 MWh rejected to the ground each year.

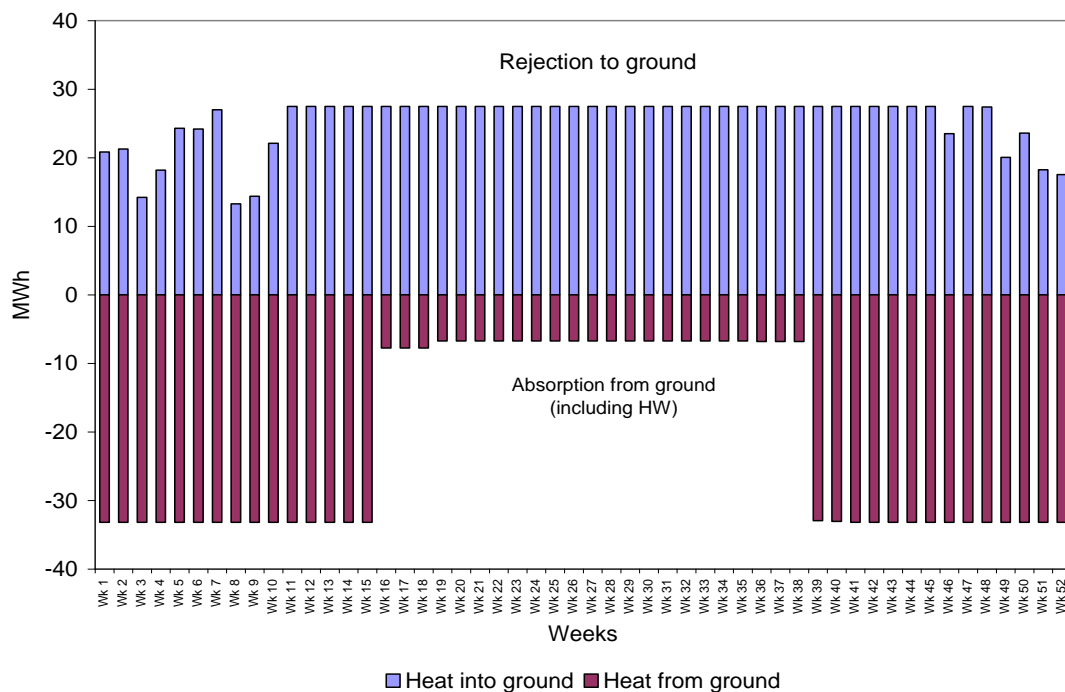


Figure 11-1 Heat rejection to the ground and absorption from the ground for the proposed system

The calculations shown in Table 11-1 predict an annual rise in ground temperature of approximately 0.5°C for a heat rejection of 200 MWh. Over the lifetime of the building (estimated 50 years) this would equate to a rise in temperature of 25 °C. Such a rise in ground temperature would clearly cause problems, both to the operation of the system and for the re-injection licence (which is normally limited to a re-injection temperature of 24°C). In practice however, the interaction will be more complicated than the simple model above. Over the lifetime of the building / system (50 years), groundwater movement will transport some of the excess energy away from the site (most likely further afield than the additional 20metres added into this calculation). In addition, energy will travel vertically into the formations above and below the aquifer by conduction, spreading the energy through a greater volume of ground than is modelled here. The calculations therefore need to be improved upon to fully understand how the system will perform over the lifetime of the building.

To this end and to include the complex hydrogeology, the proposed system needs to be incorporated into a numerical model. This brings together both the theory and the data gathered during this PhD. To investigate how the system will perform in both the short and long term the energy figures shown in Figure 11-1 were used to construct the following models.

1. Peak heat rejection
2. Average weekly heat rejection and abstraction figures over one year
3. Annual imbalance of 200MWh heat rejection over the lifetime of the system (50 years)

11.1.2 Representation of hydrogeology

The previously discussed tests and results were those for the aquifer beneath this proposed building. Both interpretations of the tracer test suggested that the flow beneath the site is carried by less than 10 fractures. If we take the results of the tracer test as being the most accurate representation of the flow between the boreholes then a maximum of 7 fractures of 1.1mm aperture carry the majority of the flow. The flow logging implies that these fractures are located within a zone between 81 and 88 mbgl. If the fractures were considered to be equally spaced then there would be approximately 1 fracture per metre depth. However, there is no evidence to suggest an even or uneven spacing of fractures. Indeed, it may even be erroneous to suggest that all of these fractures are located in the zone of high flow. Conversely, it may be more appropriate to consider the fractures to be more closely spaced, as evidenced by the flow log for borehole 2 where the ingress of flow appears to be over a 3m zone. This would result in one flowing fracture every 0.4m.

To prevent the unnecessary construction of a large number of numerical models to represent all of the possible geometrical permutations it is worth considering whether the work by Bodvarsson (1982) could be used to reduce this number of possibilities. Given that we have known flow rates, distances between boreholes and possible fracture apertures we can place some constraints on the type curves generated by Bodvarsson.

Again, the key starting point is to determine the value of θ where:

$$\theta = \frac{\rho_f C_f b}{\rho_r C_r D}$$

The same values for density and specific heat capacity of the fracture developed in previous chapters can be used here. For our base case of 7 fractures over a 7m depth, b the aperture is equal to 1.1mm, and D (max) is 0.5m (a maximum fracture spacing of 1m). In this case $\theta = 0.00186$ which again, as developed previously, equates to the type curve for $\theta \leq 0.1$. Further, calculating a value of ξ where:

$$\xi = \frac{\pi r^2 (2 + \theta)}{\rho_w C_w q D}$$

The additional parameters for this site are radius r 100m and flow rate q 0.02 m³/sec. Therefore $\xi = 1.5$. If this value is put on the type curve developed by Bodvarsson (dashed line, Figure 11-2) it can be seen that for all possible intervals of time the thermal front will be homogenous in nature at the abstraction borehole. It can also be seen that this will hold approximately true for values of ξ down to 0.75 which would represent a fracture spacing of 2m. Therefore, provided that fracture spacings are less than 2m, for the given conditions, the thermal transport will be approximately homogenous in nature. This will therefore hold true for any spacing of 7 fractures within the given high permeability zone.

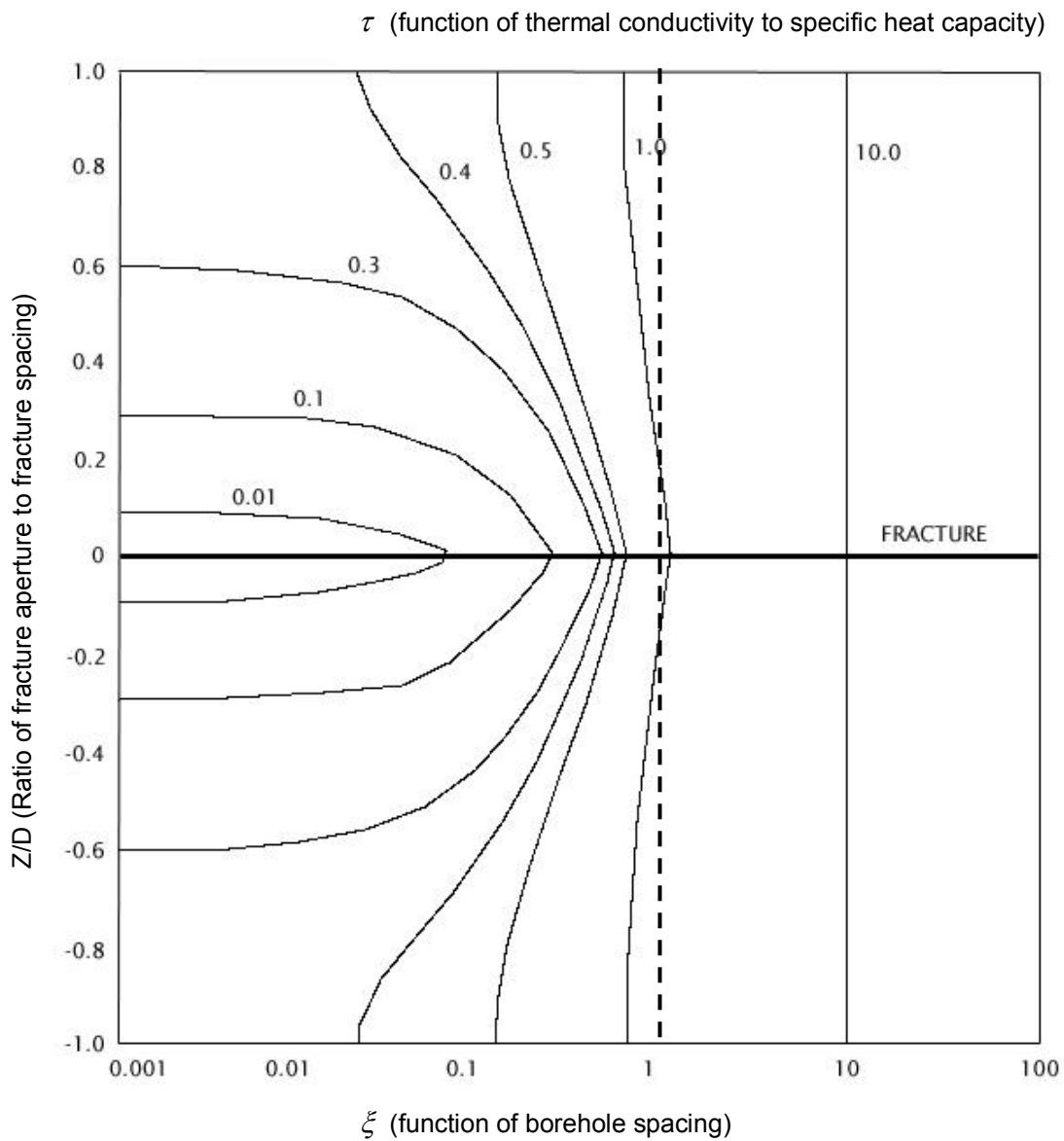


Figure 11-2 Type curve developed by Bodvarsson for $\theta \leq 0.01$

This puts an important constraint on the modelling. If the flow is assumed to be occurring in a narrow horizon (81 to 88mbgl) with equally spaced fractures of an aperture 1.1mm, the thermal transport can be represented by a homogenous medium of equivalent depth (7m) for the given borehole distances and flow rates. Only one numerical model therefore needs to be constructed, although the depth of the homogenous medium is still open to some degree of debate.

Conversely, if the flowing fractures are assumed to be spread evenly over the entire open section of the borehole (60m), the value of ξ drops to approximately 0.2. Reading off Figure 11-2 for a value of ξ of 0.2 implies that in this case, the thermal transport will be fracture dominated and the numerical model would have to consist of a number of discrete fractures.

This conclusion suggests that the results of the flow logs are extremely important when determining the thermal transport mechanisms and in the construction of subsequent numerical models. The flow logs are key in locating zones of flow/fractures and how such zones are distributed over the length of an open borehole. Although the term homogenous medium is used above, this does not imply that the entire aquifer can be treated as such. The numerical model will still have to be divided between a zone of high permeability (approximately 7m in depth) and the remainder of the aquifer (assumed to be effectively impermeable). For this particular site however, there is no need to divide the zone of high flow into discrete fractures.

11.1.3 Model construction

The numerical model to be constructed follows the same principles that were developed in previous chapters. That is to say that, where possible, symmetry is used to reduce the number of nodes and elements used by the model. The section of the aquifer where flow was recorded by the flow log is to be represented as a zone of high permeability, 7 m in total depth (Figure 11-3). The only plane of symmetry that can be used to reduce the model size is the vertical plane that divides the boreholes into two halves.

The dimensions of the model were chosen to ensure that the boundaries were sufficiently far away from the boreholes to ensure that no thermal interference occurred between the boreholes and the boundaries.

The injection borehole is to be located down gradient from the abstraction borehole. Although the hydraulic gradient is small relative to the head gradient between the injection and abstraction borehole, over 50 years the gradient will take some of the rejected heat away from the site and the abstraction borehole.

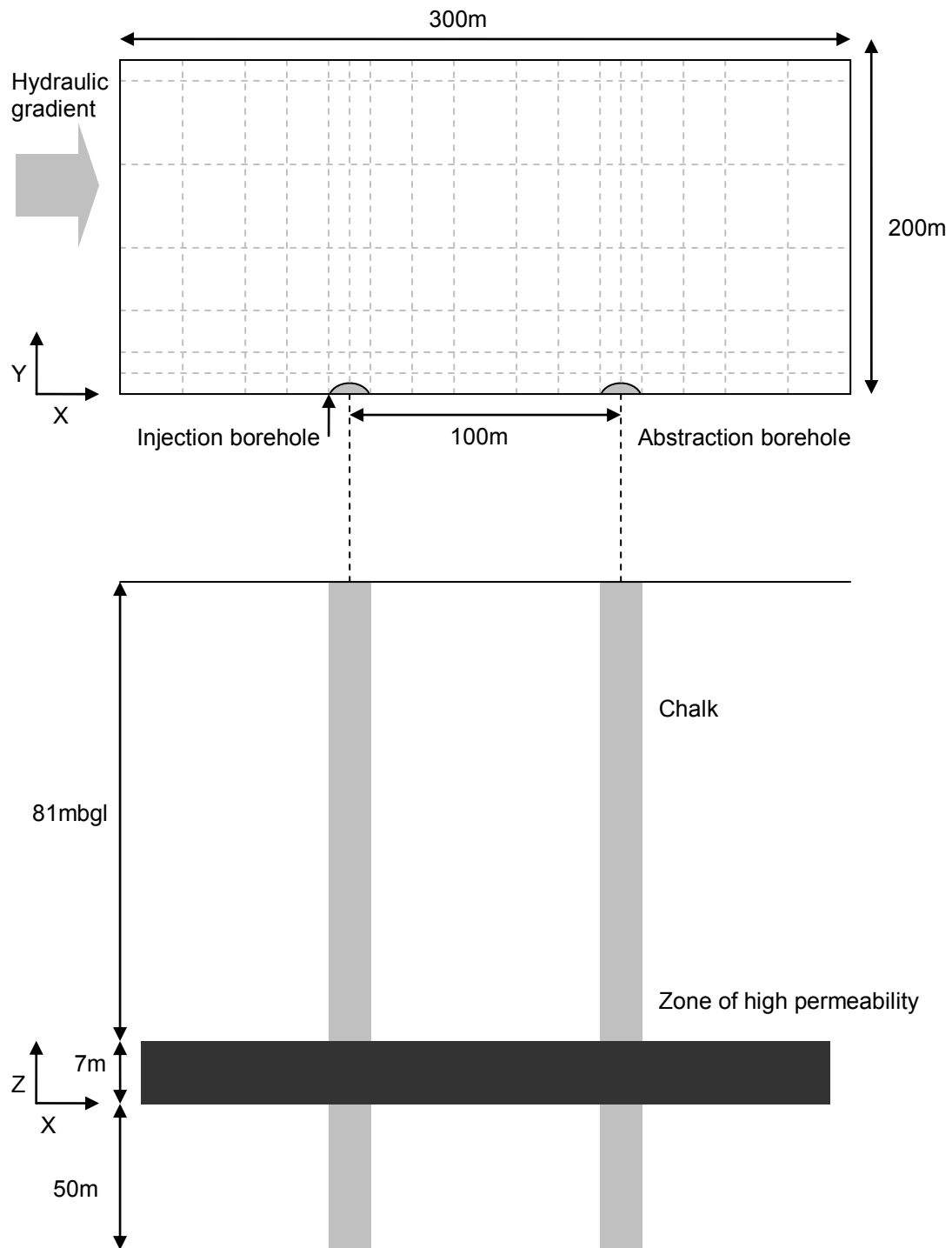


Figure 11-3 Representation of the numerical model

The value of permeability applied to the high permeability zone is important, as a background hydraulic gradient across the site will be applied to the model. The

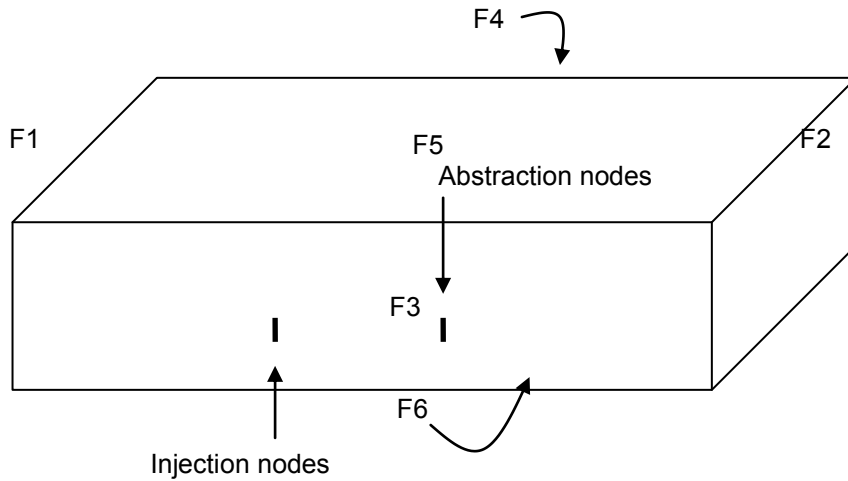
background gradient (0.001) will be applied as a pressure across boundary faces. Therefore, the permeability applied to the high flow zone will affect the flow rate of groundwater through the zone.

An initial estimate of permeability was applied to the high permeability zone based on the results of the hydraulic testing. If the average value of KD (transmissivity) from the testing is approximately 1000 m²/day then K (hydraulic conductivity) = 1.7e-3 m/s when D = 7m. Or k (permeability) = 1e-9.

This was the initial value applied to the high permeability zone in the model. When the model was run, the calculated injection and abstraction heads were less than those recorded in the trial. The permeability was then reduced to 1e-10. With this value of permeability the head difference between the injection and abstraction boreholes was 3.7m, approximately equal to that recorded during the pumping tests (3.6m).

11.1.4 Boundary conditions

The boundary conditions were allocated to the model on a face by face basis. The faces are and values / conditions added to each face are given in Figure 8-5.



Face	Pressure	Temperature
F1	Constant pressure. Fluid movement across boundary. Initial value representative of background gradient.	No flow.
F2	Constant pressure. Fluid movement across boundary. Initial value representative of background gradient.	No flow.
F3	No flow.	No flow.
F4	Constant pressure. Fluid movement across boundary. Initial value representative of background gradient.	No flow.
F5	No Flow	No flow.
F6	No flow.	No flow.

Figure 11-4 Boundary conditions for numerical model

11.1.5 Grid

Horizontal Spacing

The mesh Peclet number Pe_m (as discussed previously) is given approximately by:

$$Pe_m \approx \frac{\Delta L}{\alpha_L}$$

where ΔL is the local distance between element sides along a streamline of flow and α_L is the dispersion coefficient. Stability is guaranteed in all cases when $Pe_m < 2$, which gives a criterion for choosing a maximum allowable element dimension, ΔL , along the local flow direction. Spatial stability is usually obtained with SUTRA when $Pe_m < 4$ which gives a less-stringent criterion. This is most important in the region of the model nearest to the borehole. If we assume for this model that α_L is equal to one tenth of the horizontal zone of interest of the model (i.e. in the direction of flow) then $\alpha_L = 10\text{m}$.

If a value for ΔL of 5m is chosen for this model the mesh Peclet number is 0.5 which is well within the range of values to ensure spatial stability.

The Courant number has also already been discussed in previous chapters. The Courant number is represented numerically as follows:

$$C_o = \frac{\delta t |U|}{\delta x}$$

Where

C_o = the courant number

$|U|$ = the velocity of the fluid

δt = the timestep

δx = element dimension or ΔL

To avoid spurious numerical results it is important to keep the Courant number below 1. For this model, the approximate velocity of the fluid (as measured in the tracer test) is 0.02 m/s and the grid size (ΔL) is 5m. A timestep δt value of 100 seconds would lead to a Courant number C_o of 0.4, well below the defining limit of 1. The model was therefore initially run with a δt of 100 seconds.

Vertical Spacing

The vertical grid spacing is dictated by the zone of high permeability (assumed to be 7m thick). This was divided into seven vertical elements, each 1m thick. Above this zone of interest a vertical spacing of 5m was chosen.

Fluid injection

Fluid injection to the model is inputted as a positive injection through the nodes that represent the region of the borehole in contact with the high permeability zone. The peak fluid injection is 20 l/s. There are six nodes of fluid injection in the injection borehole and six nodes of flow in the abstraction borehole.

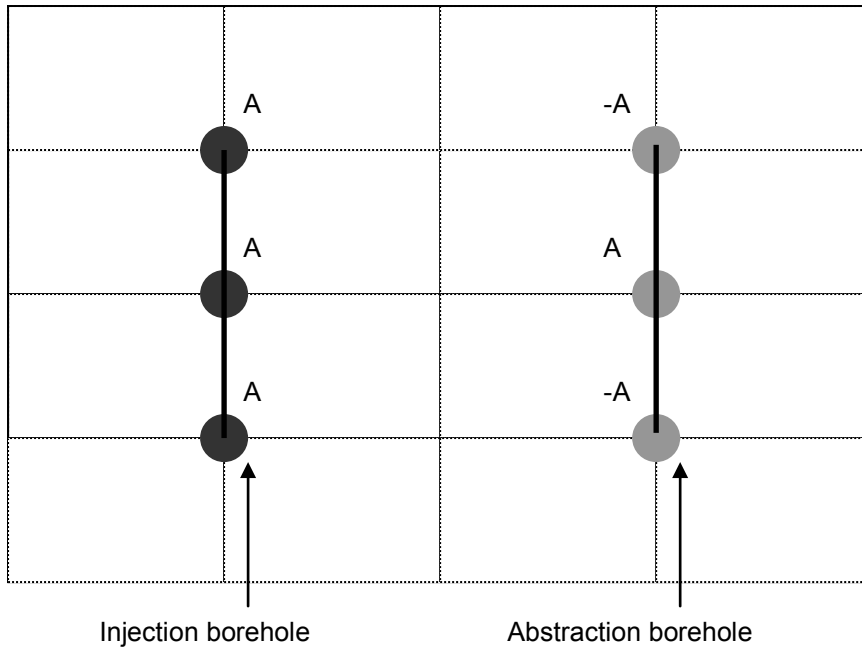


Figure 11-5 Block representation of a fracture plane and injection nodes

Total rate of injection into flow zone	20 l/s
Model uses horizontal symmetry. Total injection through model	10 l/s
Rate A	1.66 l/s

Table 11-2 Model injection and abstraction rates

All other parameters used in the numerical model are the same as those stated in Table 8-1.

11.2 Model results

The calculated temperature at the abstraction borehole (recorded at observation nodes) was plotted against time for the three scenarios stated above (conditions tabulated in Table 11-3)

Scenario	Injection rate (l/s)	Injection temperature (°C)	Duration
1. Peak flow	20	23.5	30 days
2. Weekly data	Fixed at 20	Variable depending on required energy	1 year
3. Annual	0.55	23.5	50 years

Table 11-3 Parameters for the three models

The parameters chosen for Scenario 1 are self explanatory. They represent the peak flow rate and peak re-injection temperature. This rate was sustained for a period of 30 days, the principal timeframe of interest for peak continual flow rates. For Scenario 2, the weekly energy data provided by the M&E engineers was adjusted to allow for a fixed flow rate. The injection temperature was varied to ensure that the energy rejected or abstracted from the ground was equivalent to the figures provided by the M&E engineers. These figures could have been reversed (variable flow rate, fixed injection temperature) to achieve the same result. The SUTRA code had to be recompiled (using a Compaq fortran compiler) to allow for the variations in injection temperature. A fixed flow rate for Scenario 3 was calculated by assuming that the

injection temperature was constant (23.5°C). The flow rate corresponds to an annual energy injection of 200 MWh.

One of the problems associated with running these models is that the re-injection temperature does not change in response to a change in temperature at the abstraction borehole. The models therefore assume that the re-injection licence terms (injection temperature must not exceed 24°C) are not broken. If the temperature in the borehole rises it is assumed that the system rejects additional heat to the air, not to the ground. The resulting drop in efficiency is not discussed here.

11.2.1 Peak heat rejection rates

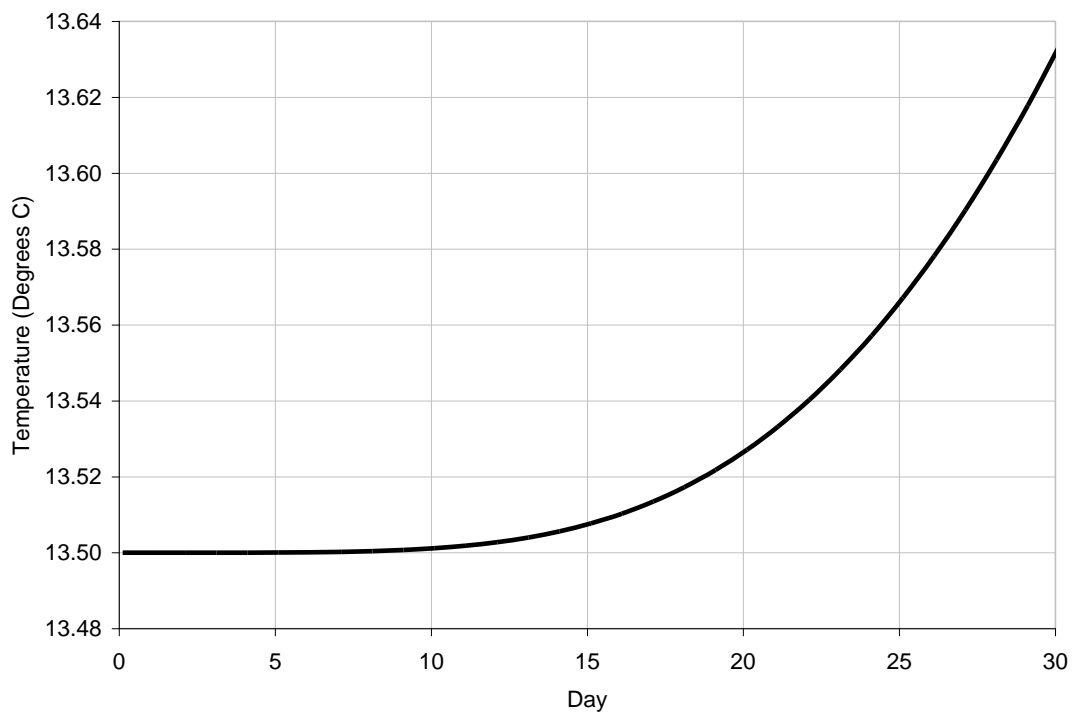


Figure 11-6 Calculated temperature in the abstraction borehole. Peak cooling.

The results of the peak injection model show that the temperature of the abstraction borehole remains fairly constant for approximately 10 days under continual peak flow

rates. After this period the injection temperature begins to rise. After 30 days the temperature in the abstraction borehole has risen by approximately 0.1 °C.

11.2.2 52 week rejection and abstraction cycle

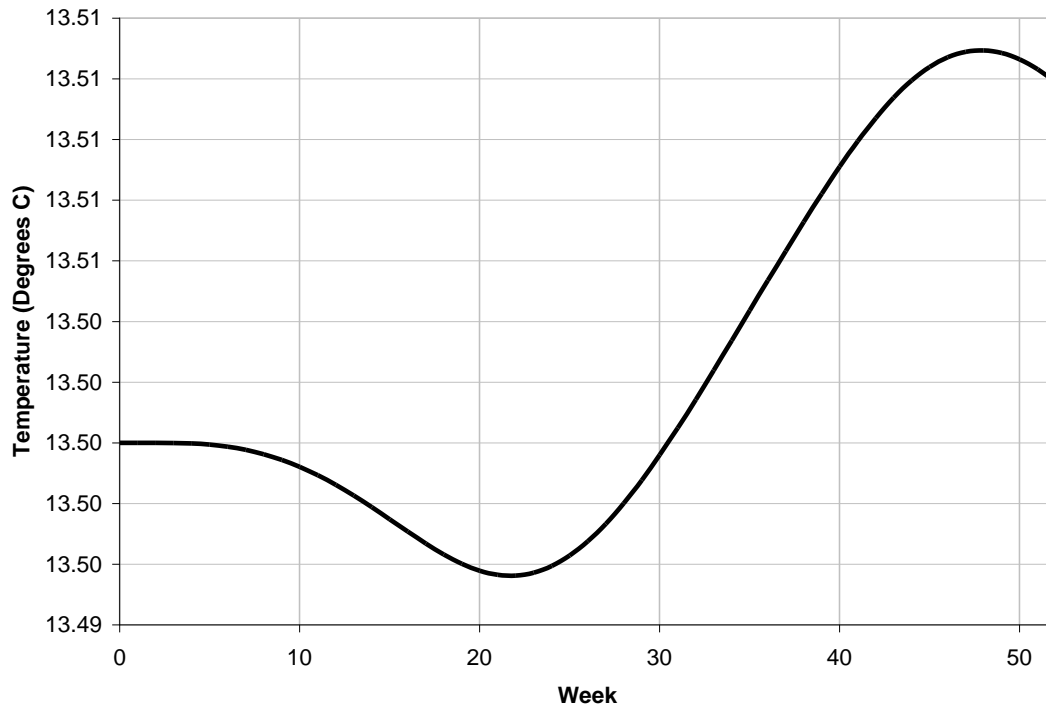


Figure 11-7 Calculated temperature in the abstraction borehole. 52 weeks.

In the 52 week model the calculated temperature in the abstraction borehole oscillates in response to the heating and cooling cycle. In the first 20 weeks, when the building requires heating, the temperature in the abstraction borehole drops as heat is abstracted from the aquifer. Over the next 20 weeks, the temperature in the abstraction borehole rises as heat is rejected from the building to the ground during cooling. The scale of the oscillations is small (a few hundredths of a degree Centigrade). For this first year of operation the temperature at the abstraction borehole rises by one hundredth of a degree. This result would appear to be in conflict with the annual change in temperature (0.5°C) predicted by the estimated

temperature change (Table 11-1). This would imply that the system is accessing a larger volume of ground than suggested in the basic modelling.

11.2.3 Yearly heat rejection cycle

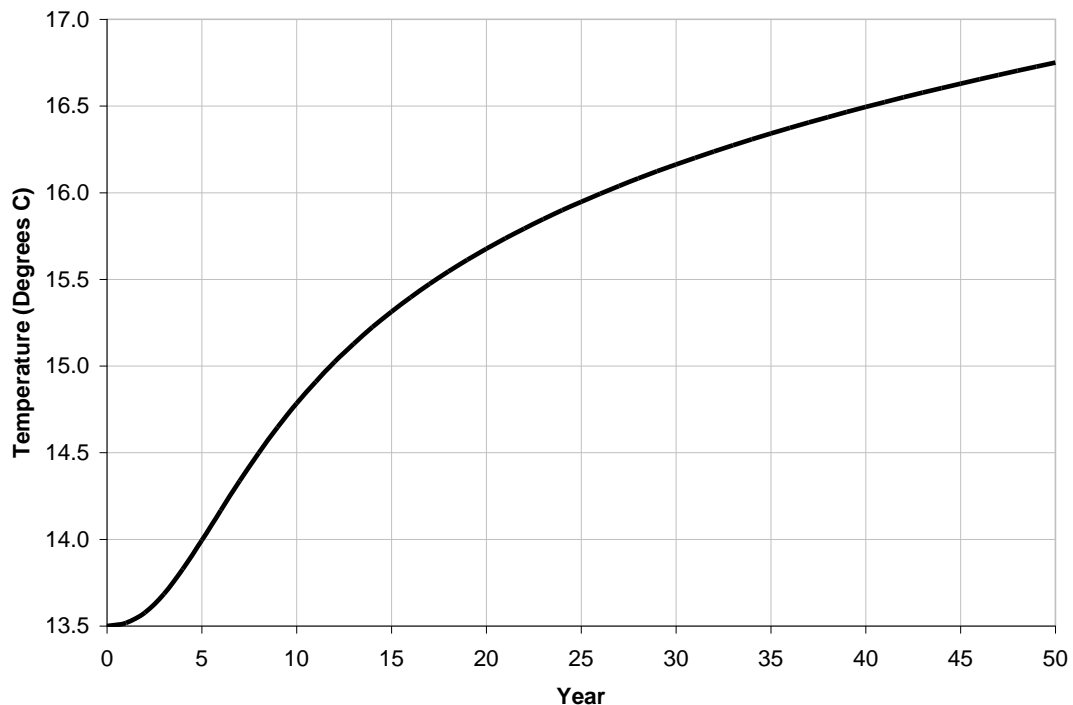


Figure 11-8 Calculated temperature in the abstraction borehole. 50 years.

The calculated yearly results appear to be split in to three phases:

1. Year 1 and 2. Small increase in temperature in the abstraction borehole, approximately 0.05°C over two years (consistent with the 52 week model)
2. Year 2 to 8. Linear increase in temperature in the abstraction borehole, approximately 0.125°C every year (one quarter of that predicted in Table 11-1)

3. Years 7 to 50. The rate of increase in temperature in the abstraction borehole tails off. The calculated temperature at the abstraction borehole after 50 years is 16.75°C.

11.3 Conclusions

The results of the peak load model and the weekly load model suggest that in the short term, the operation of the redesigned system causes little change to the temperature at the abstraction borehole. The results of the model run over the lifetime of the system suggest that over this period the system will cause the aquifer to heat up, by as much as 3°C over the lifetime of the system. The system tends towards an approximate equilibrium with the aquifer over time as the volume of ground accessed by the geothermal system increases.

To avoid such an increase in temperature in the aquifer over the lifetime of the system it may be necessary to find a method of rebalancing the ground temperature. An efficient method of achieving this is to use air blasters in the winter months to re-inject 'cold' back into the ground. Such systems have been in use for many years in the Netherlands where any open loop geothermal system must be shown to place balanced energy demands on the aquifer.

11.4 Summary

A numerical model was constructed to simulate the operation of a planned open loop geothermal system. The hydrogeological parameters of the model were determined from the results of a suite of site investigation techniques. Basic modelling suggested that the original system loads would cause the aquifer to increase in temperature at an

unsustainable rate. The building loads placed on the geothermal system were reconfigured to reject less heat to the ground. A numerical model was then run under three different conditions (peak load, weekly energy load and annual load) to understand how the system would interact with the expected hydrogeology. The results of the peak and weekly load models suggested that the revised energy rejection figures would not cause short term thermal interference during the operation of the system. The results of the annual load model suggested that over the lifetime of the system there would be changes (an increase of at least 3°C) in the temperature of the aquifer. The system must therefore find a way of rebalancing the ground temperature. This can be achieved (and is commonly done so in the Netherlands) by the re-injection of 'cold' from the external air in the winter months.

12 CONCLUSIONS AND FURTHER WORK

The PhD has focused on the interaction between an open loop geothermal system and the Chalk aquifer beneath central London. It was written to address the lack of published research and data about the long and short term effects of operating geothermal systems in the aquifer. This area of research is becoming more relevant as the number of installed systems increases.

The main aims and objectives of this PhD were threefold:

1. To understand how a geothermal system will alter the ambient temperature of the aquifer over both the short and long term
2. To predict whether the geothermal system will be prone to short circuiting due to rapid, fracture driven, thermal transport between the injection and abstraction borehole
3. To develop a procedure for developers to follow to ensure that proposed systems will function in an appropriate manner

To achieve these aims the following approach was taken:

1. A literature review of thermal transport, the geology of central London and the Chalk structure.
2. A literature review of fluid flow in fractured material and published research on open loop geothermal systems in the Chalk.
3. The development of analytical and numerical models that best represent the thermal transport displayed by the Chalk for typical geothermal flow rates and conditions.

4. A review of site investigation techniques and the development of a push pull thermal test.
5. Application of the site investigation techniques to a proposed site to collect sufficient data for the construction of a detailed numerical model. Use of the model to predict the behaviour of a proposed geothermal system.
6. Development of a standard set of procedures to be followed during the design stages of an open loop geothermal system to ensure efficient operation and environmental sustainability.

The conclusions from each of the above topics can be summarised as follows:

12.1 Literature review of geology

The results of this review showed that flow within the Chalk aquifer is dominated by fractures or high flow zones. The fracture structure and geometry may vary between closely spaced locations and it is not possible to assume a uniform permeability for the Chalk. Therefore, predicting the flow rates/ yields of an open loop geothermal system, prior to a site investigation will prove difficult. In addition, the accessible thermal mass of the aquifer (determined by the number of interconnected fractures and apertures) cannot be known without a site investigation.

12.2 Literature review of fluid flow in fractured material

The movement of fluid within fractured material has been the subject of much debate and research and has still not been, and may never be, fully resolved. The most plausible model of a single fracture remains that of a parallel plate, despite many

limitations. Calculations of flow within a parallel plate model are governed by the cube of the aperture. Therefore, using an appropriate value for the fracture hydraulic aperture is important. Without a site investigation it is extremely difficult to estimate a value for hydraulic apertures of fractures within the Chalk. In addition, although fluid flow is governed by fractures, thermal transport may not be.

12.3 Conceptual model development for Chalk

A good starting point is to treat the aquifer as being divided up into a number of parallel horizontal fractures. Bodvarsson (1982) developed this concept for hydrothermal boreholes and the analytical solutions he produced have been used here to make initial predictions about thermal transport. Given some constraints of flow rate, borehole spacing and a likely range of fracture apertures and spacings, the extent to which the thermal transport between two boreholes will be controlled by fractures has been estimated. Using a plausible range of parameters it was demonstrated that for most geothermal systems, the thermal transport in the Chalk cannot be treated as homogenous.

For more advanced models, given a known scale of interest, the most suitable conceptual model was shown to be a discrete fracture network. A small number of numerical codes are available with the capacity to model discrete fractures coupled with combined flow and transport solutions. The numerical code chosen to model the geothermal systems was SUTRA 3D (developed by the United States Geological Survey). As there are no examples in the literature on the use of SUTRA for single parallel plate fractures, the results of a SUTRA model of a single fracture were tested

against those of a proven analytical solution for heat injection into a single fracture. The results showed that the SUTRA code can be successfully used to model discrete fracture networks.

12.4 Site Investigation techniques

A suite of site investigation techniques were used to determine the key parameters of the Chalk beneath a proposed site. In addition to some of the more standardised tests a push pull thermal test was devised to try and understand the thermal behavior of the aquifer.

The results showed that a small number of fractures carried the majority of the flow. Further to this, the majority of the flow appeared to occur over a very small section (approximately 7m in depth) at approximately the same depth in both boreholes, despite a borehole separation of 100m. The only possible conclusion was that a highly permeable zone was contiguous beneath the site.

Although the push pull thermal test was executed successfully, the interpretation of the results showed that for a thermal test to provide conclusive results, observations of the integrated thermal outputs during recovery (i.e. the temperature of the recovered discharge) would be needed. The results suggest that a thermal heater test of the type described would on its own provide insufficient evidence for assessing the risk of adverse thermal breakthrough and that the combination of the tracer and thermal testing is the most effective testing regime for a fractured rock such as the Chalk.

12.5 Construction of a numerical model

The results of all of the tests were used to construct a discrete numerical model in SUTRA 3D. It was possible to reduce the number of permutations of the numerical model by firstly applying the type curves developed by Bodvarsson (1982).

The initial heating and cooling loads for a proposed system were proved to be unsustainable using simple analytical solutions. The revised heating and cooling loads for the planned geothermal system were used as inputs into a SUTRA model that best represented the hydrogeological conditions at the site. For the given conditions, the system proved to be sustainable in the short term. However, over the long term (50 years) the system was shown to raise the temperature of the aquifer by approximately 3°C. This would not be acceptable from an environmental standpoint.

12.6 Summary

The structure of the Chalk aquifer is fractured and is likely to vary significantly between sites. The fractures and high flow zones have the potential to significantly affect the performance of an open loop geothermal system. Further, depending on the structure of the Chalk, the system may adversely affect neighbouring sites and the aquifer as a whole.

At an early stage of a project, curves developed by Bodvarsson (1982) can be used to understand the likely nature of the thermal transport between injection and abstraction boreholes. The results can be used to inform system design. However, before final design decisions are taken, it is important to undertake a detailed site investigation.

The results of the site investigation can then be used to design a discrete fracture network numerical model (using the USGS SUTRA 3D code) to predict how the proposed geothermal system will function over its lifetime. It is important to model both the short (daily) and long term (the lifetime of the building) effects of the system.

The results of this PhD were used to develop a simple procedure for developers of open loop geothermal systems in the Chalk. This has been summarised in a flow chart (Figure 12-1) and in words below:

1. Apply the expected flow rates, spacing between the injection and abstraction boreholes and literature values to the appropriate Bodvarsson curves to estimate the type of thermal transport that will occur in the aquifer.
2. If the thermal front appears homogenous in all cases (even for a single fracture) then simple calculations for energy storage and transport in an aquifer can be used before the system goes to design stage.
3. If the thermal front is not homogenous in all cases, then it is recommended to use a suite of site investigation techniques.
4. The results of these tests can then be used in the appropriate Bodvarsson curves to produce a more accurate picture of the thermal front and subsequent thermal breakthrough times.
5. The data can then be used to construct a number of discrete fracture network numerical models using the SUTRA code to fully understand the short and long term affects of the proposed system.

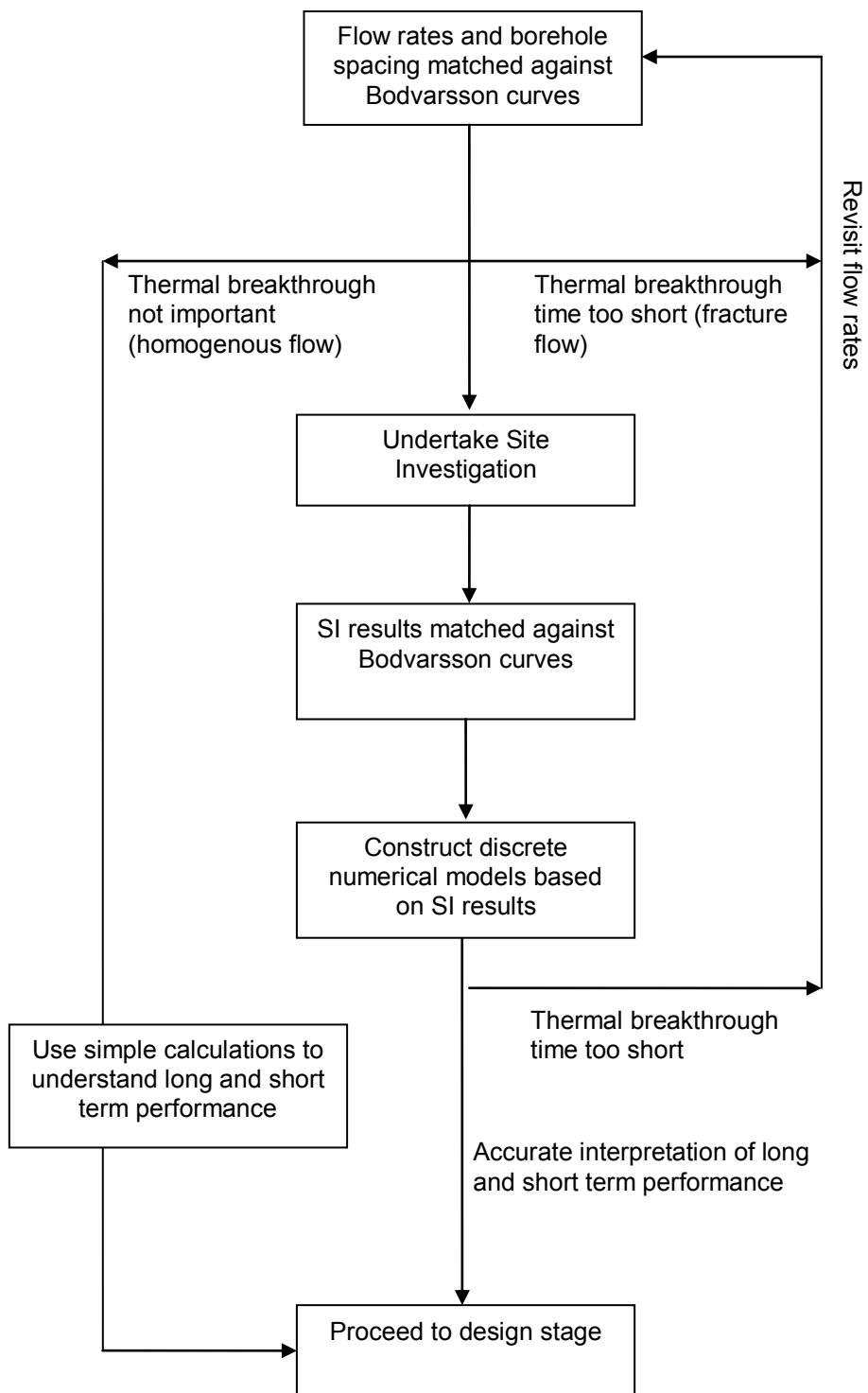


Figure 12-1 Flow chart representing the recommended procedure to be undertaken in the design of an open loop geothermal system in the Chalk.

12.7 Recommendations for further work

There is more work that could be undertaken to help understand the performance of geothermal systems in the Chalk:

1. The nature of the chemical changes that occur when heated or cooled water is passed through the Chalk. The extent to which the Chalk structure will change in response to continued usage (25+ years) of geothermal systems is not well understood. It may be the case that the temperature variations are small enough to cause little change in the structure to take place. However, it is increasingly being proposed that an open loop geothermal system be matched with a Combined Heat and Power system. This marriage would involve the rejection of higher temperature water (up to 65°C) into the aquifer. A series of experiments on saturated Chalk blocks, conducted over the medium term (1 to 3 years) would progress the understanding of the extent to which the Chalk structure changes under a range of temperature and pressure conditions.
2. A rapidly increasing number of geothermal systems are being installed in the Chalk aquifer. To what extent can an aquifer be saturated with such systems? Are existing systems already causing thermal interference with each other? Have such systems started to cause temperature changes in the aquifer, particularly during the summer? This is a piece of work that should be undertaken in conjunction with the Environment Agency. The water levels in a number of existing boreholes in the Chalk are currently monitored. In addition, the temperature of these boreholes and boreholes used for open loop geothermal systems should be monitored over a period of at least three years

to understand whether any long term temperature changes are occurring and to determine what is causing them. The Chalk could then be better managed as both a water and energy resource.

REFERENCES

Ahmadi, A., Remazeilles, V., Quintard, M., Noetinger, B., (1996). Direct calculation of large-scale properties for one-phase flow in random fractured systems. In: 5th European Conference on the Mathematics of Oil Recovery. Leoben, Austria, September 3–6.

Allen, A., Milenic, D., (2003). Low-enthalpy geothermal energy resources from groundwater in fluvio-glacial gravels of buried valleys. *Applied Energy*, 74. 9-19.

Allen, D., Michel, F., (2001). Hydrologic and thermal simulations of an ATES system in fractured limestone, Carleton university, Canada

Allen, D.M., (1996). Steady-state and transient - hydrologic, thermal and chemical modelling

of a faulted carbonate aquifer used for aquifer thermal energy storage, Carleton university, Ottawa, Canada. Doctoral Thesis. Carlton University, Ottawa.

Arup Geotechnics., (2002). Geotechnical desk study, preliminary geotechnical strategy and recommendations for additional site investigations. Arup internal document.

Arup Geotechnics., (2003). Ground storage of building energy, preliminary and desk studies. Arup internal document.

Arup Geotechnics., (2003). Scoping document for ground storage of building energy. Arup internal document.

Arup Geotechnics., (2004). Ground storage of building energy, progress report. Arup

internal document.

Barenblatt, G.I., Zheltov, I.P., (1960) Fundamental equations of filtration of homogeneous liquids in fissured rocks. *Sov Dokl Akad Nauk* 132(3), 545–8.

Barker, J. A., (1985). Block Geometry Functions Characterizing Transport in Densely Fissured Media. *J. Hydrology*, 7, 263-279.

Becker, M.W., Shapiro, A.M., (2000). Tracer transport in fractured crystalline rock: evidence of non diffusive breakthrough tailing. *Water Resources Research* 36(7), 1677–86.

Berkowitz, B., (2002). Characterizing flow and transport in fractured geological media: A review. *Advances in water resources* 25, 861-864.

Blackwell, D. D., Steele, J. L., (1989). Thermal conductivity of sedimentary rocks. In Naeser, N. D. and McCulloh, T. H. (eds), *Thermal history of sedimentary basins methods and case histories*. Springer-Verlag. New York.

Bloomfield, J., (1996). Characterisation of hydrogeologically significant fracture distributions in the Chalk: an example from the Upper Chalk of southern England. *Journal of Hydrology*.

Bodvarsson, G. (1969). On the temperature of water flowing through fractures. *Journal of Geophysical Resources*,. 74(8), 1987-1992.

Bodvarsson, G., Tsang, C.F., (1982). Injection and thermal breakthrough in Fractured Geothermal Reservoirs. *Journal of Geophysical Resources*,. 87, 1031-1048.

Bodvarsson, G. S., Stefansson, V., (1989) Some theoretical and field aspects of reinjection in geothermal reservoirs. *Water Resources Research* 25, 1235-1248.

- Bourbiaux, B., Granet, S., Landereau, P., Noetinger, B., Sarda, S., Sabathier, J.C., (1999). Scaling up matrix-fracture transfers in dual-porosity models: Theory and application. SPE 56557, SPE Annual Technical Conference and Exhibition, Houston, USA, October 3–6.
- Brandl, H. (2006). Energy foundations and other thermo-active ground structures. *Geotechnique* 56, No. 2, 81-122.
- Bromehead, C.E.N. 1925. Geology of North London. Memoirs of the Geological Survey of Great Britain, Sheet 256 (England and Wales)
- Brown, S.R., Stockman, H.W., Reeves, S.J., (1995). Applicability of the Reynolds equation for modeling fluid flow between rough surfaces. *Geophysics Resources Lett* 22(18), 2537–40.
- Cappetti, G., Parisi, L., Ridolfi, A., Stefani, G., (1995). Fifteen years of reinjection in the Larderello-Valle Secolo area: Analysis of the production data. Proc. World Geothermal Congress, 1997-2000.
- Chasteen, A.J., (1975). Geothermal steam condensate re-injection. Proc. UN Symp. Dev. Use Geothermal Resource. 2nd, 2, 1335-1336.
- Clarkson, M.H. Birks, D. Younger, P.L. Carter, A. Cone, S. Groundwater cooling at the Royal Festival Hall, London. *Quarterly Journal of Engineering Geology and Hydrogeology*, 1 August 2009; 42: 335 - 346.
- Clauser, C., (1992). Permeability of crystalline rocks. *EOS Trans AGU* 73, (21), 233, 237–8.
- Davis, A. G. & Elliott, G. F. 1958. The Palaeogeography of the London Clay sea.

Proc. Geol. Ass., Lond. 68, 255-277.

Dewey, H., Bromehead, B.A., (1921) The geology of South London. Memoirs of the Geological Survey. Sheet 270 (England and Wales).

Dewey et al., (1924) The geology of the country around Dartford. Memoirs of the Geological Survey. Sheet 271 (England and Wales).

Dijk, P.E., Berkowitz, B., Bendel, P., (1999) Investigation of flow in water saturated rock fractures using nuclear magnetic resonance imaging (NMRI). Water Resources Research 35(2), 347–60.

Dines, H.G., Edmunds, M.A., (1925). The geology of the country around Romford. Memoir of the Geological Survey. Sheet 251 (England and Wales).

Ellison R.A, Knox, R.W.O'B, Jolley, D.W and King, C., (1994). A revision of the lithostratigraphical classification of the early Palaeogene strata of the London Basin and East Anglia. Proceedings of the Geologists' Association. Vol. 105, 187-197.

Ellison R.A, Booth S.J and Strange, P.J., (1993). The British Geological Survey LOCUS project: a source of high quality geological maps and computer generated 3-D models of London. Episodes, Vol. 16, 383-388.

Ellison R.A., (2004). Geology of London. Special memoir for 1:50,000 sheets 256, 257, 270 and 271 (England and Wales). British Geological Survey, 2004.

Environment Agency. 2004. Rising groundwater levels in the chalk-basal sands aquifer of the central London basin.

Environment Agency. 2005. Groundwater levels in the chalk-basal sands aquifer of the central London basin.

F.G. Bell, M.G. Culshaw , J.C. Cripps., (1999). A review of selected engineering geological characteristics of English Chalk Engineering Geology 54, 237–269

Ge, S., (1997) A governing equation for fluid flow in rough fractures. Water Resources Research 33:53–61.

Gehlin, S., Spitler, J.D., (2002). Thermal Response test – State of the Art 2001. Report IEA ECES Annex 13.

Gelhar, L.W., (1993) Stochastic subsurface hydrology. Englewood Cliffs: Prentice-Hall.

Granet, S., Fabrie, P., Lemonnier, P., Quintard, M., (1998). A single-phase flow simulation of fractured reservoir using a discrete representation of fractures. In: 6th European Conference on the Mathematics of Oil Recovery (ECMOR VI). Peebles, Scotland, UK, September 8–11.

Gropius, M. (2010). Numerical groundwater flow and heat transport modelling of open-loop ground source heat systems in the London Chalk. Quarterly Journal of Engineering Geology and Hydrogeology, February 2010; 43: 23 - 32.

Habei, R.S., (1990). The geothermal underground injection control program of the California Department of Conservation, Division of Oil and Gas. Transactions Geothermal Resources Council 14, 1133-1140.

Hakami, E., Larsson, E., (1996) Aperture measurements and flow experiments on a single natural fracture. International Journal Rock Mechanics Mineral Science Geomechanical Abstracts 33(4), 395–404.

Horne, R.N., (1982). Effects of Water Injection into Fractured Geothermal Reservoirs

: A Summary of Experience Worldwide. Geothermal Resources Council, Davis, CA, Special Report 12, 47-63.

Hufschmiedt, P. (1985). Estimation of three-dimensional statistically anisotropic hydraulic conductivity field by means of a single well pumping tests combined with flowmeter measurements. International Symposium on Stochastic Approaches to Subsurface Flow, Fontainebleau, France, June 3 – 7, 1985.

Ineson, J., 1962. A hydrogeological study of the permeability of Chalk. Journal of the Institution of Water Engineers 16, 43–63.

Kazemi, H., Gilman, J.R., (1993) Multiphase flows in fractured petroleum reservoirs. In: Bear J, Tsang CF, de Marsily G, editors. Flow and contaminant transport in fractured rocks. New York: Academic Press.

Keller, A.A., Roberts, P.V., Kitanidis, P.K., (1995) Prediction of single-phase transport parameters in a variable aperture fracture. Geophysics Resources Lett 22(11), 1425–8.

Knox, R.W.O'B., (1996). Tectonic controls on sequence development in the Palaeocene and earliest Eocene of the southeast England: implications for North Sea stratigraphy. 209-229 in Sequence stratigraphy in British geology. Parkinson. D.N (editor). Geological society of London, Special publication, No.103.

Lauwerier, H.A., (1955). The transport of heat in an oil layer caused by the injection of hot fluid. Applied Science Resources 5, 2-3, 145-150

London Energy Partnership. (2004). London renewables – integrating energy into new developments. Greater London Authority.

- Mayor of London. (2004). Green light to clean power. The mayor's energy strategy. Greater London Authority.
- McDonald, A., Allen, D., (2001). Aquifer properties of the Chalk of England. Quarterly journal of Engineering Geology and Hydrology.
- Meheust, Y., Schmittbuhl, J., (2001) Geometrical heterogeneities and permeability anisotropy of rough fractures. J Geophys Res, 106(B2), 2089–102.
- Mourzenko, V.V., Thovert, J.F., Adler, P.M., (1995). Permeability of a single fracture: validity of the Reynolds equation. Journal Phys II Fr 5(3), 465–82.
- Muskat, 1937. The Flow of Homogeneous Fluids Through Porous Media, Ann Arbor.
- National Research Council. (1996). Rock fractures and fluid flow: contemporary understanding and applications. Washington,DC: National Academy Press.
- Novakowski, K.S., Lapcevic, P.A., Voralek, J., Bickerton, G., (1995) Preliminary interpretation of tracer experiments conducted in a discrete rock fracture under conditions of natural flow. Geophys Res Lett, 22, (11), 1417–20.
- OECD Nuclear Energy Agency., (1990). Proceedings of the 3rd NEA/SKB Symposium on In Situ Experiments Associated with the Disposal of Radioactive Waste. International Stripa Project, Stockholm, 3– 4 October. Paris: OECD Nuclear Energy Agency.
- Packsoy, H., Turgot, B., Gurbuz, Z., (2003). First Aquifer Thermal Energy Storage (ATES) plant in Turkey. Proceedings of the 9th International Conference on Thermal Energy Storage, Warsaw, 77-81.
- Patsoules, M.G., Cripps, J.C., (1990). Survey of macro-and micro-fracturing in

Yorkshire chalk. In: Proceedings of the International Chalk Symposium, Brighton, UK. Thomas Telford Press, London, pp. 87–93.

Price, M., (1987). Fluid flow in the Chalk of England. In: Goff, J.C., Williams, B.P.J. (Eds.), Fluid Flow in Sedimentary Basins and Aquifers Geological Society Special Publication No. 34. The Geological Society, London, pp. 141–156.

Price, M., (1996). Discussion on Chalk fracture systems: implications for flow and solute transport. Quarterly Journal of Engineering Geology 29, 93–96.

Pyrak-Nolte, L.J., Meyer, L.R., Cook, N.G.W., Witherspoon, P.A., (1987) Hydraulic and mechanical properties of natural fractures in low permeable rock. Proc 6th Int Cong ProcRock Mech, 225–31

Rao, P.S.C., Jessup, R.E., Rolston, D.E., Davidson, J.M., and Kilcrease, D.P., (1980). Experimental and Mathematical Description of Non adsorbed Solute Transfer by Diffusion in Spherical Aggregates Soil. Sci. SOC.A m. J., 44, 684-688.

Rasmuson, A., Neretnieks, I., (1986) Radionuclide transport in fast channels in crystalline rock. Water Resour Res, 22, 1247–56.

Raven K.G., Novakowski, K.S., Lapcevic, P.A., (1988) Interpretation of field tracer tests of a single fracture using a transient solute storage model. Water Resour Res 24, 2019–32.

Sahimi, M., (1995). Flow and transport in porous media and fractured rock: from classical methods to modern approaches. Weinheim, Germany: VCH.

Sanner, B., Reuss, M., Mands, E., (2000). Thermal Response Test – Experiences in Germany. Proceedings of Terrastock 2000, Stuttgart, Germany, 177-182.

Sanner, B., 1999. Prospects for ground-source heat pumps in Europe. - Newsletter IEA Heat Pump Centre 17/1, pp. 19-20, Sittard.

Sauty, J. P., Gringarten, A. C., Fabris, H., Thiery, D., Menioz, A. and Landel, P. A., (1982). Sensible energy storage in aquifers. 2. Field experiments and comparison with theoretical results. *Water Resources Research*, 18, No. 2. 253-265.

Sauty, J.P., (1980). An Analysis of Hydrodispersive Transfer in Aquifers. *Water Resources. Research*, 16, 1, 69-103.

Sherlock, R.L.(1960). *British regional geology: London and Thames Valley*. HMSO, London.

Sinha,R., Asakawa,K., Pope, G.A., Sepehrnoori, K., (2004), Simulation of Natural and Partitioning Interwell Tracers to Calculate Saturation and Swept Volumes in Oil Reservoirs. SPE 89458, Proceedings of the 2004 SPE/DOE Fourteenth Symposium on Improved Oil Recovery held in Tulsa, Oklahoma, U.S.A., April 17–21.

Soper, N.J, Webb, B.C and Woodcock, N.J., (1987). Late Caledonian transpression in north west England. Timings, geometry and geotectonic significance. *Proceedings of the Yorkshire Geological Society*, Vol. 46, 175-192.

Spitler, J.D., Yavuzturk, C., Rees, S., (2000). In Situ Measurement of Ground Thermal Properties. *Proceedings of Terrastock Vol. 1, Stuttgart*, 165-170.

Stefansson, V., (1997) *Geothermics Vol. 26, No. 1*, 99-139. Geothermal reinjection experience.

Sumbler, M.G., 1996. *British regional geology: London and the Thames valley* (4th edition). (London: HMSO for the British Geological Survey)

Toynnton, R., (1983). The relation between fracture patterns and hydraulic anisotropy in the Norfolk Chalk, England. *Quarterly Journal of Engineering Geology* 16, 169–186.

USGS., (2003). SUTRA – A model for saturated unsaturated variable density ground water flow with solute or energy transport. *Water-resources investigations report* 02-4231.

Vandergraaf, T.T., (1995). Radionuclide migration experiments under laboratory conditions. *Geophys Res Lett* 1995, 22(11), 1409–12.

West, G., Dumbleton, A.J., (1972). Some observations on swallow holes and mines in the Chalk. *Quarterly Journal of Engineering Geology* 5, 171–178.

Whitaker, W., (1872). The geology of the London Basin, Part I. The Chalk and the Eocene Beds of the Southern and Western tracts. *Memoirs of the Geological Survey*, Sheets 1,2 and 7.

Whitaker, W., (1889). The geology of London and part of the Thames Valley, Vol.2. *Memoir of the Geological Survey*, Sheets 1,2 and 7.

Willemsen, A., Groeneveld, G. J., (1989). Environmental impacts of aquifer thermal energy storage (ATES): modelling of the transport of energy and contamination from the store. *In: Jousma, G. et al. (eds.), Groundwater Contamination: Use of Models in Decision-Making*, 337-351. Kluwer Academic Publishers.

Xu, Moujin, Yoram Eckstein., (1995). Use of weighted least squares method in evaluation of the relationship between dispersivity and field scale. *Goundwater* 33, no.6. 905-908.

Zabarnay, G.M., Shurchkov, A.V., Chetveryk, H.O., (1998). The computer programs for calculation of some parameters of geothermal systems. Institute of Engineering Thermophysics, Ukrainian National Academy of sciences, Kiev, 126.

APPENDICES

PUBLISHED PAPERS

2007. Law, R. Nicholson, D. Mayo, K. Aquifer thermal energy storage in the fractured London Chalk. A thermal injection / withdrawal test and its interpretation. *Proceedings, Thirty-Second Workshop on Geothermal Reservoir Engineering Stanford University, Stanford, California, January 22-24, 2007 SGP-TR-183*

2008. Law, R. Nicholson, D. Modelling of the Chalk aquifer in central London for a proposed open loop cooling system. *Proceedings, EcoStock, 2008*

2008. Law, R. Whitaker, D. Aspects of sustainability in ground energy systems. *Proceedings GeoCongress, 2008.*

2010. Law, R. Mackay, R. Determining fracture properties by tracer and thermal testing to assess thermal breakthrough risks for groundsource heating and cooling in the Chalk. *Quarterly Journal of Engineering Geology and Hydrogeology, 43, 1–12 – In press.*

AQUIFER THERMAL ENERGY STORAGE IN THE FRACTURED LONDON CHALK. A THERMAL INJECTION / WITHDRAWAL TEST AND ITS INTERPRETATION

Ryan Law, Duncan Nicholson, Karen Mayo

Arup Geotechnics

e-mail: r.law@arup.com

ABSTRACT

To comply with current renewable energy targets substantial new building developments in London are using the water held within the Chalk aquifer as a source for heating or cooling. Owing to the fractured structure of the Chalk there is the possibility of rapid transport occurring between the abstraction and injection boreholes at a site. This has the potential to cause thermal interference between the boreholes and a consequent loss of performance and, ultimately, eventual failure of the system.

The nature of the thermal transport that occurs at a site will primarily be dependent on the fracture frequency in the aquifer. To help determine the frequency of the fractures beneath a proposed site in central London a thermal injection and abstraction test was designed and undertaken. The test was the first of its kind in the United Kingdom and its interpretation will be used to assist with the design of the proposed heating and cooling system.

The test consisted of heating and storing water on site, followed by injection into a packered section of a borehole. Once the hot water was injected the pump was reversed and the water abstracted. The temperature of the packered section of the borehole was monitored with thermistors throughout the test. The results were then interpreted with the United States Geological Survey (USGS) SUTRA 3D code.

The results suggest that the fracture frequency beneath the site is sufficiently high to limit the possibility of rapid thermal transport occurring between the two boreholes. The results have been used in further numerical models that predict the long term performance of the proposed system in this flow regime.

INTRODUCTION

There has been an increasing interest in using the water contained within the Chalk aquifer underneath central London as a source for heating or cooling a building, in combination with either ground source heat pumps or heat exchangers (Arup, 2006). This is in direct response to a change in the planning framework, instigated by the Mayor of London (Mayor of London, 2004). The Mayor's strategic policy on renewable energy states that substantial new developments should meet 10% of their total energy requirements from renewable sources. Indeed, it is anticipated that these targets may go further and require 20% from renewables and a 35% reduction in carbon emissions. Using the water within the Chalk aquifer is currently the principal method that developers have identified for meeting these targets.

Under the abstraction licensing legislation the Environment Agency currently requires that in order to maintain current water levels in the Chalk aquifer new abstractions must re-inject the majority of the water abstracted (Environment Agency, 2005). Re-injection of water at a different temperature to that at which it has been abstracted presents a number of problems including:

1. The possibility of heating or cooling the aquifer beneath the site during the lifetime of the building.
2. The possibility of rapid thermal transport between the injection and abstraction boreholes beneath the site due to the fracturing within the Chalk.

To better understand the long term performance of proposed ground source systems (problem 1 above) Arup has used a number of numerical models based on the USGS SUTRA 3D code (Law, 2005). The SUTRA code is well proven and is capable of coupling groundwater flow with convective and conductive heat transport. These models have to

date treated the Chalk as a homogenous medium. The flow within the Chalk aquifer actually occurs through a number of fractures, with the Chalk matrix acting as an impermeable material (Price 1987, Bloomfield, 1996). Although the fracturing is often dense (Moench, 1995) there is the possibility that a small number of distinct fractures may link the abstraction boreholes with the injection boreholes (Figure 1.)

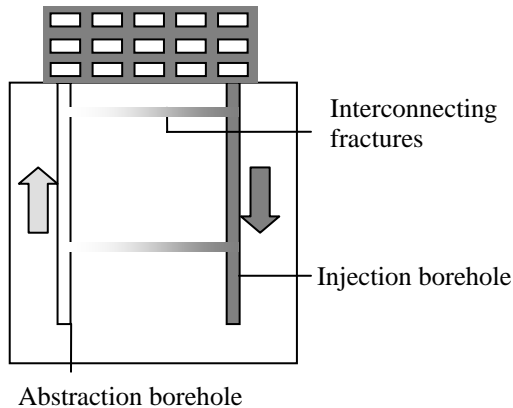


Figure 1. Illustration of the potential thermal interference caused by fractures linking abstraction and injection boreholes

The flow between the boreholes would, in such conditions, be channeled through a smaller volume or cross-sectional area of fracture. Flow rates would therefore be much faster than for a homogenous medium. The smaller the number of fractures that carry the flow, the faster the flow rates will be. Faster flow rates are likely to cause faster thermal breakthrough times between the injection and abstraction boreholes. Conversely, as the number of fractures carrying the flow increases, so does the volume and surface area through which the water flows, decreasing the velocity. In addition, the surface area of the Chalk matrix exposed to the hot / cold re-injected water is increased, causing greater energy dissipation from the fracture into the matrix. These two factors are the properties of the aquifer that need to be determined before a realistic appraisal of the proposed heating and cooling system can be made.

THERMAL TEST ASSUMPTIONS

The thermal test itself is based on the assumption that fluid transport within the Chalk can be represented by a number of parallel horizontal fractures. This is not an unreasonable assumption for the Chalk in which fractures, when observed, are often parallel and broadly follow bedding plane structures (Bloomfield, 1996).

As the operational flow rates will be fixed at a constant rate for a proposed system it is only the frequency of the fractures that will alter the thermal breakthrough times. The fracture aperture will only affect the head required to drive the flow.

The frequency of the fractures should theoretically determine the response of the aquifer to the injection and abstraction of heated water. The fracture frequency will affect both the fluid velocity and the dissipation of energy into the Chalk matrix. This theory was tested in a number of different numerical models previous to the actual test to prove that the response for different fracture frequencies would be sufficiently different to be measurable during the test. This work is in the process of being reported.

The longer the test, the greater the fluid penetration and therefore the more accurate the interpretation of the aquifer structure beneath the site. However, this has to be balanced with both the man hours required to undertake the test and the ability to heat sufficient quantities of water on site.

THE THERMAL TEST PROCEDURE

The thermal test consisted of heating a total of 6000 litres of water (by means of immersion heaters) in a number of thermally insulated containers (Figure 2).



Figure 2. Plastic insulated containers for heated water storage

Once the water was sufficiently heated to a temperature close to the likely peak injection temperature for the proposed system, the water was pumped into a 3.66m packed section of the

borehole. The pump was placed within the packed section along with three thermistors; one at the base, one at the middle and one at the top of the section (Figure 3). The location of the packed section corresponded to the section of the borehole where peak flow rates had been observed in previous flow metre testing, in this case 144m below ground level. Figure 4 shows the equipment and packer being lowered into the borehole.

The flow rate from the heated containers to the packed section of the borehole was kept at a constant 5 l/s. Once the heated water had been exhausted the flow rate was reversed and the water abstracted at a constant 5 l/s.

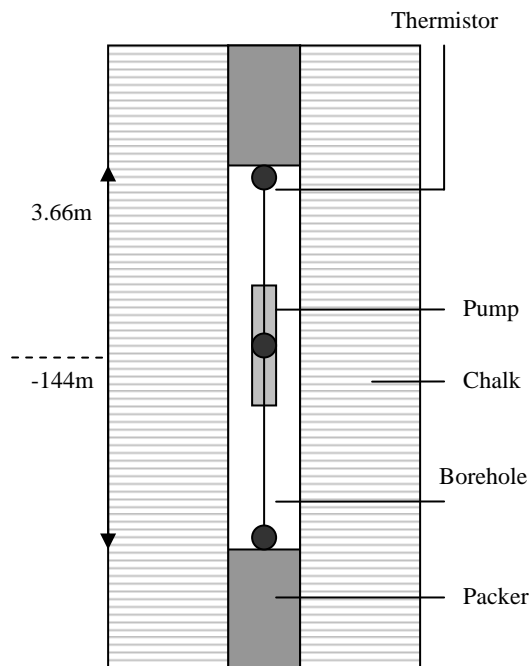


Figure 3. Schematic section of thermal test equipment



Figure 4. Equipment being lowered into the borehole

TEST INTERPRETATION

The principal method used to interpret the test was numerical modeling. Analytical solutions have been developed for an injection / abstraction test for the oil industry (Kocabas and Horne, 1990) for a constant injection rate and temperature followed by a constant abstraction rate. However, the injection rate for the test itself, although close to constant, did vary throughout the test. In addition, the temperature of the water within the packed section of the borehole was not constant throughout the test. Analytical solutions also become increasingly complex when dealing with radial flow (Moench, 1995). To represent the actual conditions that occurred during the test numerical modeling with time variable inputs was considered to be the most appropriate approach.

ANALYTICAL COMPARISON

To test the validity of the numerical model construction and the USGS SUTRA code for this type of problem a comparison was made between an analytical solution for thermal injection through a single fracture and the results derived from a numerical model. The analytical solution for thermal transport in a single fracture is well known and is based on the work by Lauwerier, 1955. The equations that need to be solved to determine the temperature at any point within the fracture are as follows:

$$(C\rho)_f \frac{\delta T}{\delta t} + \rho_w C_w V \frac{\delta T}{\delta x} = \frac{\lambda_m}{h} \frac{\delta T_m}{\delta z}$$

Eq.1

$$(C\rho)_f \frac{\delta T}{\delta t} + \rho_w C_w V \frac{\delta T}{\delta x} = (\lambda)_f \frac{\delta^2 T}{\delta x^2}$$

Eq.2

where:

ρ_w = density of water

C_w = specific heat capacity of water

ϕ_f = porosity of the fracture

$(C\rho)_f$ = total volumetric heat capacity of the fracture (includes any material in the fracture)

V = velocity of the water $V = \frac{q}{(\rho_w A \phi_f)}$

q = water injection rate

$\frac{\delta T}{\delta x}$ = temperature gradient in the water in the fracture

$(\lambda)_f$ = bulk thermal conductivity of the fracture

λ_m = bulk thermal conductivity of the material around the fracture

$\frac{\delta^2 T}{\delta x^2}$ = rate of change of temperature gradient in the fracture

h = the vertical depth of the fracture

$\frac{\delta T_m}{\delta z}$ = the temperature gradient in the material surrounding the fracture.

Equations 1 and 2 can be solved (Zabarnay, 1998) with the following boundary conditions:

$T_{(x,t)}$ = temperature within the fracture at any point

$T_{m(x,z,t)}$ = temperature of the impermeable surrounding material.

T_2 = initial temperature of the aquifer

T_1 = injection temperature

$T_{(\infty,\infty,t)} = T_2$

$T_{(x,y,0)} = T_1$

$T_{(x,0)} = T_1$

$T_{(0,t)} = T_2$

$T_{m(x,z,0)} = T_1$

$T_{m(x,z,t)} = T_1; x \rightarrow \infty, z \rightarrow \infty$

The solution then becomes:

$$\theta_{(x,t)} = erf \left(\frac{\frac{\lambda_m x}{C_w \rho_w V}}{h \sqrt{\frac{\lambda_m}{C_m \rho_m} \left(t - \frac{(C\rho)_f x}{C_w \rho_w V} \right)}} \right)$$

when $t > \frac{(C\rho)_f x}{C_w \rho_w V}$

Eq. 3

And

$\theta_{(x,t)} = 1$ when $t < \frac{(C\rho)_f x}{C_w \rho_w V}$

Where

$\theta_{(x,t)} = (T_{(x,t)} - T_2) / (T_1 - T_2)$

Equation 3 was solved in an Excel spreadsheet and the temperature at a number of different points along the fracture plotted against time. The parameters used are those shown in Table 1.

Parameter	Value	Units
C_w	4182	J/kg°C
ρ_w	1000	kg/m ³
ρ_r	2800	kg/m ³
λ_f	2.8	W/m
C_r	890	J/kg°C
q	0.5	l/s
ϕ_m	0.3	dimensionless
ϕ_f	0.98	dimensionless
t	variable	s
h	0.001	m

Table 1. Parameters used in the analytical solution

The numerical model in SUTRA consisted of a single fracture split horizontally by symmetry to save on model running time.

In order for the numerical model to treat the fracture as flowing water the dispersivity was set to zero. The model grid dimensions were set to comply with the Courant number which represents the relationship between the velocity of the fluid and the grid size of the model. A Courant number less than 1 is preferred for numerical accuracy:

$$C = v \frac{\Delta t}{\Delta l}$$

Where:

C = Courant number

v = average linear velocity of the fluid

Δt = numerical time step

Δl = dimension of the largest grid cell in the direction of flow

Fluid enters SUTRA through individual nodes and is then applied across a cell (Figure 5)

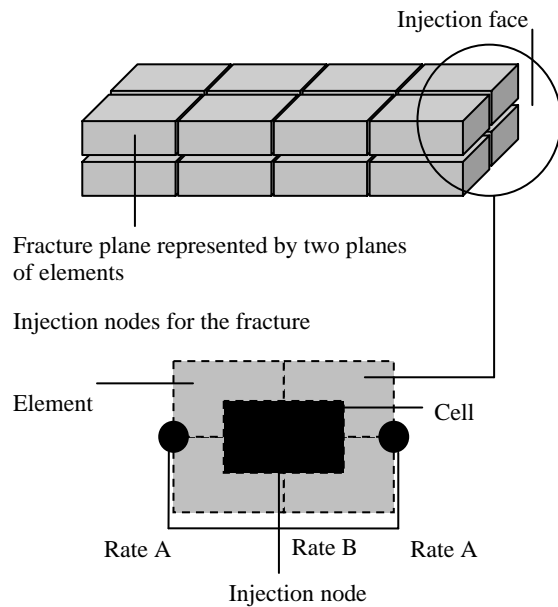


Figure 5. Representation of fracture plane in the numerical model

A single injection cell therefore spans four elements. The fracture plane itself was represented by two rows of elements to ensure that the fluid entered the model through the elements with the correct hydraulic and thermal parameters. In addition, nodes on the outer edge of the model were allocated half the injection rate of the other injection nodes (Rate A and Rate B respectively). The fracture hydraulic conductivity applied to the model was that derived from the cubic law for a 1mm fracture, although as the injection rate

through the nodes is constant this parameter will only affect the pressure required to achieve this flow.

The results from the comparison between the analytical modeling and the numerical modeling can be seen in Figure 6. This shows that the correlation between the two results is extremely good for all distances from the injection point. The method used to represent the fracture and the model construction and running (time stepping, grid definition) are clearly acceptable.

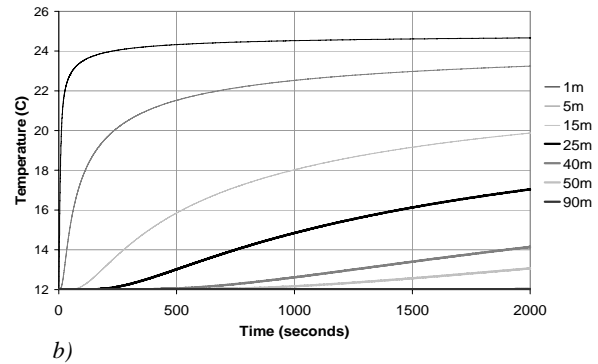
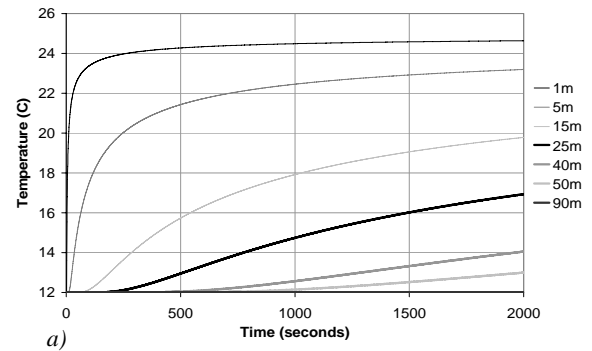


Figure 6. Comparison of results for a) analytical and b) numerical modeling for a single fracture

THERMAL TEST MODEL CONSTRUCTION

As with all numerical models a balance has to be maintained between the model resolution and the model running time. To reduce the model grid size and thus the running time, horizontal and vertical symmetry was used to split the packed section of the borehole (Figure 7). After this alteration, the model running time was reasonably fast.

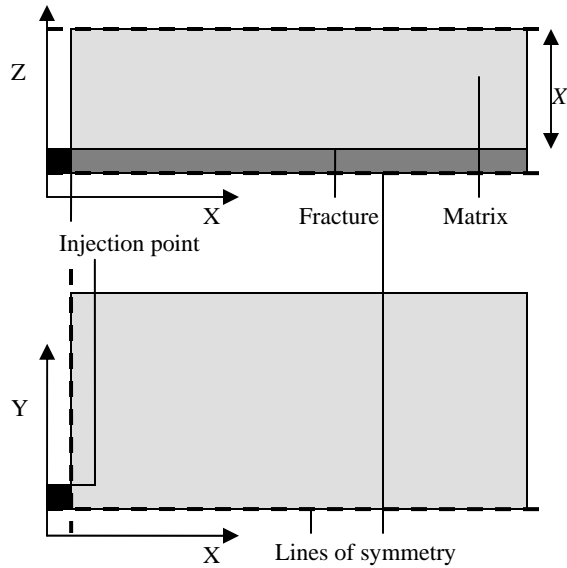


Figure 7. Lines of symmetry and model layout

MODEL OPERATION

The data from the injection period of the actual test was input as a time dependent variable into the SUTRA code. The average temperature recorded in the borehole during injection was used as the temperature input. The code was then recompiled using the Compaq Fortran compiler before being run. The dimension of the matrix above the fracture (X in Figure 7) was varied for each model run and the flow rate altered accordingly. The modeling commenced with a fracture frequency of one for the 3.66m packered section and was progressively increased by reducing the distance X .

RESULTS

The results of the thermal test can be seen in Figure 8. The results show that a near constant flow rate was achieved during the test. The moment when the flow is reversed can also be seen. The temperature recorded at the thermistors varied by up to a maximum of $3\text{ }^{\circ}\text{C}$ during the test from which it is inferred that the water in the packered section of the borehole was not well mixed during the injection process. The temperature rose to a peak of $32\text{ }^{\circ}\text{C}$ before the abstraction occurs and then dropped off during abstraction. Once the abstraction has finished there was a slight temperature rise in the borehole.

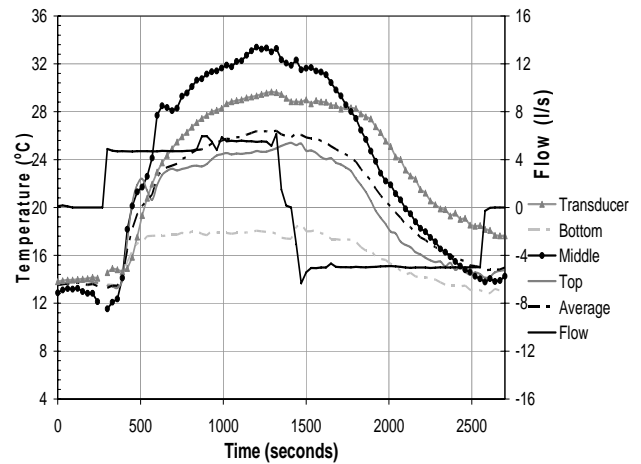


Figure 8. The results of one of the thermal tests

The results of the average temperature recorded during the test and those generated by the numerical model for different fracture frequencies can be seen in Figure 9. Fracture frequencies within the packered section of 2, 16 and 32 are shown to highlight the different predicted responses.

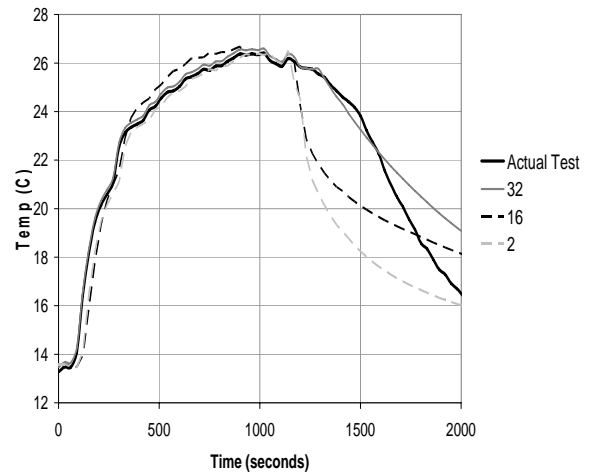


Figure 9. Thermal test results compared with numerical modeling results for different fracture frequencies

It can be seen from Figure 9 that the actual result from the test could not be matched exactly to a particular fracture frequency. However, it is clear that the response obtained from the test is more similar to the curve generated for a higher fracture frequency than for a lower frequency. Flow is clearly not occurring through a small number of isolated fractures (the response curve generated for a fracture frequency of 2 over the packered section, particularly in the early stages of abstraction, is markedly different to that obtained from the test). Even a fracture frequency of 16 still gives a more rapid drop

in temperature during abstraction than that achieved during the test. A closer representation of the test is achieved when the fracture frequency rises to approximately 32 (one every 0.11m). Although this result is still not identical to that observed during the test it is much closer than those obtained with lower fracture frequencies.

The difference in the heat dissipation pattern for different fracture frequencies can be seen in Figures 10 and 11. Figure 10 shows the extent and nature of the thermal penetration for a single fracture. In this case, the penetration distance is approximately 7m from the borehole during the injection period. Conversely, for a fracture frequency of 32 (one every 0.11m) the penetration is closer to 3m and the thermal penetration pattern is markedly different.

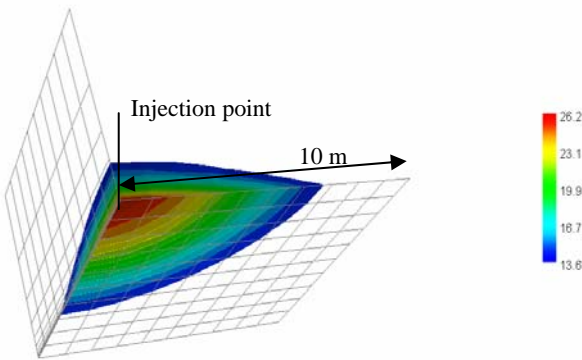


Figure 10. Thermal dissipation pattern for a single fracture

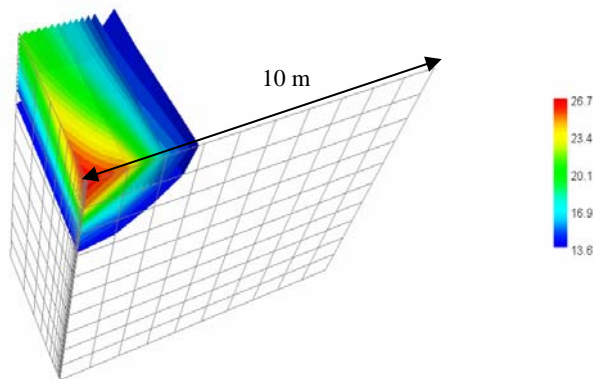


Figure 10. Thermal dissipation pattern for a fracture frequency of one every 0.1m

CONCLUSIONS

A thermal test was designed and implemented at a central London site to investigate the nature of the thermal transport. The results of the test indicate that the flow was not carried by a single or small number of fractures. The fractures that carry the flow can be

approximately represented as a series of horizontal fractures with a frequency of one every 0.1m (approximately 32 fractures over the packed section of the borehole). This result can be used in subsequent models that predict the performance of the system over the lifetime of the building.

DISCUSSION

There are some issues that arise from this sort of test and its interpretation. Of primary importance is the penetration that is gained during the test. With a penetration distance of approximately 3m it is likely that the test is, to a degree, representing the acidised portion of the Chalk aquifer. The flow in this acidised section of the aquifer will occur through preferentially enlarged channels. As the distance from the borehole increases the channels are likely to become less enlarged and the flow will travel through a greater number of fractures. The test will therefore be conservative and under estimate the fracture frequency.

REFERENCES

- Arup. (2006), Internal project lists.
- Mayor of London (2004). Green Light to Green Power – The Mayor’s energy strategy.
- Environment Agency (2005). Rising Groundwater Levels in the Chalk-Basal Sands Aquifer of the Central London Basin.
- Law, R., Nicholson, D (2005). A 3 dimensional model of the potential impacts on an aquifer of two energy storage systems. Proceedings, Consoil.
- Price, M., (1987). Fluid flow in the Chalk of England. In: Goff, J.C., Williams, B.P.J. (Eds.), Fluid Flow in Sedimentary Basins and Aquifers Geological Society Special Publication No. 34. The Geological Society, London, pp. 141–156.
- Bloomfield, J., (1996). Characterisation of hydrogeologically significant fracture distributions in the Chalk: an example from the Upper Chalk of southern England. Journal of Hydrology.
- McDonald, A., Allen, D., (2001). Aquifer properties of the Chalk of England. Quarterly journal of Engineering Geology and Hydrology.
- Kocabas, I., Horne, R.N., (1990). A new method of forecasting the thermal breakthrough time during re-injection in Geothermal reservoirs. Proceedings, 15th workshop on Geothermal Reservoir Engineering, 1990.
- Lauwerier, H.A., (1955). The transport of heat in an oil layer caused by the injection of hot fluid. Applied Science Resources 5, 2-3, 145-150.
- Zabarnay, G.M., Shurchkov, A.V., Chetveryk, H.O., (1998). The computer programs for calculation of some parameters of geothermal systems. Institute of

Engineering Thermophysics, Ukrainian National Academy of sciences, Kiev, 126.

Moench, A.F, (1995). Convergent radial dispersion in a double-porosity aquifer with fracture skin: analytical solution and application to a field experiment in fractured Chalk.

MODELLING OF THE CHALK AQUIFER IN CENTRAL LONDON FOR A PROPOSED OPEN COOLING SYSTEM

R. Law, D. Nicholson

ARUP Geotechnics

London

1. BACKGROUND

As part of the growing interest in aquifer thermal energy storage (ATES) in the United Kingdom a proposal has been made to use the chalk aquifer underlying central London to cool a new building development. The economic case for the system has been made by freeing up valuable floor space that would normally be used for conventional cooling systems. The use of an ATES system is in direct response to the Mayor of London's Energy strategy proposal (2004) which states that developments referred to the Mayor are 'to generate at least 10% of the site's energy needs (power and heat) from renewable energy on the site where feasible'.

Recent regulations from the Environment Agency in England state that licenses are unlikely to be granted for abstractions greater than 0.2 Ml/day (*Environment Agency, 2005a*). For an ATES system of any size therefore, the majority of the water abstracted from the central London aquifer will have to be re-injected. As the proposed building does not have a balanced energy demand throughout the year (a net cooling demand) there is a continual injection of heated water into the aquifer. This heated water has the potential to migrate to the abstraction boreholes and affect the long term performance of the system. The key concern for the system design is at what point in time and under what conditions the temperature at the abstraction borehole causes the cooling system to stop functioning effectively. To provide some design guidelines, Arup Geotechnics constructed a number of numerical models to simulate the response of the aquifer to different system configurations.

2. GEOLOGY AND HYDROGEOLOGY

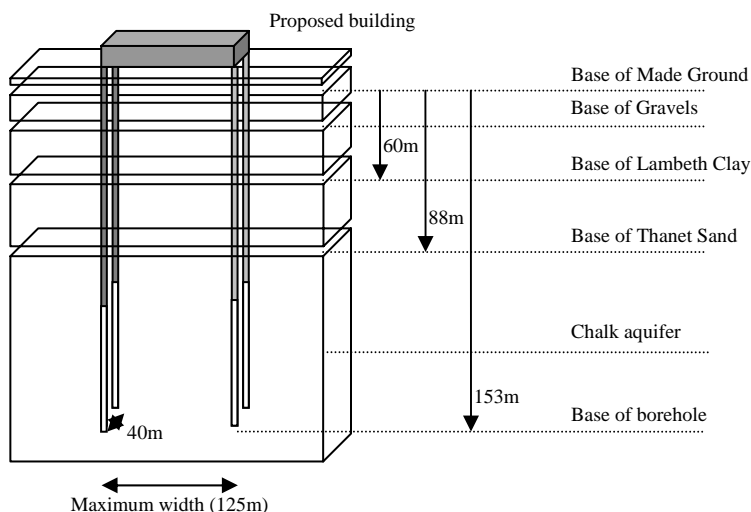


Figure 1. Representation of the site, boreholes and geology

The site is located in the central London area and falls within the London Basin, an asymmetric syncline in Cretaceous and Tertiary deposits. The Basin is faulted in a number of places. The faulting affects aquifer continuity and the flow of water. The sequence of strata at the site can be summarised as, Made Ground, Alluvium & Gravels, London Clay / Lambeth Group, Thanet Sand Formation, Chalk, (Figure 1). The site is underlain at a depth of around 90 m by the chalk which forms the aquifer. The chalk aquifer is typically hydrogeologically linked to the Thanet Sand Formation. The intact chalk is generally considered to be impermeable (*Bloomfield 1995, Bose*

1985, Macdonald 2001) but fissures and fractures in the chalk can make the overall rock mass highly permeable and allow very rapid transmission of water between the recharge and abstraction boreholes.

The degree of fissuring in the chalk can be highly variable. The mass permeability of the chalk typically decreases with depth and it is generally considered, for engineering purposes, that almost all the water entering boreholes is yielded by the upper 60–100 m of the chalk (Macdonald, 2001). The chalk is widely exploited for water abstraction in Central London and a review of available records indicates that 15 l/s is a reasonable design value for average borehole yield in the area.

The proposed site will have two abstraction and two injection boreholes, each approximately 150 m deep (Figure. 1) placed as far apart as the site will permit (approx. 125 m) to minimise heat interference between the boreholes. Each injection / abstraction borehole will be separated from the other by approximately 40 m. At present the background hydraulic gradient beneath the site is approximately 1/1000 (bearing of 40 degrees).

3. SYSTEM CONFIGURATIONS

A number of different system configurations have been modelled to test the overall sustainability of the proposal for different energy demands. Initial calculations suggested that using the aquifer to meet 100% of the cooling demands of the building would prove unsustainable. Models were run that represented energy demands of 20%, 30%, 40% and 50% of the total cooling demand. The total monthly cooling demands are listed in Table. 2. In addition, further analyses were undertaken on the 40% model. These included:

1. An average bleed flow of 0.2 MI/day (used as an average over the year and varied to meet peak demands). 0.2 MI/day was selected as this is the maximum amount that could potentially be permitted by the Environment Agency in the area of the site.
2. The addition of a background hydraulic gradient of 1/100.
3. A reduced delta T (the temperature differential for the cooling system) for the system of 5°C (consequent re-injection temperature of 17°C).
4. The effects of fracture flow/ the presence of high permeability zones in the chalk.

4. MODEL ASSUMPTIONS

- The aquifer is to be used for cooling only. All the extracted water is re-injected into the aquifer (other than when bleed flow is modelled). The injection occurs at the same rate as the abstraction.
- Water is extracted from the aquifer at 12°C.
- Delta T is 10°C. As the water being extracted from the aquifer is at 12°C it is assumed that the re-injected water is at 22°C.
- The energy required to cool the building is in part met from the aquifer, the remainder being met by conventional means.
- The model does not take daily fluctuations in energy demand into account. Short-term peaks in demand will therefore not feature in the results, and the total number of boreholes and maximum flow rate to meet peak daily demand is not addressed in the current modelling exercise.
- The model does not account for any water used within the building as grey water.
- The model ignores the effects of any abstraction boreholes that are not on the site. From geological records, the nearest borehole is approximately 95m away. Environment Agency data indicates that this is currently not licensed for extraction.
- For the purposes of this assessment, based on information from the building designers, it is assumed that the system will cease to function adequately once a temperature of 18°C has been reached at the abstraction boreholes.

5. NUMERICAL MODEL

The models use the program SUTRA 3D (Saturated-Unsaturated Transport) to calculate the temperature at the abstraction boreholes over time. SUTRA 3D is a modelling code that can be used to simulate density-dependent, saturated or unsaturated, water movement and the transport of either energy or dissolved substances in a subsurface environment. SUTRA 3D was released by the United States Geological Survey (USGS) in September 2003. Thermal energy transport includes advection and conduction and assumes local thermal equilibrium between the rock and the fluid.

SUTRA 3D calculates numerically the fluid pressures and temperatures at discrete points in space and time. The numerical approximation of the governing equations is based on a hybridisation of finite-element and integrated-finite-difference methods. The method of weighted residuals is employed for the finite-element approximations of the fluid mass and energy flux terms in the balance equations. All the other flux and storage terms are approximated using the integrated-finite-difference method. This hybrid approach improves the stability of the numerical solution. SUTRA 3D is a well proven code. Further details can be obtained from the USGS website.

6. MODEL DESIGN

The models were designed to focus on the interactions between the boreholes. They provide limited information on the environmental impacts associated with the general thermal migration from the site. As the boreholes are only injecting into and abstracting from the chalk, this is the only lithology that has been considered in the model. Further to this, to increase the resolution and the accuracy of the model, a one metre deep horizontal slice through the chalk and the boreholes has been taken instead of the full 60 m depth. This makes the assumption that the flow between the boreholes and the chalk is constant with depth. This may not be the case as the chalk permeability normally decreases with depth. However, predicting this variation in any meaningful sense is difficult. In addition, taking a 1m vertical slice ignores conductive vertical heat flux through the top and bottom of the chalk formation. Vertical losses through conduction were considered to be small compared to the main transfer of heat between the boreholes by advective processes.

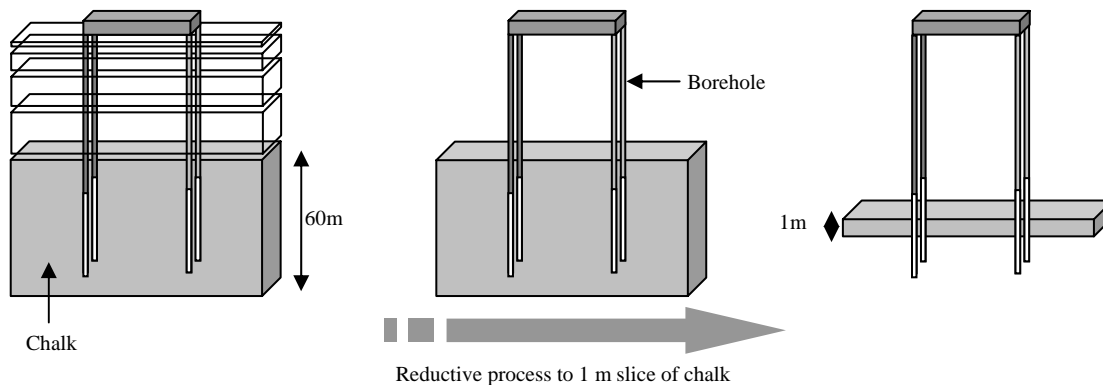


Figure 2. Reduction of the system to a simplified model

The main models assume an average hydraulic conductivity for the chalk, taken from literature values. As the flow rates between the two boreholes are fixed, differing values of hydraulic conductivity will not affect the thermal transport. They will only affect the calculated drawdowns. As flow through the chalk is dominated by fractures, it is conceivable that water velocities will be faster in the fractures than the velocities predicted by an averaged hydraulic conductivity. Additional models have explored the possible impacts of this faster flow.

As the principal result of interest is the change of temperature at the abstraction boreholes, the temperature of the nodes that represent the abstraction boreholes have been plotted against time. The models operate under the assumption that if the temperature of the abstraction boreholes is raised by a degree then the corresponding injection temperature is also raised by a degree.

7. MODEL PARAMETERS

The parameters used for the non-fracture flow models are listed in Tables 1 and 2. Complete references are given at the end of this paper.

Table 1. Hydrogeological parameters

Parameter	Units	Value	Reference
Chalk hydraulic conductivity	m/s	5x10 ⁻⁶	(2)
Porosity	-	30%	(2)
Density	kg/m ³	2700	(2)
Specific heat capacity	kJ/kg°C	0.9	(4)
Thermal conductivity	W/m°C	2.7	(1)
Hydraulic gradient	-	1/1000 (bearing 40°)	(5)

The cooling energy requirement of the building has been apportioned between the boreholes and scaled down to represent one metre of borehole for input into the model.

As an example, the monthly cooling requirement of the building in month 1 is 164 MWh. Taking the specific heat capacity of water to be 4.182 kJ/kg°C, the density of water to be 1 kg/l and delta T to be 10°C, the average flow needed over the month is 5.45 l/sec split between two abstraction boreholes.

The average flow rate per borehole is therefore 2.725 l/s. This corresponds to a flow rate per metre of 0.045 l/s.

It is important to note that the quoted flow rates above are the average for the whole month. Peak flow rates may be several times greater than the average and must be taken into account when considering the number of boreholes required.

The models were run using flow rates generated from these cooling figures until the cut off temperature of 18°C was reached at the abstraction boreholes.

Table 2. Building total cooling demands and flow rates

Month	Demand (MWh)	Total flow rate (l/s)	Flow rate per borehole (l/s)
1	164	5.45	2.73
2	152	5.05	2.53
3	224	7.44	3.72
4	345	11.46	5.73
5	406	13.48	6.74
6	484	16.07	8.04
7	521	17.30	8.65
8	484	16.07	8.04
9	400	13.28	6.64
10	341	11.32	5.66
11	210	6.97	3.49
12	162	5.38	2.69

8. FRACTURE FLOW / ZONING

Fracture flow is the primary method of fluid transport in the chalk, with very little flow occurring through the intact chalk. Accurately predicting the orientation and size of fractures and their effect on flow patterns is difficult. In addition, flow within the chalk can be confined to a number of zones whose total depth may be significantly less than that of the open borehole. For example, chalk in the upper 10m zone may become more weathered and hence more fractured, prior to deposition of the Thanet Sand. Both fracture flow and zones of increased flow will have an effect on the velocity of fluid transport in the aquifer. This may affect the velocity of heat migration.

As a method of checking the validity of treating the chalk as a homogenous medium, a discreet fracture model was constructed. This assumed that the flow in the chalk was carried by a small number of horizontal fractures spread evenly over the 60 m borehole (Figure 3.A). Using a field study by Bloomfield as a guide, 1mm fractures were placed at 1m intervals throughout the borehole.

In order to take account of the possible effects of zones, a model was constructed that assumed all the flow between the boreholes occurred through a 10 m zone of chalk (Figure 3.B). In addition, to represent a worse case scenario,

one model assumed that all the flow in this 10 m zone was carried by 5 x 1 mm aperture fractures, each separated by 2 m.

In the fracture flow model, flow has been assumed to be through the fractures only, with the remainder of the matrix being impermeable. Fracture hydraulic conductivity was determined using cubic law (*National Academic Press, 1996*). However, as the flow rate between the two boreholes is fixed, the hydraulic conductivity will only influence the head gradients between the boreholes, not the transport times.

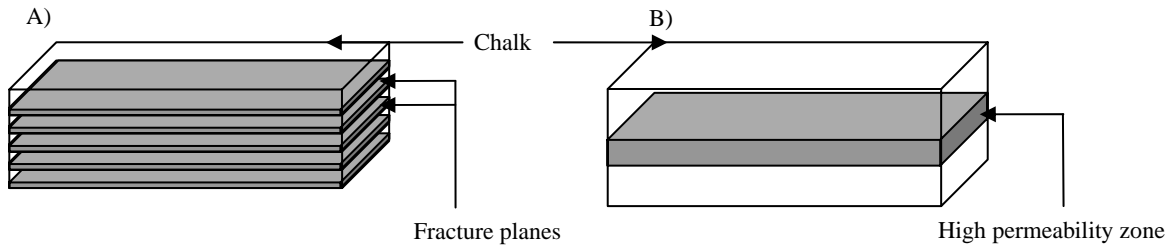


Figure 3. Fracture and zone representation

9. RESULTS

Energy demands

The temperature profile over time at the central abstraction borehole for all four cooling demands is shown in Figure 4.

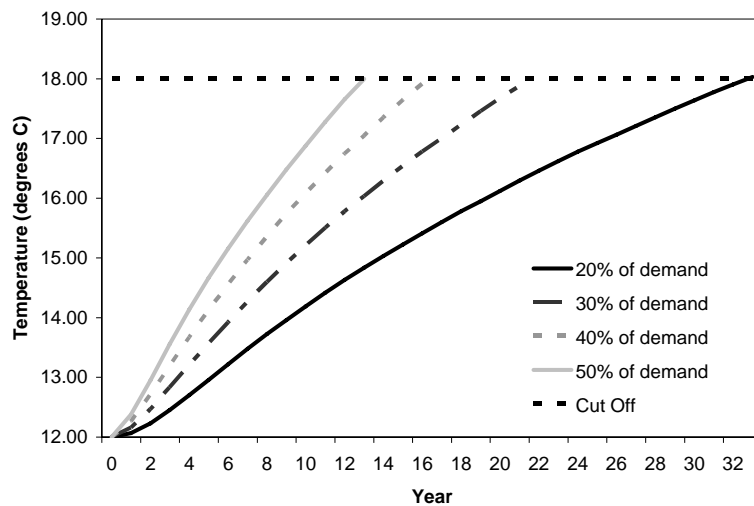


Figure 4. Temperature at the abstraction borehole for different energy demands

It can be seen that as the cooling load applied to the groundwater system increases, the rate of temperature rise at the abstraction boreholes increases and the time before the cut off temperature is reached decreases.

The effect of the increase in demand is exaggerated by the feedback system between the two boreholes. As the demand increases, so do the flow rates. This in turn reduces the transport time between the abstraction and injection boreholes and causes the temperature of abstraction to rise more quickly thus raising the injection temperature. This causes a larger temperature gradient between the injection borehole and its surroundings which leads to faster temperature diffusion rates.

Hydraulic gradient and drawdowns

The results suggest that a relatively high background gradient of 1/100 makes little difference to the temperatures at the abstraction boreholes over time. This is due to the head gradients generated by the injection and abstraction boreholes being far greater than any potential background gradient. The actual background gradient for the site is an order of magnitude lower at 1/1000.

The average drawdown for the configuration is 7.7 m (40% energy demand). This is around 3 m lower than that generally encountered in existing abstraction boreholes for similar flow rates. This would imply that the hydraulic conductivity assigned to the model is on the conservative side. The drawdowns are only significant when

considering viability of the system / checking the validity of the model parameters. They do not influence the heat transport time.

Reduction in Delta T

The reduction in delta T for a 40% re-injection model has effectively doubles the flow rate. As with all the modelled cases peak flow rates will be much higher than average flow rates.

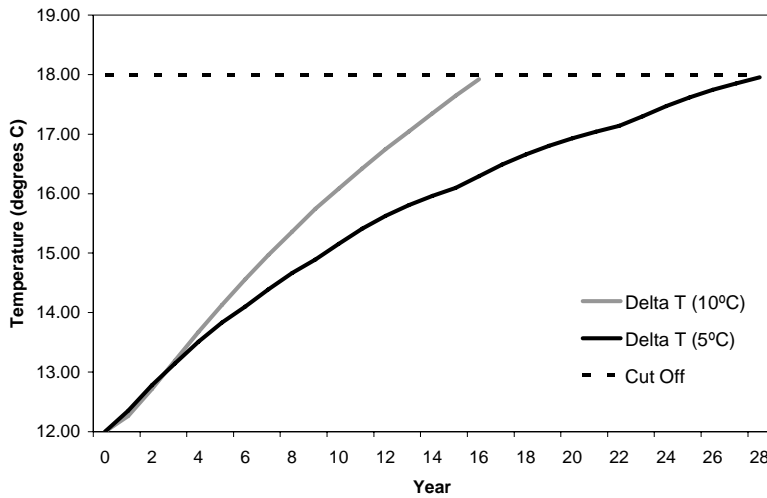


Figure 5. Temperature at the abstraction borehole for a reduction in Delta T

The temperature at the abstraction borehole initially increases at a similar rate for both systems. For a delta T of 5°C the increased flow rates cause the initial temperature rise to be similar to a delta T of 10°C (Figure 5.). However, over the longer term, the temperature at the abstraction borehole increases at a slower rate than with a delta T of 10°C. The system reaches its cut off temperature of 18 °C after approximately 17 years with a delta T of 10°C versus approximately 29 years with a delta T of 5°C. The lowering of delta T decreases the temperature gradient between the abstraction and injection boreholes and creates a greater pressure cone around the injection borehole which, over time, spreads the heat through a larger volume of aquifer.

Bleed Flows

Figure 6 shows the effect of bleed flows on the 40% re-injection model. Using an average bleed flow over the year of 0.2 MI/day lengthens the time before the cut off temperature is reached by approximately 40 years to 56 years. This is longer than would be expected from simply reducing the energy demands of the system in proportion to the quantity of bleed flow. It appears that at this lower injection rate, the system as a whole is closer to reaching equilibrium with the surrounding aquifer (the rate of heat production by the building is matched to the removal rate of the aquifer).

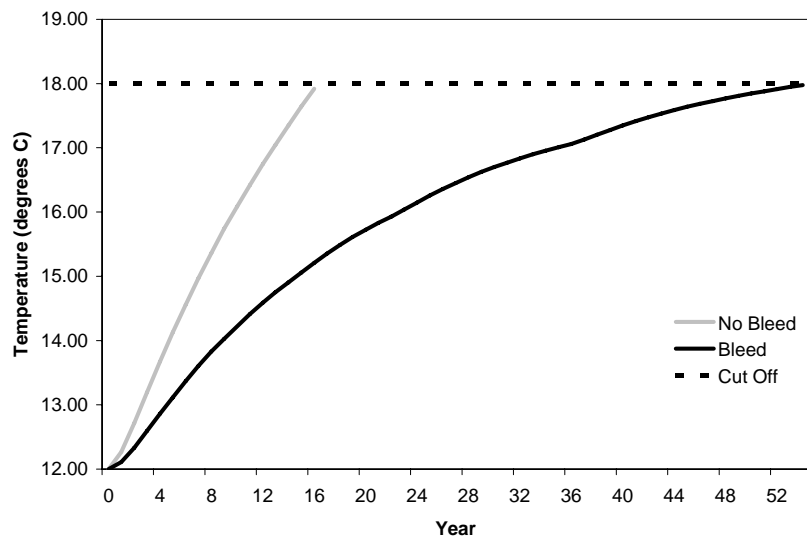


Figure 6. Temperature at the abstraction borehole with a bleed flow

The effect of using a selective bleed flow compared to an average bleed flow is negligible over time. The use

of selective bleed flows (i.e. those that vary during the year) requires more complex control systems than for constant bleed flow, so there appears to be little practical advantage in using selective bleed flow.

Fracture flow / high permeability zones

Figure 7 shows the difference between treating the chalk as a homogeneous medium and as a discretely fractured medium. The results show little difference. The slight difference between the two results is due to differences in the model grid designs. It appears as though the distance between the abstraction and injection boreholes is sufficiently large and the velocity of the water sufficiently low enough to cause a significant amount of heat to be transported away from the fracture into the intact chalk before it reaches the abstraction borehole. This would not necessarily be true for faster flow rates.

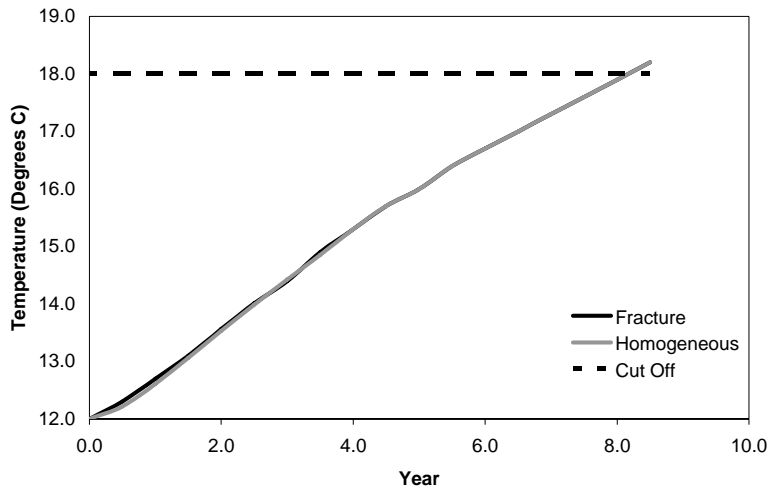


Figure 7. Temperature at the abstraction borehole for discrete and homogenous models

The effect of all the flow being concentrated through a zone of 10 m significantly decreases the time before the cut off temperature is reached. For the 40% cooling demand model, the failure temperature of 18°C is reached after approximately 8.5 years. Where flow is assumed to be linear over the full 60 m of chalk, the same temperature is reached after 17 years. Fracture flow in this worse case scenario still appears to have little impact upon the time to failure suggesting that it will have no impact upon the heat migration in the other cases.

10. CONCLUSIONS

The background hydraulic gradients of the magnitudes that can plausibly exist in the aquifer cannot be relied upon to remove any significant portion of the heat generated by the system. Reducing the cooling demand placed upon the aquifer significantly reduces the year on year rate of increase of the temperature of the abstracted groundwater.

The use of bleed flow (where a portion of the cooling water is discharged to waste, rather than re-injected into the aquifer) at a rate of 0.2 MI/day has the capacity to extend the time before the cut off temperature of 18 °C is reached. If the aquifer is used to meet a small percentage (20% or less) of the total cooling demand then the bleed flow could account for all of the re-injection flow, rendering the system completely sustainable in terms of long term increases in aquifer temperature.

Reducing the delta T for the cooling system causes an initial faster break through time for temperature at the abstraction borehole but over a longer duration lengthens the time before the cut off temperature is reached.

Zones of preferential or concentrated flow within the chalk could potentially reduce the time before the system reaches the cut off temperature by effectively increasing the flow rates between the two boreholes. It seems unlikely that fracture flow at these flow rates will have a significant impact on the system. If high flow zones are encountered the boreholes could be cased off through these zones to reduce the short circuiting effect.

11. RECOMMENDATIONS

It is likely that a groundwater cooling system can be made sustainable in terms of long term increases in aquifer temperature by a combination of design measures that include reducing the cooling loads placed on the groundwater system (by meeting a proportion of the total building cooling demand from groundwater, with the remainder from conventional plant), decreasing delta T (thereby reducing the temperature of the re-injected water) and using bleed flows to discharge a proportion of the warmer water to waste.

A workable system could employ a bleed system and a variable delta T to allow the aquifer to meet a proportion of the building cooling demand (between 20% and 40%). The installation of a simple monitoring system at the central abstraction borehole would allow an assessment to be made of the proportion of energy demand that could be placed upon the aquifer each year. However, any reduction in delta T will have the effect of increasing flow rates. The boreholes would have to be configured to cope with any subsequent increase in water demand.


Field testing to determine the nature of thermal flux within the fractured chalk would prove beneficial. A field thermal test for an open system is currently under development. In addition, standardised specifications for ATES boreholes need to be developed.

REFERENCES

- (1). ASHRAE (2003). Applications handbook SI (2003). P 32.16
- (2). Bell F.G, Culshaw M.G and Cripps J.C (1999). A review of selected engineering geological characteristics of English Chalk. *Engineering Geology* 54 (237-269)
- (3). Bloomfield, J (1995). Characterisation of hydrogeologically significant fractures in the Chalk; an example from the Upper Chalk of southern England. *Journal of Hydrology* 184 (1996) 355-379
- (4). Bose J.E, Parker J.D and MQuiston F.C (1985). Design/ data manual for closed loop, ground coupled heat pump systems. ASHRAE 1985.
- (5). Environment Agency (2005a). Groundwater levels in the Chalk-Basal Sands aquifer of the central London basin, May 2005.
- (6). Environment Agency (2005b). Chalk groundwater licensing policy for London. Feb 2005.
- (7). Macdonald, A.M and Allen D.J (2001). Aquifer properties of the chalk of England. *Quarterly Journal of Engineering Geology and Hydrogeology*. 34, 571-384
- (8). Mayor of London (2004). Green Light to Green Power – The Mayor’s energy strategy.
- (9). Rock Fractures and Fluid Flow (1996). National Academic press (p120) – Cubic law
- (10). Voss, C.I., and Provost, A.M (2002). SUTRA. A model for saturated-unsaturated variable-density groundwater flow with solute or energy transport. U.S. Geological Survey Water-Resources Investigations Report 02-4231, 260 p

Aspects of Sustainability in Ground Energy Systems

David Whitaker¹ and Ryan Law², Arup Geotechnics.



ABSTRACT: In the temperate regions of the world the energy demand of buildings is split between energy used for heating and energy used for cooling. The thermal mass of the ground may be utilised to store energy from one season to the next and so reduce the net annual energy demand in cities. Open and closed loop borehole systems and energy foundations are all methods of exploiting the thermal capacity of the ground. The long term stability of all ground energy systems depends upon adoption of an operating regime which maintains a balance between heat rejection and abstraction. This is not as widely appreciated as it should be. A case history from the UK is presented which illustrates sustainable aspects of implementing ground energy storage schemes for commercial buildings.

INTRODUCTION

The long term stability of all ground energy systems, open and closed, depends upon adopting a scheme design and an operating regime which maintain an approximate balance between heat rejection and abstraction. It is often said that the basis for ground sourced energy schemes is the relatively constant temperature of the ground below about 15m. It may be, however, that the reason for this equilibrium is that energy flows in this zone are rather low relative to the thermal mass. When assessing the long term sustainability of a ground energy scheme involving much more than a handful of closed boreholes or energy piles, or more than one or two open boreholes, the question: “Where is the energy coming from (or going to)?” must be answered. The natural geothermal gradient in most parts of the world is insignificant in the context of ground sourced energy, and solar radiation is remote from deep strata. Groundwater flow rates are seldom large enough to carry a significant part of the temperature deficit or surplus beyond the site boundaries. A simple calculation of the energy fluxes within the top 100m of the ground surface suggests that large ground energy schemes depend substantially on thermal capacity and not upon replenishable sources.

REPLENISHMENT OF GROUND ENERGY – CLOSED LOOPS

Design calculations for ground energy systems, and for closed systems in particular, usually omit reference to the ultimate source of the net energy abstraction. This is in contrast to groundwater supply engineering, in which a hydrogeological evaluation of sustainable resources is as important as the design of the abstraction system.

Bandyopadhyay et al (2006) have reviewed the design of many systems and concluded that "...models developed for loop design take into account the long term drift of ground temperature....However...the boundary heat flow either from the atmosphere or from...depth below the (ground heat exchanger) is ignored." Rybach & Eugster (2002) observe that "the oldest...(ground energy)...installations are not older than about 15 – 20 years, thus experience and...detailed studies on long-term performance...are lacking."

Where the question of long term performance and sustainability has been recognized and attempts have been made to understand the issues, efforts have been focused on modelling and measurement of conditions in the close vicinity of the ground heat exchangers. The ground surface, if it is included in the model at all, is represented as a fixed head (temperature) boundary. The meteorological, geophysical, and hydrogeological processes which control thermal recharge to a ground energy scheme are not explicitly modelled.

Let us carry out some basic calculations of energy flux and thermal capacity, considering notional ground heat exchanger loops. The continental geothermal flux is between 0.025 and 0.160W/m² approximately (Badino, 2005); an average figure might be about 0.05W/m². If the geothermal heat flow rising through one hectare of granite terrain could be efficiently captured, it would light eight 60 watt light bulbs. On the other hand, the average net solar flux, that part of the total solar influx which reaches the ground surface, is about 50W/m² in the UK. Clearly, in the undisturbed condition that influx is exported from the surface (or else the ground would be warming up), but a proportion could potentially be induced to flow towards an energy abstraction. It could be likened to the infiltrating portion of rainfall which has the potential to replenish groundwater storage and thereby support an abstraction.

For a horizontal near-surface ground heat exchanger it is perhaps easy to see how the winter depletion is replenished by summer recharge. Even for vertical ground heat exchangers the balance seems to be quite achievable, on first inspection. Thus, assume the average input of solar radiation at the ground surface is 18kWh/m² per month, equivalent to a constant 25W/m² (50% of the net solar flux at the surface). Assume a single energy borehole of 70m depth is operated so as to yield 3.5kW. If all the incident solar energy could be captured and extracted, a catchment area of only 140m² would be required, which would be equivalent to a circular area of radius only 6.7m.

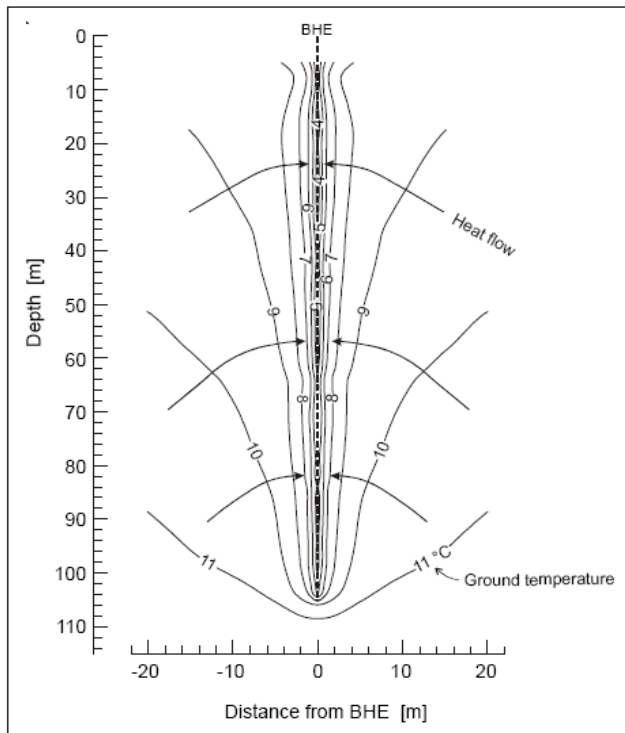


Figure 1. Calculated temperature isolines around a BHE (from Rybach and Eugster, 2002)

To achieve this, however, there would have to be a predominantly vertical thermal gradient within the ground around the energy borehole, which is not possible with the conductor tubing aligned with the length of the borehole. Figure 1, from Rybach and Eugster (2002), shows the temperature isolines around a single borehole heat exchanger (BHE): heat flow is radial and near horizontal, indeed upwards rather than downwards. The simple notion of solar energy incident upon the ground surface immediately above an energy borehole supporting the energy extraction of that borehole clearly cannot hold. The radius of influence of the borehole is going to be much greater than 6.7m. The point, however, is that, assuming all the heat

energy abstracted from a borehole heat exchanger is derived from solar recharge at the ground surface, each borehole requires an average catchment area of 140m^2 . Energy piles and closed energy boreholes within an array, however, are generally sited at closer centres than this; for example, less than 5m apart.

Interference between adjacent vertical ground heat exchangers at close spacings will become significant unless they are operated so as to exploit thermal capacity, or thermal mass, as opposed to intercepting thermal flux originating from solar recharge. The peripheral units may generate a temperature gradient over a sufficiently large area that abstraction from those peripheral heat exchangers is balanced by solar input, but “internal” boreholes are bounded by other units and these are unable to access any significant source of recharge. The larger the field of energy boreholes the more of these are “internal” and dependent upon energy storage due to the thermal capacity of the ground.

Considering the case of an array of closed energy boreholes, the thermal capacity available for energy storage and abstraction may be calculated quite easily. Assume the boreholes are positioned at 5m centres and are 70m long and the ground is a damp quartz sand with specific heat capacity $840\text{J}/(\text{kg}\cdot\text{K})$. The thermal capacity of a cylinder of ground of radius 2.5m and length 70m is then approximately $2.3 \times 10^6\text{kJ}/\text{K}$, equivalent to about $640\text{kWh}/\text{K}$. Let the average temperature of this cylinder of ground be changed by 10°C : the total amount of energy which is available in storage is 6.4MWh. Over a six-month extraction period (4320 hours) this would

support a yield of 1.5kW approximately. Operation at any higher average rates, or for longer, would require energy transport from some source of recharge, or remote storage, into the envelope of ground occupied by the pile, otherwise the temperature change will be greater than 10°C. Note that with reference to Figure 1, an average temperature change of ten degrees would mean that the temperature change immediately adjacent to each borehole would be significantly more than ten degrees. There is no other source of energy: each borehole in the array is in an identical situation to the one for which this calculation is performed (except for the peripheral ones, which are relatively few in number if the array is a large one).

A review of the literature on case histories suggests that, indeed, most ground energy systems based on closed vertical ground heat exchangers do operate on the storage principle and are therefore not sustainable unless either the abstraction is reversed seasonally (it does not have to be a year but in practice this is most practical) so that the total of heating and cooling is approximately balanced within the year, or the system is “rested” periodically (Rybach, 2007).

It is quite possible that there have been many ground energy schemes based on closed loop ground heat exchangers which are in effect over-abstracting heat or coolth. While the consequences to the operator of over-abstraction of groundwater are water level lowering, falling well yields and increased pumping costs, in the case of ground energy schemes the effects are seen as increasing (or decreasing) temperature of entering flow and reduced efficiency of heat pumps. The wider environmental costs are, of course, also significant in both cases. The Environment Agency in the UK is adopting a precautionary approach to the licensing of open borehole schemes, although it has no jurisdiction over closed systems.

REPLENISHMENT OF GROUND ENERGY – OPEN SYSTEMS

An open system comprising pairs of abstraction and recharge wells (doublets) is designed to operate either on the hot well – cold well principle, or on the basis of using the flow of groundwater between the two wells to allow energy transfer between the groundwater and the aquifer matrix.

In the latter case it can be advantageous to make use of the background hydraulic gradient to carry recharged groundwater offsite: in this way a proportion of the energy deficit (heat or coolth) is exported beyond the boundaries of the site. In practice, however, the natural hydraulic gradient is seldom large enough and flow beneath the site is dominated by the artificial gradient between the injection and abstraction wells (Arup, 2006). In the Chalk beneath London for example, typical drawdowns associated with an open system in which wells are operated at 5 - 10l/s are within the range of 3 - 5 m (McDonald, 2001). These are matched by equivalent injection heads, so that the head difference between pairs of wells in a doublet may be 6 - 10m. A building footprint in central London will seldom exceed 100m at its maximum dimension which means that the local gradient will be between 0.06 and 0.1. Typical background hydraulic gradients for central London, however, are of the order of 0.001. The hydraulic gradient generated by the abstraction and injection wells is therefore up to 100 times greater than the background gradient. Only a small proportion of the re-injected water, carrying the temperature anomaly, will be carried

off in the regional groundwater flow system and the majority of the heat rejected from the building will remain beneath the site as shown in Figure 2.

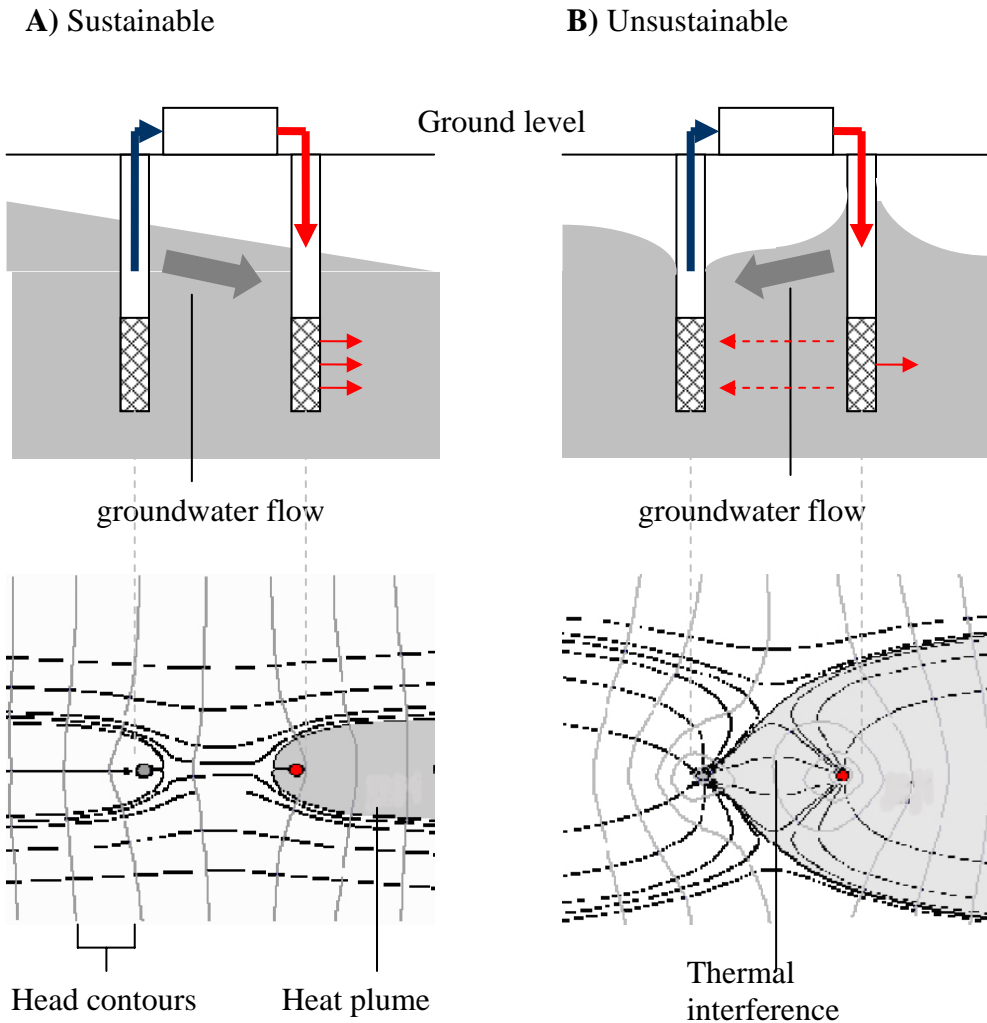


Figure 2. Effect of artificial hydraulic gradient

Hydrogeological conditions can be complex, particularly in fractured aquifers such as the Chalk. Assumptions of flow rate and residence time between injection and abstraction wells based on constants applicable to an intergranular flow regime can be seriously in error. There have been a number of cases reported in the literature (Packsoy, 2003; Allen, 1996) where a lack of knowledge about the hydrogeology caused problems to occur.

In an open system once the number of pairs of abstraction and injection wells has been chosen, the individual pumping rates are fixed. The volume flux or Darcian rate of groundwater flow through the aquifer between injection well and abstraction well is therefore also fixed; however, the true seepage velocity depends upon the nature of the permeability. Flow might actually be rapid within a small number of fractures or it may occur as slow seepage along a very large number of (tortuous) pore tubes in an intergranular aquifer: the permeability could be identical in either case. The implications of very different flow regimes for thermal behaviour between the

boreholes, however, are major. The residence time – the length of time during which the groundwater is in contact with the aquifer matrix – would be very different in the two extreme cases. Also, the surface area of the interface would be quite different: much greater in the case of the intergranular aquifer, which would improve thermal transfer across the boundary. On the other hand turbulent conditions, which are more likely to occur in the fissure flow case, assist the process of thermal transfer.

The short and medium term sustainability of a ground energy scheme based on abstraction and recharge doublets is consequently very dependent upon the hydrogeology at the site. The long term sustainability, however, depends upon a balance between the heat rejection and heat abstraction loads.

CASE STUDY – HYBRID ENERGY PILE AND OPEN BOREHOLE SYSTEM

The geology of the London area comprises largely clay strata of low permeability overlying the Chalk aquifer. Above about 100m depth the geology is only suited to closed systems while the Chalk is more suitable for open systems. A ground energy system was to be used to both heat and cool the new development, which is a large office, residential and retail complex. The energy demands of the building are large, and a hybrid scheme was devised comprising an array of energy piles and an open borehole system (Figure 2). In this way the maximum utilization of energy storage potential of the ground beneath the site could be made.

The overall objective was to meet 10% of the total energy demand from renewable sources, and the ground sourced scheme was required to contribute a large part of that figure. Restrictions on new abstractions from the confined aquifer meant that groundwater abstracted from the borehole system should be returned to the aquifer through recharge boreholes at the same site.

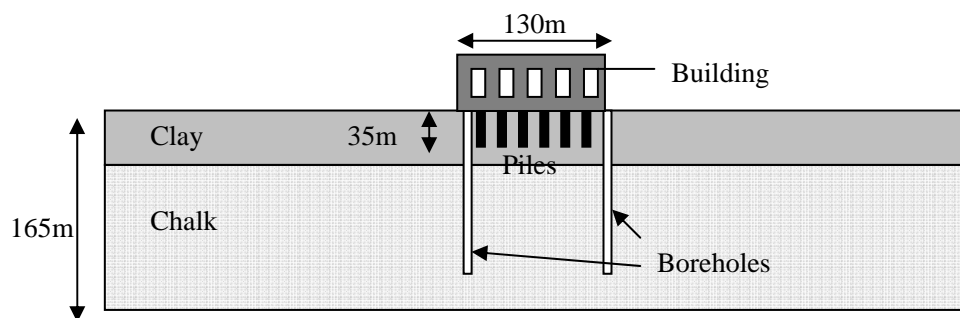


Figure 2. Schematic representation of the proposed system (not to scale)

An iterative approach was followed to design the scheme. Once the thermal ground model had been developed, an energy abstraction/rejection system was chosen which would provide the maximum energy transfer capacity. This involved using some 180 of the structural piles for energy transfer, and siting 4 pairs of abstraction and injection boreholes within the site. Numerical models were developed of the upper part of the system, to simulate pile operation, and of the aquifer incorporating the borehole array. The numerical models were constructed using the United States Geological Survey (USGS) SUTRA code.

The design load profiles were revised and refined in successive model iterations to

maximize the short term and annual yield without causing long term temperature changes beneath the site. Early iterations demonstrated poor long term performance, and these findings resulted in some quite major revisions being made to the building HVAC design. The major changes were towards achieving an annual balance in the heating and cooling loads applied to the piles and a near-balance in the case of the borehole system, and adjusting the distribution and timing of the loads on the two parts of the scheme.

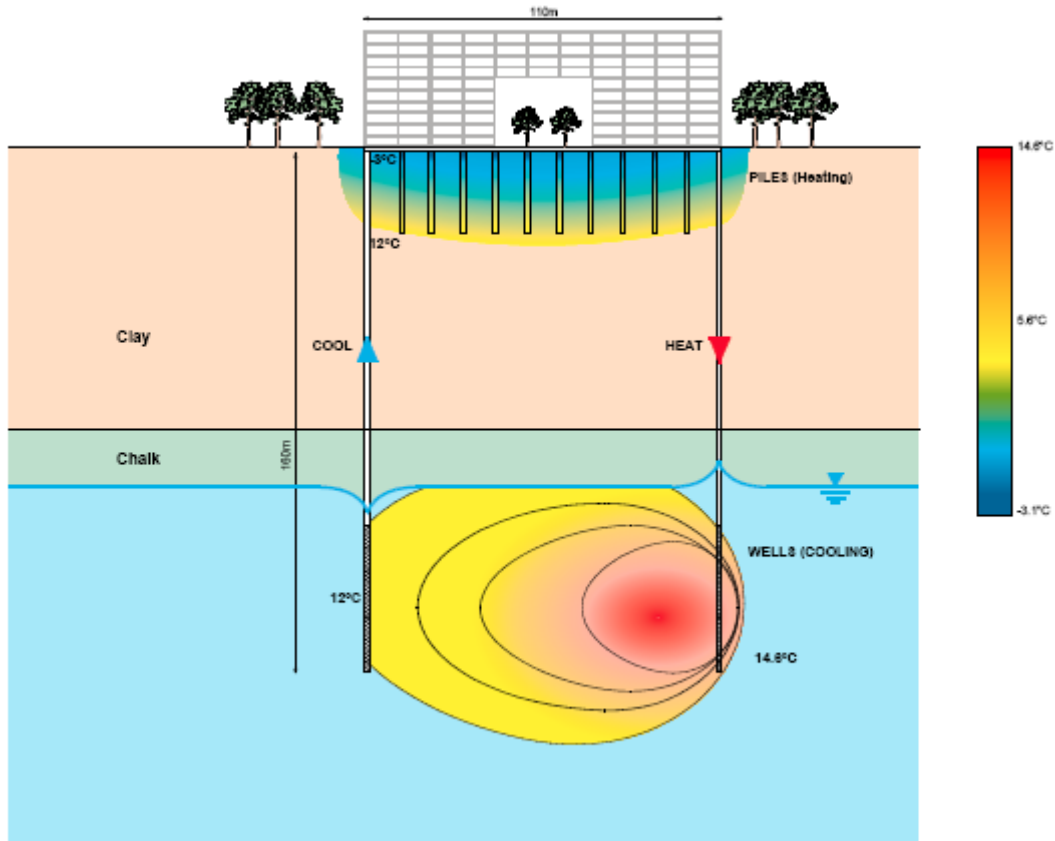


Figure 3. Simplification of model predictions after 2 years operation

Figure 3, which is a simplification of the output from an early run of the model using the demand figures given in Table 1, shows that the spread of energy outward from the ground surrounding the energy piles is minimal. The temperature of the ground surrounding the energy piles (used for heat abstraction only) had dropped to approximately 10°C after only two years of operation, indicating that the system is significantly out of balance and consequently unsustainable in the long term. It is clear from the figures in Table 1 that there is a substantial imbalance between the total heating and cooling demands.

In Figure 3 it can be seen that the open borehole system has caused a temperature deficit in a larger volume of ground (aquifer) than the energy piles. The temperature of the aquifer surrounding the open system (used for heat rejection only) has been

Table 1. Initial energy loads

	Energy Piles (kW)	Boreholes (kW)	Number of Hours	Total Demand (MWh)
Cooling Demand	0 kW	1650 kW	2500	4125
Heating Demand	450 kW	0 kW	500	225
Net				3900 (Cooling)

raised by almost two degrees after two years. The model predicted that after a period of 10 years the system would no longer function as the entering fluid temperatures would have exceeded the economical limits of the heat exchanger.

CONCLUSIONS

In order for ground energy systems to function in a sustainable manner in the long term the system configuration and energy demands must be matched to the ground conditions. Numerical models can assist with predicting the performance of ground energy systems at the design stage to avoid potential problems that may only be discovered after many years of operation.

REFERENCES

- Allen, D.M. (1996). "Steady-state and Transient Hydrologic, Thermal and Chemical Modelling of a Faulted Carbonate Aquifer used for Aquifer Thermal Energy Storage". Carleton University, Ottawa, Ontario, Canada. *Unpublished Ph.D. thesis*, Ottawa-Carleton Geoscience Centre and the Department of Earth Sciences, Carleton University, Ottawa, Ontario, Canada, 642 pp.
- Badino, G., (2005). "Underground drainage systems and geothermal flux". *Acta Carsologica*, 34 (2), 277-316
- Bandyopadhyay, W.D. Gosnold, M. Mann, (2006). "Thermal study of a large ground heat exchanger in clay soil the cold weather environment of northern USA: some initial findings". *Research report*, Stockton University.
- Kavanaugh, S.P., and K. Rafferty, (1997). "Ground-source heat pumps: Design of geothermal systems for commercial and institutional buildings." Atlanta: American Society of Heating, Refrigerating and Heating Engineers, Inc.
- MacDonald, A. M. and Allen, D. J., (2001). "Aquifer properties of the Chalk of England". *Quarterly Journal of Engineering Geology and Hydrogeology*. 34, 371 – 384.
- Packsoy, H., Turgot, B., Gurbuz, Z., (2003). "First Aquifer Thermal Energy Storage (ATES) plant in Turkey". *Proc., 9th International Conference on Thermal Energy Storage*, Warsaw, 77-81.
- Rybach, L. (2007) "Geothermal Sustainability." *Proc., European Geothermal Congress 2007*, Unterhaching, Germany, 30 May-1 June 2007.
- Rybach, L., and W.J. Eugster, (2002). "Sustainability Aspects of Geothermal Heat Pumps." *Proc., 27th Workshop on Geothermal Reservoir Engineering*, Stanford University, Stanford, California, p. 50-64.

Quarterly Journal of Engineering Geology and Hydrogeology

Determining fracture properties by tracer and thermal testing to assess thermal breakthrough risks for ground source heating and cooling in the Chalk

R. Law and R. Mackay

Quarterly Journal of Engineering Geology and Hydrogeology 2010; v. 43; p. 269-278
doi:10.1144/1470-9236/08-089

see <http://eprints.bham.ac.uk/455/>
